



UNIVERSITEIT VAN PRETORIA
UNIVERSITY OF PRETORIA
YUNIBESITHI YA PRETORIA

THE INFLUENCE OF SURFACE ROUGHNESS IN THE TRANSITIONAL FLOW REGIME

MSC 422 – Final Report

Marilize Everts s29037078
Study Leader: Prof J.P. Meyer
2012

100
1908 - 2008



UNIVERSITEIT VAN PRETORIA
UNIVERSITY OF PRETORIA
YUNIBESITHI YA PRETORIA

MECHANICAL AND AERONAUTICAL ENGINEERING
MEGANIESE EN LUGVAARTKUNDIGE INGENIEURSWESE
INDIVIDUAL ASSIGNMENT COVER PAGE /INDIVIDUELE OPDRAG DEKBLAD

Name of Student / Naam van Student	
Student number / Studentenommer	
Name of Module / Naam van Module	
Module Code / Modulekode	
Name of Lecturer / Naam van Dosent	
Date of Submission / Datum van Inhandiging	
Declaration: 1. I understand what plagiarism is and am aware of the University's policy in this regard. 2. I declare that this _____ (e.g. essay, report, project, assignment, dissertation, thesis, etc.) is my own, original work. 3. I did not refer to work of current or previous students, memoranda, solution manuals or any other material containing complete or partial solutions to this assignment. 4. Where other people's work has been used (either from a printed source, Internet, or any other source), this has been properly acknowledged and referenced. 5. I have not allowed anyone to copy my assignment.	Verklaring: 1. Ek begryp wat plagiaat is en is bewus van die Universiteitsbeleid in hierdie verband. 2. Ek verklaar dat hierdie _____ (bv. opstel, verslag, projek, werkstuk, verhandeling, proefskrif, ens.) my eie, oorspronklike werk is. 3. Ek het nie gebruik gemaak van huidige of vorige studente se werk, memoranda, antwoord-bundels of enige ander materiaal wat volledige of gedeeltelike oplossings van hierdie werkstuk bevat nie. 4. In gevalle waar iemand anders se werk gebruik is (hetsy uit 'n gedrukte bron, die Internet, of enige ander bron), is dit behoorlik erken en die korrekte verwysings is gebruik. 5. Ek het niemand toegelaat om my werkopdrag te kopieër nie.
Signature of Student / Handtekening van Student	
Mark awarded / Punt toegeken	

Appendix B

REPORT CARD FOR THESIS MSC 412 and 422

20.12.....

Name Marilize Everts Reg. no. 29037078.....

Topic Determine the influence of surface roughness in the transitional flow regime

Leader Prof. JP Meyer.....

Commencement date:

2012-03-01.....

Date	Par	Par	Comments
1/3/2012		ME	First meeting
7/3/2012		ME	Discuss protocol.
14/3/2012		ME	Discuss literature study
22/3/2012		ME	Prep set-up & literature study
28/3/2012		ME	Experimental set-up.
16/4/2012		ME	Design
2/5/2012		ME	Design
9/5/2012		ME	Design
17/5/2012		ME	Design & Report.

25/5/2012

1/8/2012

ME

ME

Designs Report
Roughness of surface discussion

Registration for Thesis MSC 412 and 422

20.12.....

Name Marilize Reg. no. 29037078.....

Address 571 Norval Street, Moreleta Park, 0044.....

Topic Determine the influence of surface roughness in the transitional flow regime

Study Leader Prof. JP Meyer.....

Signature

ABSTRACT

Title: The Influence of Surface Roughness in the Transitional Flow Regime

Author: M. Everts

Student number: 29037078

Study Leader: Prof J.P. Meyer

Commencement Date: 2012-03-01

Completion Date: 2012-10-19

Heat exchangers are usually designed that they do not operate in the transitional flow regime, mainly due to the uncertainty and perceived chaotic flow behavior and instabilities in this region. However, due to changes in operating conditions and design constraints, heat exchangers are often required to operate in this region. Although much research has been devoted to flow in the transitional flow regime, little information is available on the influence of surface roughness in this flow regime. Thus, the aim of this study was to determine the influence of surface roughness in the transitional flow regime. An experimental set-up was developed, built and validated, and heat transfer and pressure drop measurements at different heat fluxes were taken for water in a smooth and roughened tube with a relative roughness of 0.058, with the same outer diameters. The Reynolds number was varied between 1 000 and 7 000 for the smooth tube, and between 500 and 7 000 for the roughened tube, to ensure that the whole transitional flow regime was covered. Heat transfer and pressure drop measurements were taken at three different heat fluxes (8.66, 11.14 and 13.92 kW/m²) for water in a smooth and roughened tube over the transitional regime. Both tubes had a diameter of 15.88 mm, a square edge inlet and a length of 1.8 m. The Prandtl numbers of the water ranged between 5 and 7. The data obtained from the experiments have been compared to recently published results. Both adiabatic and diabatic friction factor results showed that surface roughness increased the friction factors significantly and transition occurred earlier as well. Although surface roughness increased the heat transfer in the turbulent region, the opposite is true for the laminar region, since it partially obstructs the secondary flow path. The heat transfer results further showed that transition is delayed for increasing heat fluxes and that the diabatic friction factor was higher due to the effect of secondary flow, especially in the laminar regions.

ACKNOWLEDGEMENTS

I would like to acknowledge the following people for their help and support

- Prof J.P. Meyer for offering his support and guidance and placing his substantial knowledge at my disposal.
- Mr D. Gouws and Prof S. Els for their technical advice and support with the experimental set-up and testing.
- Mr J.C. Everts, Mrs M. Everts, Mr M. Kapp and Mrs N.M. Kotze for their continuous moral support.

TABLE OF CONTENTS

1. Introduction	1
1.1 Background	1
1.2 Problem Statement	1
1.3 Aim.....	2
1.4 Objectives.....	2
1.5 Scope of Work	2
2. Literature Study	3
2.1 Introduction	3
2.2 Reynolds and Grashof Numbers	3
2.3 Reynolds Analogy	4
2.4 Different Inlet Geometries	5
2.5 Uniform Heat Flux Boundary Condition.....	6
2.6 Transitional Flow in Smooth Tubes: Work Done by Ghajar.....	6
2.6.1 Diabatic Investigation	6
2.6.1.1 Fluid Properties	6
2.6.1.2 Influence of Inlet Geometry on Pressure Drop Measurements, Friction Factors and Heat Transfer	7
2.6.1.3 Forced and Mixed Convection	8
2.6.2 Adiabatic Investigation	9
2.7 Transitional Flow in Smooth Tubes: Work Done by Meyer	10
2.7.1 Diabatic Investigation	10
2.7.2 Adiabatic Investigation	12
2.8 Transitional Flow in Enhanced Tubes: Work Done by Meyer.....	13
2.8.1 Diabatic Investigation	13
2.8.1.1 Heat Transfer	13
2.8.1.2 Friction Factors	14
2.8.2 Adiabatic Investigation	14
2.9 Surface Roughness	15
2.10 Conclusion	16
3. Experimental Set-up.....	17
3.1 Introduction	17
3.2 Design Calculations.....	17
3.2.1 Diabatic Conditions	17
3.2.2 Minor Pipe Losses	19
3.2.3 Overall System Pressure Loss	20
3.2.4 Insulation and Heat Loss	20
3.3 Experimental Set-up.....	21
3.3.1 Tube Diameters	23
3.3.2 Surface Roughness	23
3.3.3 Calming Section	28
3.3.4 Test Section	29
3.4 Data Reduction.....	31
3.4.1 Friction Factor	31
3.4.2 Heat Transfer Coefficient	31

3.4.3	Energy Balance	32
3.5	Instruments.....	32
3.5.1	DC Power Supply.....	32
3.5.2	Thermocouples	32
3.5.3	Heating Wire	33
3.5.4	Pressure Transducers	33
3.5.5	Flow meters	34
3.6	Experimental Procedure.....	34
3.7	Validation	35
3.7.1	Adiabatic Friction Factors	35
3.7.2	Diabatic Friction Factors	38
3.7.3	Heat Transfer Coefficients	39
3.8	Conclusion	40
4.	Results	42
4.1	Introduction	42
4.2	Smooth Tube.....	42
4.2.1	Friction Factors	42
4.2.2	Heat Transfer	44
4.3	Roughened Tube	47
4.3.1	Friction Factors	47
4.3.2	Heat Transfer Coefficients	49
4.4	Conclusion	51
5.	Conclusion and Recommendations	53
6.	References	55
	Appendix A: Surface Roughness.....	A1
A.1	Sand Paper.....	A2
A.2	Steel Brush.....	A3
A.3	Hammering Process.....	A5
A.4	Sand Grading Analysis	A7
	Appendix B: Calibration.....	B1
B.1	Thermocouple Calibration	B2
B.2	Pressure Transducer Calibration	B7
	Appendix C: Matlab Codes	C1
C.1	Thermocouple Calibration	C2
C.2	Adiabatic Tests.....	C3
C.3	Diabatic Tests	C6
C.4	Data Comparison.....	C9
C.5	Secondary Flow	C10
	Appendix D: Protocol and Progress Reports.....	D1
D.1	Protocol.....	D2
D.2	First Progress Report.....	D6
D.3	Second Progress Report.....	42

LIST OF TABLES

Table 2.1: Transition Reynolds Numbers for Different Heat Fluxes	7
Table 3.1: Temperature Differences at Different Heat Fluxes	19

LIST OF FIGURES

Figure 2.1: Different Inlet Geometries	5
Figure 2.2: Secondary Flow	6
Figure 3.1: Experimental Set-up	21
Figure 3.2: Positive Displacement Pump and Accumulator	22
Figure 3.3: Experimental Set-up	23
Figure 3.4: Moody Chart (Toprak, 2006)	24
Figure 3.5: Steel Brush	24
Figure 3.6: Steel Wire Mesh	25
Figure 3.7: Steel Rod	25
Figure 3.8: Measuring Hammered Section	25
Figure 3.9: Frictions Factor Comparison for Smooth and Roughened Tubes	26
Figure 3.10: Pressure Comparison for Smooth and Roughened Tubes	27
Figure 3.11: Thermal Resistance Experiment	27
Figure 3.12: Sand Roughened Tube	28
Figure 3.13: Calming Section	28
Figure 3.15: Schematic of Test Section	29
Figure 3.14: Square-edged Inlet	29
Figure 3.16: Thermocouples Attached to Tube	30
Figure 3.17: Pressure Tap	30
Figure 3.18: Mixer	30
Figure 3.19: Power Supply	32
Figure 3.20: Heating Wire	33
Figure 3.21: Differential Pressure Transducer	34
Figure 3.22: Coriolis Flow Meters	34
Figure 3.23: Validation of Adiabatic Friction Factor Results Inside the Smooth Tube	37
Figure 3.24: Validation of Adiabatic Friction Factor Results Inside the Roughened Tube	38
Figure 3.25: Validation of Diabatic Friction Factor Inside the Smooth Tube	39
Figure 3.26: Validation of Heat Transfer Data for the Smooth Tube	40
Figure 4.1: Local Heat Transfer Coefficients for the Smooth Tube When 8.66 kw/m ² Heat Flux	43
Figure 4.2: Experimental Friction Factors for the Smooth Tube as a Function of Reynolds Number for Different Heat Fluxes	44
Figure 4.3: Experimental Heat Transfer Data for the Smooth Tube in terms of Nusselt Numbers against Reynolds Numbers for Different Heat Fluxes	45
Figure 4.4: Local Heat Transfer Ratio for the Smooth Tube for Different Heat Fluxes	46
Figure 4.5: Smooth Tube Heat Transfer Data in terms of the Colburn j-factors for Different Heat Fluxes	47
Figure 4.6: Experimental Friction Factors for the Smooth Tube and Roughened Tubes as a Function of Reynolds Number for Different Heat Fluxes	44
Figure 4.7: Experimental Heat Transfer Data for the Smooth Tube and Roughened Tubes in terms of Nusselt Numbers against Reynolds Numbers for Different Heat Fluxes	45
Figure 4.8: Local Heat Transfer Ratio for the Roughened Tube for Different Heat Fluxes	50
Figure 4.9: Experimental Data for the Smooth Tube in terms of the Colburn j-factor	51

NOMENCLATURE

A	Area	m^2
D	Diameter	m
C_p	Constant pressure specific heat	J/kg K
EB	Energy Balance	
f	Friction factor	
Gr	Grashof number	
g	Gravitational acceleration	m/s^2
h	Convection heat transfer coefficient	$W/m^2 \text{ } ^\circ C$
I	Current	A
j	Colburn j-factor	
k	Thermal conductivity	W/m K
K	Minor losses	
L	Length	m
L_c	Characteristic linear dimension	m
m	Flow parameter	
\dot{m}	Mass flow rate	kg/s
N	Number of turns	
Nu	Nusselt number	
ρ_r	Resistivity	Ω/m
Pr	Prandtl number	
\dot{Q}	Heat transfer rate	W
\dot{q}	Heat flux	W/m^2
R	Resistance	Ω
Re	Reynolds number	
St	Stanton number	
T_s	Temperature of surface	$^\circ C$
T_∞	Temperature of fluid sufficiently far from surface	$^\circ C$
V	Mean velocity of object relative to the fluid	m/s
	Voltage	V

GREEK LETTERS

α	Thermal diffusivity	m^2/s
β	Coefficient of volume expansion	
ε	Heat transfer effectiveness	
ρ	Density of the fluid	kg/m^3
μ	Dynamic fluid viscosity	kg/ms
ν	Kinematic Viscosity	m^2/s
Δh	Head loss	m
ΔP	Pressure drop	Pa
ΔT	Temperature Difference	$^\circ C$

SUBSCRIPTS

avg	Average
b	Property evaluated at bulk temperature
conv	Convection
i	Inner
lam	Laminar flow
o	Outer
tot	Total
trans	Transitional flow
turb	Turbulent flow
w	Property evaluated at wall temperature Wire property
cp	Constant property solution (isothermal)
vp	Variable property solution (non-isothermal)

1. INTRODUCTION

1.1 BACKGROUND

Flow in tubes has been extensively investigated since as early as 1883 especially focusing on laminar and turbulent flow, while research has been done on the transitional flow regime since the 1990's. The transitional flow regime is where the Reynolds Number changes from laminar to turbulent flow and it is usually avoided due to flow instabilities and uncertainties.

Transition occurs at a Reynolds number of 2 300 for uniform and steady flow in a horizontal smooth tube with a rounded entrance (ASHRAE, 2009). However, this Reynolds number is significantly affected when the inlet geometry and smoothness of the tube are changed, which typically occur in heat exchangers in order to increase the heat transfer and efficiency. When designing heat exchangers, the aim is to increase the heat transfer, while reducing the pressure drop. Turbulent flow provides good heat transfer coefficients and high pressure drops, while the opposite is true for laminar flow. Therefore, transitional flow will be able to provide higher heat transfer coefficients compared to laminar flow, but also lower pressure drops compared to turbulent flow. Although heat exchanger designers are usually advised to avoid flow in the transitional flow regime (mainly due to the large fluctuations and uncertainties) it is not always possible, due to design constraints. Thus, it is important to investigate flow through tubes with different inlet geometries, inside surfaces as well as different boundary conditions.

Up to now, there are mainly two groups of people who have investigated flow in the transitional flow regime. Professor A. J. Ghajar from Oklahoma State University as well as Professor J.P. Meyer from the University of Pretoria, have both investigated flow through smooth tubes in the transitional flow regime under diabatic conditions and adiabatic conditions. Meyer also investigated the influence of enhanced tubes. Extensive work has been done in the Heat Transfer Laboratory of the University of Pretoria on heat transfer in the transitional flow regime, as well as on the influence of different inlet geometries and enhanced tubes on flow in this flow regime. These studies proved that the transitional flow regime can be accurately described and is not as chaotic and unpredictable as was believed earlier. However, since this research was mainly focused on the influence of different inlet geometries and secondary flow due to applied heat fluxes, the influence of a uniform surface roughness has not yet been investigated.

1.2 PROBLEM STATEMENT

As indicated above, previous work has been done on flow in the transitional flow regime, but these studies focused primarily on the influence of inlet geometries and secondary flow due to the heat flux applied. The influence of surface roughness in the transitional flow regime has not yet been investigated.

1.3 AIM

The purpose of this study was to investigate the influence of surface roughness at different heat fluxes.

1.4 OBJECTIVES

The main objectives of this study will be:

- To obtain the heat transfer and friction factor data for Reynolds numbers between 1 000 and 7 000 for water flowing through a smooth and roughened tube of the same diameter.
- To determine the boundaries of the transitional region for flow through a roughened tube.
- To investigate the influence of surface roughness in the transitional flow regime.

These objectives will be obtained by capturing the required information by means of an experimental system.

1.5 SCOPE OF WORK

In chapter 2, a literature study is presented which was compiled on the basis of the work done by Professor Meyer from the University of Pretoria and by Professor Ghajar from Oklahoma State University, respectively, on flow in the transitional flow regime.

In chapter 3 details are given of the experimental set-up. An experimental set-up was designed and built to measure the heat flux, mass flow rate, pressure and temperature of flow through a smooth and roughened horizontal tube. Two copper tubes with an outer diameter of 15.88 mm and a length of 1.8 m were used. The one tube was smooth on the inside, whereas the other tube was roughened in order to obtain a relative roughness of 0.058. The Reynolds numbers ranged between 1 000 and 7 000 for the smooth tube, and between 500 and 7 000 for the roughened tube, in order to ensure that the entire transitional flow regime, as well as part of the laminar and turbulent flow regimes, was covered. Three different heat fluxes (8.66, 11.14 and 13.92 kW/m²) were applied to the tubes by using T-type thermocouple wire. The Colburn j-factors, and Nusselt numbers as a function of heat flux and Reynolds numbers were determined from the experimental heat transfer data. The pressure drop measurements were used to determine the adiabatic and diabatic friction factors. The data reduction and experimental validation are also covered in this chapter

Chapter 4 contains the experimental results and Chapter 5 contains the conclusion as well as recommendations for further work.

2. LITERATURE STUDY

2.1 INTRODUCTION

The transitional flow regime is where the fluid motion changes from laminar to turbulent flow. Little design information is currently available about the heat transfer and pressure drop in the transitional flow regime. Heat exchanger designers are therefore advised to remain outside this region, mainly due to the flow instability and uncertainty in this region.

Up to now, there have been mainly two groups of people who have investigated flow in the transitional flow regime. Professor A. J. Ghajar from Oklahoma State University and Professor J.P. Meyer from the University of Pretoria have both investigated smooth tubes in the transitional flow regime under diabatic and adiabatic conditions, while Meyer has investigated the influence of enhanced tubes as well. Their work will briefly be discussed in this chapter; a few fundamental concepts are, however, first revised.

2.2 REYNOLDS AND GRASHOF NUMBERS

Reynolds showed, as early as 1883, that the critical value at which transition occurs, is dependent on the surrounding disturbances. Thus, for tubes, this value is a function of the tube diameter, fluid velocity and viscosity. This is also known as the Reynolds number, which is a dimensionless number of the ratio of the inertial forces to viscous forces. It also characterizes flow regimes, for example, laminar flow in a tube occurs at lower Reynolds numbers, usually below 2 300, while turbulent flow occurs at Reynolds numbers larger than 4 000. The transitional flow regime is where the fluid motion changes from laminar to turbulent flow. For a round pipe with water flowing through it, the Reynolds numbers in this region will be between 2 300 and 10 000 (Cengel, 2006, p. 365).

For pipe-flow, the Reynolds number can be calculated using the following formula:

$$Re = \frac{\rho v D}{\mu} \quad (2.1)$$

While the flow regime in forced convection is governed by the Reynolds number, the flow regime in natural convection is governed by the Grashof number. This is a dimensionless number which represents the ratio of the buoyancy force to the viscous force acting on a fluid. Furthermore, it provides the main criterion to determine whether a fluid is laminar or turbulent in natural convection (Cengel, 2006, pp. 509-510).

$$Gr_L = \frac{g\beta(T_s - T_\infty)L_C^3}{\nu^2} \quad (2.2)$$

2.3 REYNOLDS ANALOGY

The Reynolds Analogy describes the relationship between pressure drop and heat transfer and enables us to determine the friction, heat transfer or mass transfer coefficients when only one of them is known. This analogy is restricted to cases where $Pr = 1$.

The equations can therefore be written as:

$$\frac{f}{2} = \frac{Nu}{Re Pr} \quad (2.3)$$

The Nusselt number is a dimensionless heat transfer coefficient and is named after William Nusselt. It describes the enhancement of heat transfer in a fluid layer as a result of convection relative to this layer. Hence, pure conduction heat transfer is represented by a Nusselt number of 1 (Cengel, 2006). The Nusselt number is defined as:

$$Nu = \frac{hD}{k} \quad (2.4)$$

The Prandtl number is a dimensionless parameter that describes the relative thickness of the velocity and thermal boundary layers and is named after Ludwig Prandtl. The Stanton number is also dimensionless parameters and can be described as follows (Cengel, 2006, pp. 365,812):

$$Pr = \frac{v}{\alpha} = \frac{\mu C_p}{k} \quad (2.5)$$

$$St = \frac{h_{conv}}{\rho V C_p} = Nu \frac{1}{Re Pr} \quad (2.6)$$

Due to the restrictions of the Reynolds Analogy, it has been modified to cover a range of Prandtl numbers between 0.6 and 60. This new analogy, known as the Modified Reynolds Analogy or Chilton-Colburn Analogy, can be expressed as:

$$C_{f,x} \frac{Re_L}{2} = Nu_x Pr^{-1/3} \quad (2.7)$$

$$\frac{C_{f,x}}{2} = \frac{h_x}{\rho c_p V} Pr^{2/3} = j \quad (2.8)$$

The Prandtl and Stanton numbers can also be used to determine the Colburn j-factor, which is defined as follows:

$$j = St Pr^{0.6} \quad (2.9)$$

Meyer and Olivier further modified the Reynolds Analogy to be valid for all flow regimes, although it is restricted to water flowing through a smooth tube (Meyer & Olivier, 2010, p. 493). It can be expressed as:

$$St Pr^{2/3} = f Pr^{-2/3} \quad (2.10)$$

2.4 DIFFERENT INLET GEOMETRIES

The heat transfer coefficient along the tube and thus the transition from laminar to turbulent flow is affected by the type of inlet geometry. There are typically four different types of inlets that are used in the experiments and are shown in Figure 2.1.

1. Square-edged
This type of inlet is characterized by a sudden contraction of flow and simulates the header of a shell-and-tube heat exchanger.
2. Re-entrant
This entrant contains a square-edged inlet with a tube inside and simulates a floating header in a shell-and-tube heat exchanger.
3. Bellmouth
This inlet contains a smooth and gradual contraction and aims to reduce fouling, although it is not commonly used in heat exchangers.
4. Hydro-dynamically fully-developed inlet
The diameter of this inlet section is the same as the pipe diameter of the test section. This inlet is used to obtain a fully-developed velocity profile, since the velocity profile of the other three inlets is always developing.

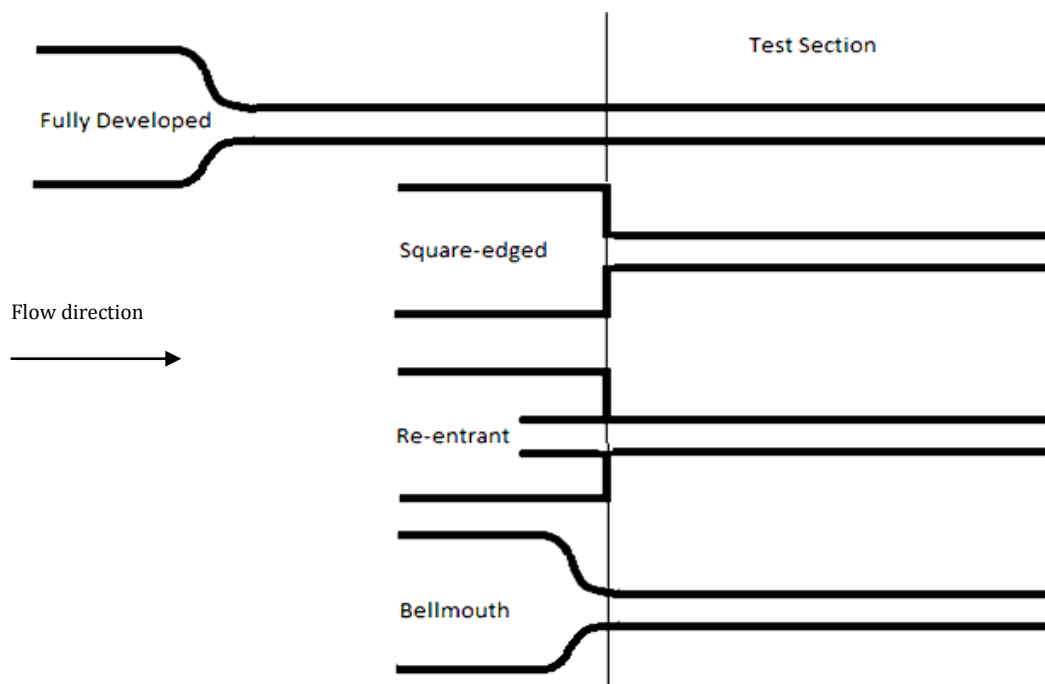


FIGURE 2.1: DIFFERENT INLET GEOMETRIES

2.5 UNIFORM HEAT FLUX BOUNDARY CONDITION

A uniform heat flux boundary condition means that the peripheral and radial conduction of heat in the tube wall is included. Therefore, the bulk fluid temperature will increase from the inlet to the outlet. The temperature of the fluid near the wall will be higher than the fluid temperature near the centerline, thus the density will be lower as well. The temperature difference causes a secondary flow due to convection. This leads to a decreasing kinematic viscosity with an increasing x/D which leads to an increase in Reynolds number along the tube. Secondary flow is usually produced when the fluid in horizontal tubes is heated. The fluid near the tube wall has a higher temperature and lower density and circulates upward, while the fluid in the centre with a lower temperature and higher density circulates downward, as shown in Figure 2.2. The uniform heat flux boundary condition cause a stronger influence of gravity (buoyancy effects) on forced convection and the response is also greater for horizontal than for vertical flow.

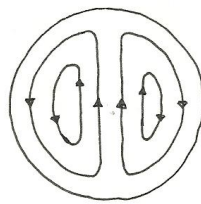


FIGURE 2.2: SECONDARY FLOW

2.6 TRANSITIONAL FLOW IN SMOOTH TUBES: WORK DONE BY GHAJAR

2.6.1 DIABATIC INVESTIGATION

2.6.1.1 FLUID PROPERTIES

In a constant heat flux study done by Ghajar and Tam (1994), the heat transfer results showed that transition varied from inlet (3 diameters from inlet) to outlet (192 diameters from inlet) of the tube. The Reynolds number limits for transitional flow for these regions were:

- Re-entrant: inlet = 2 000 – 6 700 outlet = 2 100 – 8 500
- Square-edged: inlet = 2 400 – 7 300 outlet = 2 500 – 8 800
- Bell-mouth: inlet = 3 400 – 9 400 outlet = 3 800 – 10 500

This variation was explained from the variation in fluid properties. As a constant heat flux was applied, the fluid was under a uniform heat flux boundary condition and heated along the axial length. This caused the viscosity to decrease and the Reynolds number to increase.

In most pipe flow friction analyses it is assumed that the fluid properties are constant throughout the flow field. This is an idealization since the transport properties of most fluids vary with temperature (Ghajar & Tam, 1997, p. 52). There are two methods to correct the constant property correlations, namely the reference-temperature method and the property-ratio method.

A characteristic temperature is chosen at which the non-dimensionalised properties (C_f , Re , Pr , etc) are evaluated using the reference-temperature method. The constant property results at that temperature can then be used to predict the variable-property behaviour.

The property-ratio method is often used in literature and the properties are evaluated at the bulk temperature. The variable-property effects are then used as a function of the ratio of one property evaluated at the bulk temperature to that temperature evaluated at the wall temperature. The variation in viscosity is responsible for most property effects in liquids. Thus, the property-ratio method for liquids is correlated by:

$$C_{vp} = C_{cp} \left(\frac{\mu_b}{\mu_w} \right)^m \quad (2.11)$$

2.6.1.2 INFLUENCE OF INLET GEOMETRY ON PRESSURE DROP MEASUREMENTS, FRICTION FACTORS AND HEAT TRANSFER

Ghajar and Tam (1994, pp. 79-89) did a study to provide a heat transfer database across all flow regimes in the entrance and fully developed regions for different inlet configurations. This data base can be used to assist heat exchanger designers in predicting the heat transfer coefficient along a circular horizontal tube. Ghajar further plotted graphs to show the effect of secondary flow on the heat transfer coefficient. This illustrated that secondary flow will dominate after a certain length-to-diameter ratio. The geometry of the inlet also influences the development of the heat transfer coefficient along the pipe. The influence of the inlet geometry at the beginning and end of transition was shown when the average heat transfer coefficients in terms of the Colburn j-factor were plotted against the bulk Reynolds number. Based on these experimental results, the limits for the Reynolds number range are

- Re-entrant $2\,000 < Re < 8\,500$
- Square-edged $2\,400 < Re < 8\,800$
- Bell-mouth $3\,800 < Re < 10\,500$

It is therefore clear that the heat transfer coefficient as well as the beginning and end of transition, is influenced by the inlet geometry. Secondary flow increased along the pipe, which caused the kinematic viscosity to decrease. Thus, the local bulk Reynolds number (beginning and end of transition) also increased.

In another study, a uniform heat flux boundary condition is applied by attaching welding cables to the copper plates at the pressure drop test section. Three different heat fluxes (3, 8 and 16 kW/m²) were used in this investigation and the results obtained were as follows (Ghajar & Tam, 1997, pp. 52-64):

TABLE 2.1: TRANSITION REYNOLDS NUMBERS FOR DIFFERENT HEAT FLUXES

Heat flux [kW/m ²]	Re-entrant	Square-edged	Bell-mouth
0	$2\,870 < Re < 3\,500$	$3\,100 < Re < 3\,700$	$5\,100 < Re < 6\,100$
3	$3\,060 < Re < 3\,890$	$3\,500 < Re < 4\,180$	$5\,930 < Re < 8\,730$
8	$3\,350 < Re < 4\,960$	$3\,860 < Re < 5\,200$	$6\,480 < Re < 9\,110$
16	$4\,090 < Re < 5\,940$	$4\,450 < Re < 6\,430$	$7\,320 < Re < 9\,560$

The results prove that heating has a significant influence on the transition region. The increase in the friction factor causes an increase in the lower and upper limits of the transition region, compared to adiabatic flow (0 kW/m²). Ghajar also plotted the friction factor against Reynolds number and the results showed that, while the influence of the heating was significant in the laminar and transition regions, it had almost no effect on the friction factors in the turbulent region. This is due to the secondary flow, since the velocity profile of the fluid changes due to mixed convection, therefore the shear stress, fluid density as well as the friction factor, is also changed. As the heat flux increases, the shear stress increases due to the change of velocity profile and so the friction factor also increases. It can also be seen that the Reynolds numbers at the beginning and end of the transition region increase with an increase in the heat flux applied. The heating therefore delays the flow transition, or stabilizes the flow, thus causing it to go into transition at higher Reynolds numbers.

The effect of the inlet geometry is identical when compared to the isothermal conditions. Early transition occurred at the inlet that caused the most disturbances, while transition was delayed at the inlet that caused the least disturbance.

2.6.1.3 FORCED AND MIXED CONVECTION

Natural and forced convection depend on how the fluid motion is initiated. In natural convection, the fluid motion is caused by natural means, for example the buoyancy effect. When heat is applied to the tube, the temperature difference produces a secondary flow due to the buoyancy effects, thus the fluid near the pipe wall circulates upwards due to the higher temperature, while the lower temperature fluid near the central region circulates downward. These counter rotating vortices can increase the heat transfer significantly. Natural convection is mainly dependant on the Prandtl and Grashof numbers, which accounts for the density variation in the fluid. In forced convection, the fluid motion is caused by external means such as a pump or fan. The buoyancy forces are also present in any forced convection flow and it is important to know when it can be neglected, since it influences the forced convection heat transfer in horizontal pipes in ways that depend on the Reynolds, Prandtl and Grashof numbers, as well as the inlet geometry, wall boundary conditions and length-to-diameter ratio. The influence is also stronger when a uniform heat flux boundary condition is applied, compared to a uniform wall temperature, especially in the laminar and lower-transition regions. The response is also greater for horizontal flow, compared to vertical flow.

The convection heat transfer coefficient is a strong function of velocity, thus it will be significantly higher in forced convection compared to natural convection. Accordingly, natural convection is often neglected in forced convection heat transfer analyses. However, the error involved in this assumption can be high, thus a parameter, Gr/Re^2 , was introduced in order to determine the importance of natural convection in forced convection analyses. It can be summarized as follows (Cengel, 2006, p. 531):

- $\frac{Gr}{Re^2} < 0.1$ Forced Convection negligible
- $0.1 < \frac{Gr}{Re^2} < 10$ Mixed Convection
- $\frac{Gr}{Re^2} > 10$ Natural Convection negligible

Mixed convection is when both natural and forced convection are significant in the heat transfer analysis. It is not only dependant on the Reynolds and Prandtl numbers, but also on the Grashof number in order to account for the density variation of the test fluid. The presence of natural convection along with forced convection leads to higher Nusselt numbers in laminar flow.

The local heat transfer data obtained from the experiments can also be used to determine the boundary between forced and mixed convection (Ghajar & Tam, 1994, pp. 83-84). For forced convection, the ratio of the local peripheral heat transfer coefficient at the top and bottom of the tube is close to unity (0.8 – 1.0), while it is much less than unity for natural convection.

The inlet geometry has a significant influence on the boundary between forced and mixed convection. Based on the experimental results, the transition region limits for the re-entrant and square-edged inlets are:

- Re-entrant $2\,157 < Re < 8\,475$
- Square-edged $2\,514 < Re < 8\,791$

These transition region limits are dependent on x/D since the physical properties of the fluid vary with temperature. Forced convection dominated at higher Reynolds numbers and the heat transfer ratio varied between 0.9 and 1, while mixed convection dominated at lower Reynolds numbers. For mixed convection, the heat transfer coefficient ratio decreased with an increase in the length-to-diameter ratio, and beyond 125 diameters from the tube entrance, the free convection activity increased, while forced convection was less dominant. The increase in the transition limits is solely due to the variation in the physical properties of the pipe. Due to the increase of the fluid bulk temperature along the pipe, the kinematic viscosity of the fluid decreases and this, in turn, causes an increase in the local bulk Reynolds numbers (Ghajar & Tam, 1995, pp. 287-297).

Mixed convection dominates in the laminar and lower transition flow regions, while natural convection can be assumed to be negligible in turbulent flow. The inlet configuration will therefore have a minor influence on the heat transfer coefficient.

2.6.2 ADIABATIC INVESTIGATION

The following limits for the transition range were obtained from experiments done by Ghajar and Madon on the pressure drop measurements of laminar-transition-turbulent flow (Ghajar & Madon, 1992, p. 132):

- Re-entrant $1\,980 < Re < 2\,600$
- Square-edged $2\,070 < Re < 2\,840$
- Bell-mouth $2\,125 < Re < 3\,200$

The experimental set-up used for this study was designed in such a way that the flow in the test section was fully developed. Thus, the measurements in the entrance region of transitional flow were not considered. The fully developed skin friction coefficient was determined from the measured pressure drop readings. (The skin friction coefficient corresponds to a friction coefficient that accounts for pressure drop arising from shear stresses at the wall only.) The

data obtained indicated the influence of the inlet configuration at the start and end of transition. Once again, the inlet that caused the most disturbances showed an early transition.

Isothermal flow conditions were also investigated by Ghajar and Tam, by ensuring that the inlet and outlet bulk temperatures were equal within 0.4 °C (Ghajar & Tam, 1997). The Reynolds number ranges for these conditions are:

- Re-entrant $2\ 870 < Re < 3\ 500$
- Square-edged $3\ 110 < Re < 3\ 700$
- Bell-mouth $5\ 100 < Re < 6\ 100$

The Reynolds number for the start of transition is taken as the first sudden change in the friction factor. The Reynolds number for the end of transition corresponds to the Reynolds number of the friction factor that first reaches the fully developed turbulent friction factor line. The bulk Reynolds number for this study is significantly larger compared to the previously mentioned study. This may be due to the properties of the test fluid, since different ethylene-glycol-water mixtures were used. However, it can still be concluded that the transition Reynolds number range can be manipulated by using different inlet geometries. By comparing these Reynolds number ranges with the diabatic results obtained from Ghajar when a constant heat flux was applied, it follows that the secondary flow, due to the applied heat, increases the Reynolds number ranges. The Reynolds number ranges for the transition region was higher during diabatic investigations than during adiabatic investigations, thus transition is delayed when heat flux is applied.

2.7 TRANSITIONAL FLOW IN SMOOTH TUBES: WORK DONE BY MEYER

While Ghajar used different ethylene-glycol-water mixtures as the test fluid for all his experiments, water was used as the test fluid in the experiments done by Meyer. A constant wall temperature boundary condition was also used for the heat transfer experiments, while Ghajar mainly used a constant heat flux boundary condition.

2.7.1 DIABATIC INVESTIGATION

Since the viscosity difference between the fluid at the wall and the bulk fluid, as well as the effect of secondary flow, influences the friction factors, it is important to investigate the diabatic friction factors. The results obtained from a heat transfer study done with water as the test fluid, showed that transition is independent of the type of inlet that was used. Transition for all inlet geometries was between Reynolds numbers of 2 100 and 3 000. These results were then confirmed by pressure drop data that was measured independently from the heat transfer data (Meyer & Olivier, 2011). This inlet-independency is due to the buoyancy effect, since the buoyancy-induced secondary flows suppress the growth of the hydrodynamic boundary layer to such a degree that the flow is fully developed. Thus, transition occurs at the fully developed inlet's transition point and the effects of the inlet geometries are dampened by the secondary flow. The secondary flow effects dominate the boundary-layer in such a way that the inlet geometry effects are negligible.

This, however, is not applicable to all fluids and might be limited to water and other low Prandtl number fluids. The results obtained from the studies done by Ghajar showed that transition was inlet-dependant under diabatic conditions. Ghajar used water-glycol mixtures with heat transfer for these studies which caused the different conclusions.

The data further showed an overall increase in the friction factors, compared to their adiabatic experimental results. This is mainly due to the effects of secondary flow. The friction factor is proportional to the wall shear stress, which is proportional to the velocity gradient at the wall. The secondary flow distorts the velocity profile in such a way that the gradient at the wall is much steeper, resulting in higher friction factors.

The following correlations were developed from the experimental data obtained by Olivier and are valid for all inlet geometries:

- Friction Factors

$$StPr^{\frac{2}{3}} = fPr^{\frac{2}{3}} \quad (2.12)$$

By expanding the Stanton number using equation 2.6, the following correlation for the friction factor is obtained:

$$f = \frac{Nu}{Re} Pr^{\frac{1}{3}} \quad (2.13)$$

This correlation accurately predicted the friction factors for all the flow regimes within 1%. Although it is valid for all flow regimes, it is restricted to water in smooth tubes only, because the results differ for high Prandtl number fluids.

- Laminar heat transfer

$$Nu_{lam} = 2.686 \left[Re^{0.105} Pr^{1.133} \left(\frac{D}{L} \right)^{0.483} + 1.082 \left(Gr^{0.362} Pr^{-2.987} \left(\frac{L}{D} \right)^{0.202} \right)^{0.277} \right]^{2.226} \left(\frac{\mu}{\mu_w} \right)^{0.152} \quad (2.14)$$

This correlation predicted the heat transfer data accurately within 7 % and is valid for developing and fully developed flow. Although the form is similar to those developed by previous authors, the GrPr-term contains a negative power in the Prandtl number since fluids with high Prandtl numbers have a higher viscosity and tend to resist secondary flow motion.

Comment: $940 < Re < 2\,522$
 $4.43 < Pr < 5.72$
 $1.5 \times 10^5 < Gr < 4.3 \times 10^5$
 $0.695 < \frac{\mu}{\mu_w} < 0.85$
 $289 < \frac{L}{D} < 373$

- Turbulent heat transfer

$$Nu_{\text{turb}} = 0.032 Re^{0.802} Pr^{0.059} \left(\frac{\mu}{\mu_w} \right)^{0.14} \quad (2.15)$$

This form of this correlation corresponds to the Dittus-Boelter equation and accurately predicted the heat transfer data within 1.5%.

Comment: $3\,000 < Re < 17\,800$
 $3.37 < Pr < 5.06$
 $1.5 \times 10^5 < Gr < 4.3 \times 10^5$
 $0.678 < \frac{\mu}{\mu_w} < 0.788$

- Transitional heat transfer

$$Nu_{\text{trans}} = \left[Nu_{\text{lam}} + e^{(Re-2\,717)/202} + Nu_{\text{turb}}^{0.845} \right]^{0.845} \quad (2.16)$$

This heat transfer correlation is a combination of the laminar and turbulent correlations and accurately predicted the heat transfer data within 1%.

Comment: $2\,000 < Re < 3\,000$
 $4.47 < Pr < 5.3$
 $2.8 \times 10^5 < Gr < 4.1 \times 10^5$
 $0.702 < \frac{\mu}{\mu_w} < 0.797$
 $289 < \frac{L}{D} < 373$

2.7.2 ADIABATIC INVESTIGATION

The friction factors obtained from an adiabatic study (Meyer & Olivier, 2010) showed that the type of inlet geometry has a significant influence on the transition from laminar to turbulent flow. Transition for the bell-mouth inlet only occurred at a Reynolds number of approximately 7 000, which is significantly higher than that for the fully developed inlet tube, thus, as mentioned earlier, transition is delayed for smoother inlets. The effect of hysteresis was also investigated and found negligible since the difference in the data for increasing and decreasing Reynolds numbers was less than 0.7%. Two different tube diameters were used in the experiments and it was concluded that larger tube diameters led to a greater delay for transition.

The following correlation was developed from the experimental data obtained by Olivier and is valid for Reynolds numbers between 500 and 20 000:

$$f = \frac{16}{Re} \left[1 + \left(0.0791 Re^{-0.25} \left[1 + \left(\frac{\left(\frac{16}{2200} \right) \left(\frac{Re}{2200} \right)^2}{0.0791 Re^{-0.25}} \right)^{-12} \right]^{-1/12} \frac{Re}{16} \right)^8 \right]^{1/8} \quad (2.17)$$

The Reynolds numbers range for the transition from laminar to turbulent flow started at approximately 2 100 and ended at approximately 2 900. This data corresponds to the results obtained for the Bell-mouth-inlet by Ghajar and Madon (1992).

2.8 TRANSITIONAL FLOW IN ENHANCED TUBES: WORK DONE BY MEYER

The efficiency of heat exchangers can be increased by increasing the heat transfer surface area. This will also decrease the flow rate in the tubes which leads to lower compressor and pumping power required. For this reason, more heat exchangers will start to operate in the transitional regime.

Garcia et al. (2005) investigated the thermo hydraulic behaviour in laminar, transitional and turbulent flow by investigating helical wire coils fitted inside a round tube. They found that at very low Reynolds numbers in laminar flow, the wires behave similar to a smooth tube, and heat transfer is not improved. At Reynolds numbers between 200 and 1 000, the heat transfer rate is significantly increased since the perturbation caused by the wire hinders the establishment of the recirculation caused by buoyancy forces, so that forced convection heat transfer occurs. At Reynolds numbers between 1 000 and 1 300, the heat transfer is significantly increased as well, but this time due to the fact that the wire inserts promoted transition from laminar to turbulent flow. It was further found that the heat transfer rate can be increased by 200 % while maintaining a constant pumping power in the transitional region. In the turbulent flow regime, the heat transfer is increased up to four times and the pressure drop up to nine times compared to smooth tubes.

The results obtained from previous research performed on transitional flow, and especially the results of Nunner and Koch, were analysed by Obot (Obot, et al., 1990). Nunner inserted different types of circular rings along the length of the tube and investigated the heat transfer. It was found that the roughness height was the main contributing factor that influenced transition.

Meyer (2011, p. 55) investigated the friction factors and Nusselt numbers for enhanced tubes. The outer walls of the enhanced tubes had a diameter of 15.8 mm and the inner-walls 14.6 mm. The tubes had fins with a height of 0.395 mm and a fin apex angle of 27° inside. One tube had 25 fins with a helix angle of 18°, while the other tube had 35 fins with a helix angle of 27°.

2.8.1 DIABATIC INVESTIGATION

2.8.1.1 HEAT TRANSFER

The heat transfer coefficients for the enhanced tubes were calculated using the nominal surface area which is based on the nominal diameter. Therefore their performance can easily be compared with the results of the smooth tubes.

An interesting conclusion drawn from the diabatic heat transfer results is that transition for all the tubes and flow types for fully developed and developing flow appeared at approximately the same Reynolds numbers. Thus, for smooth tubes, transition is independent of the inlet geometry and this was confirmed with the diabatic friction factor results. This was due to the buoyancy-induced secondary flow inside the tubes, since water, which has a low Prandtl number was used as the test fluid. These flow patterns usually occur in the transitional region of low Prandtl number fluids. It also appeared that the roughness has little or no effect on the transition region during heat transfer.

The heat transfer results further showed that the fins contribute negatively to the heat transfer process in the laminar regime since they act as a barrier for secondary flow, thus preventing the bulk fluid and the fluid at the tube wall from mixing with one another. The flow between the fins is cooler than in the rest of the tube, therefore their viscosity is higher and this leads to a higher shear stress. As a result, the fins have almost no effect on the spinning of the fluid at low velocities.

The turbulent results, however, showed a significant increase in the heat transfer, although the inlet geometry still had no influence on the turbulent regime. Between Reynolds numbers of 3 000 and 8 000, the results differ from those of the smooth tubes, since the j-factors increase with Reynolds number. This is due to the fins that break the laminar viscous sub-layer, which accounts for up to 60 % of the fluid's temperature drop during turbulent flow. The helix angle of the fins caused a further increase, since fins with a greater helix angle spin the fluid more effectively.

A performance evaluation for these enhanced tubes was also performed and it was found that the enhanced tubes became viable when the smooth tube Reynolds numbers exceeded 6 000 and peaked at Reynolds numbers of approximately 10 000. Thus, there was no performance enhancement in the transition region.

2.8.1.2 FRICTION FACTORS

The friction factor and heat transfer data showed similar trends, with the result that higher friction factors were obtained when compared to the data of smooth tubes.

In the laminar and turbulent regions, the friction factors were higher compared to the smooth tubes. This is due to the fins that enhance the amount of mixing by spinning the fluid. A secondary transition was observed in the turbulent results between Reynolds numbers of 3 000 and 10 000. The secondary transition was developed when the velocity of the fluid was high enough for the helical fins to effectively spin it. The intensity of the spinning increased with an increase in velocity, but stopped at a Reynolds number of approximately 10 000, from where the friction factor started to decrease. The friction factors of this secondary transition region, as well as the fully turbulent region were dependant on the helix angle, thus higher friction factors were obtained for greater helix angles.

The friction factors in the transition region are independent of the Reynolds numbers and the transition occurred between the same Reynolds numbers of 2 000 and 3 000, similar to those of the smooth tubes. The critical Reynolds numbers were also found to be independent of the tube or inlet geometry. This was also found in the heat transfer results, thus it can be concluded that the results are independent of the measuring techniques.

2.8.2 ADIABATIC INVESTIGATION

There are three main conclusions that can be drawn from a comparison between the experimental results of the smooth and enhanced tubes, namely:

1. There was an upward shift in the friction factors of the enhanced tubes.
This is due to the increase in surface roughness which increases the resistance to flow.
2. Transition occurred earlier compared to smooth tubes.
This is caused by the increased surface roughness.
3. There is a smooth second increase in the friction factors at Reynolds numbers between 3 000 and 10 000, which appears to be a secondary transition.
From the experimental results it follows that the effectiveness of the fins increases with an increase in Reynolds numbers, thus with an increasing velocity. This secondary transition may be caused by the effective rotation the fins bring about the fluid, since the secondary transition did not occur in the results of studies using ring insert or dimpled tubes.

The results showed that the fins were ineffective at lower Reynolds numbers and that they become effective at rotating the fluid only as the velocity is increased. It was also concluded that the developing boundary layer leads to an increase in the friction factors for fully developed flow. In contrast, for developing flow, the tube roughness has a greater influence than the effect of the boundary layer on the wall shear stress. The end of transition appeared to be affected by the helix angle, since transition for the 27° helix angle occurred earlier than the 18° helix angle. It can subsequently be concluded that the roughness and angle of the fins has an influence on the stability of the boundary layer.

When Meyer further compared a 19.1 mm tube with a 15.8 mm tube, the fully developed flow results showed that transition was only influenced by the roughness height. Three 15.8 mm enhanced tubes with a fin-height-to-diameter ratio of 0.027 showed that transition occurred at a Reynolds number of approximately 1 870. The fourth tube had a diameter of 19.1 mm and the fin-height-to-diameter ratio of 0.022 showed that transition only occurred at a Reynolds number of 2 070. Since the same inlet geometry was used, it can be concluded that the only geometrical aspect that influences transition is the fin-height-to-diameter ratio.

The laminar and turbulent friction factors were significantly higher than those of the smooth tubes, but were also independent of the inlet geometry. The second transitional region which occurred at Reynolds numbers between 3 000 and 10 000 was very stable and predictable, compared to the first transitional region (Meyer & Olivier, 2010, p. 7).

2.9 SURFACE ROUGHNESS

Up to now, there have been no studies done on the influence of surface roughness in tubes on heat transfer in the transitional flow regime. Smooth tubes were mostly considered, except for Meyer and Olivier who investigated enhanced tubes as well. Dimpled tubes and tubes with spiral inserts along the length of the tube have been investigated by Garcia *et al.*, but no studies have yet been done on tubes with a uniform surface roughness. The influence of surface roughness in the transitional regime will therefore be investigated in this research report.

2.10 CONCLUSION

It is evident from the above results of the experiments done by Ghajar, Meyer and co-workers that the geometry of the inlet influences the establishment of secondary flow, the beginning and end of the heat transition region, as well as the development of the heat transfer coefficient along the pipe. This effect however, is negligible when the test fluid is water or low Prandtl number fluids, as was found in the studies done by Meyer.

The transition Reynolds number range is also influenced when heat flux is applied. The laminar and transitional friction factors were increased by heating and this caused an increase of the bulk Reynolds number, compared to the isothermal conditions. Heating delays the flow transition or stabilizes the flow, thus causing it to go into transition at higher Reynolds numbers.

Enhanced tubes were also investigated by Meyer and it was found that transition is independent of the inlet geometry under diabatic and adiabatic conditions. The adiabatic heat transfer and friction factors in the turbulent flow regime were higher compared to the smooth tubes. In contrast, the laminar heat transfer coefficients were lower due to the fins that obstruct the secondary flow and increase the mixing of the fluid. The helix angle had a negligible effect in the laminar and transition regions and it is concluded that the fin-height-to-diameter ratio is the only geometrical aspect that influences transition. However, a secondary transition occurred between Reynolds numbers of 3 000 and 10 000 and was characterized by an increasing friction factor with the Reynolds number. This is due to the fins that rotate the fluid, thus, the friction factors increased with an increase in helix angle. The diabatic friction factors followed a trend similar to that of the adiabatic friction factors.

The influence of surface roughness in the transitional flow regime will be further investigated as no previous research has been done on tubes with a uniform surface roughness.

3. EXPERIMENTAL SET-UP

3.1 INTRODUCTION

The experimental set-up is discussed in this chapter. It gives an overview of the design calculations that have been done to obtain the maximum and minimum operating conditions of the system, the components of the system, the test section, as well as the instruments used. The experimental procedure, data reduction and validation of the experimental set-up are also included in this chapter.

3.2 DESIGN CALCULATIONS

The laminar and turbulent conditions were investigated since these will yield the maximum and minimum conditions which the experimental set-up must be able to accommodate. The maximum and minimum Reynolds numbers were chosen as 1 000 and 7 000 and the fluid properties were evaluated at the inlet temperature of the water, which was 20°C. The length of the test section was 1.8 m and the tube diameter relative roughness was initially chosen as 15.88 mm and 0.05, respectively, for the calculations.

The inlet velocity was determined by using equation 2.1 and the mass flow rate was determined from the following equation:

$$\dot{m} = \rho AV \quad (3.1)$$

3.2.1 DIABATIC CONDITIONS

The Moody Chart shows that the friction factor for laminar flow is not affected by the relative surface roughness. Thus, the following Poiseuille equation was used to determine the laminar friction factor of the smooth and roughened tubes:

$$f_{lam} = \frac{64}{Re} \quad (3.2)$$

The turbulent friction factor, however, is dependent on the relative surface roughness; therefore the First Petukhov Equation was used to determine the turbulent friction factor for the smooth tube.

$$f_{turb} = (0.79 \ln Re - 1.64)^{-2} \quad (3.3)$$

The turbulent friction factor for the roughened tube was determined from the Modified Colebrook equation:

$$\frac{1}{\sqrt{f}} = -1.8 \log \left[\frac{6.9}{Re} + \left(\frac{\varepsilon}{3.7D} \right)^{1.11} \right] \quad (3.4)$$

The pressure drop for the smooth and rough tubes (both flow regimes) was calculated as follows:

$$\Delta P = \frac{fL\rho V^2}{2D} \quad (3.5)$$

A constant heat flux has been applied to the tubes by means of T-thermocouples with the following properties (Omega, 2012):

- Resistivity: 50 $\mu\Omega/m$
- Thermal conductivity: 19.5 W/mK
- Maximum operating temperature: 150 °C
- Melting temperature 1225-1300 °C
- Overall wire diameter: 0.001 m
- Constantan diameter 0.00025 m

The power supply used for the experiments could supply a maximum power of 1.5 kW and 360V.

The number of turns of the thermocouple wire along the tube and the length of the thermocouple wire were determined as follows:

$$N = \frac{L}{D_w} \quad (3.6)$$

$$L_w = \pi D_o N \quad (3.7)$$

In order to decrease the resistance of the wire, three thermocouple wires were placed in parallel. Thus, each wire was a third of the initial length calculated above.

The resistance of the wire was determined using the following equation:

$$R = \rho_r \frac{L}{A} \quad (3.8)$$

$$R_{\text{parallel}} = \left(\frac{3}{R} \right)^{-1} \quad (3.9)$$

Since a maximum of 360 V could be supplied by the power source, the power supplied and the current through the wire were then determined from:

$$Q = \frac{V^2}{R} \quad (3.10)$$

$$I = \frac{V}{R} \quad (3.11)$$

The power and current were calculated as 1 275 W and 3.542 A. Finally the temperature difference between the inlet and outlet was determined, using the flowing equation:

$$\Delta T = \frac{\dot{Q}}{\dot{m}c_p} \quad (3.12)$$

The temperature difference was calculated as 24.4 °C for laminar flow and 3.487 °C for turbulent flow. Thus, the average temperature difference across the tubes was calculated to be 13.94 °C. These conditions were acceptable since the temperature difference was large enough to obtain accurate measurements from the thermocouples. Temperature differences less than 1 °C are difficult to measure and could lead to inaccurate results.

The heat flux supplied to the copper tubes was obtained by dividing the heat applied by the surface area as follows:

$$\dot{q} = \frac{\dot{Q}}{A} \quad (3.13)$$

Since the experiments had to be conducted at different heat fluxes, three different heat fluxes corresponding to three different power inputs which lead to reasonable temperature differences were investigated using the above method. The results are tabulated in Table 3.1. The maximum conditions appear in the first column, while the remaining three columns show the results at the desired heat fluxes.

TABLE 3.1: TEMPERATURE DIFFERENCES AT DIFFERENT HEAT FLUXES

Q [W]	1275		1250		1000		750	
q [kW/m ²]	14.20		13.92		11.14		8.35	
	Laminar Re = 1 000	Turbulent Re = 7 000	Laminar Re = 1 000	Turbulent Re = 7 000	Laminar Re = 1 000	Turbulent Re = 7 000	Laminar Re = 1 000	Turbulent Re = 7 000
V [V]	360	360	356.427	356.427	318.798	318.798	276.087	276.087
I [A]	3.542	3.542	3.507	3.507	3.137	3.137	2.717	2.717
ΔT	24.4	3.478	23.92	3.418	19.134	2.735	14.351	2.051
ΔT avg	13.94		13.67		10.93		8.201	

3.2.2 MINOR PIPE LOSSES

In addition to the friction loss, there are also additional minor losses due to:

- Pipe entrances or exits
- Sudden expansion and contraction
- Bends, elbows, tees and other fittings
- Open or partially closed valves
- Gradual expansions or contractions

The loss coefficients were obtained from tables and afterwards the system head loss was computed using the following equation (White, 2009, p. 383):

$$\Delta h_{tot} = \frac{v^2}{2g} \left(\frac{fL}{D} + \Sigma K \right) \quad (3.14)$$

The pressure losses in the pipes and fittings were determined by (Cengel, 2006, p. 465):

$$\Delta P_L = \Delta h_{tot} \rho g \quad (3.15)$$

For laminar flow the head loss and pressure drop were calculated as 0.0181 m and 177.2 Pa, respectively, in the smooth and roughened tubes. These values increased significantly in turbulent flow to 0.55 m and 5.38 kPa in the smooth tube, and 1.02 m and 9.94 kPa in the roughened tube.

3.2.3 OVERALL SYSTEM PRESSURE LOSS

The total pressure loss value of the experimental set-up was determined by adding the pressure loss of the test section to the pressure loss due to the pipes and fittings. This value was compared to the pump capacity in order to verify that the pump is sufficient. If the requirements were not met, other parameters of the test section, for example the length or tube diameter, had to be adjusted.

The maximum pressure loss for this experimental set-up was 10.7 kPa and occurred during turbulent flow in the roughened tube. This was less than the maximum capacity of 500 kPa of the SP3 Cemo pump that had been used.

3.2.4 INSULATION AND HEAT LOSS

Armaflex tubes with a thermal conductivity of 0.034 W/m²K were used as insulation for the copper tubes in order to prevent heat loss to the surroundings. Turbulent flow conditions were used for the calculations, since most heat transfer occurs during turbulent flow.

Free convection occurs on the outside of the insulation to the surroundings, thus the outer heat transfer coefficient was between 2 and 25 W/m²K. The latter (25 W/m²K) was therefore used for the remaining calculations. The inner heat transfer coefficient for turbulent flow was obtained from the following Nusselt number relation:

$$Nu = \frac{hD}{k} = 0.023Re^{0.8}Pr^{0.4} \quad (3.16)$$

The turbulent inner heat transfer coefficient is 2249 W/m²°C and, by using the exit water temperature, the surface temperature can be determined from:

$$T_s = T_e + \frac{q_s}{h} \quad (3.17)$$

The surface temperature at the end of the tube was determined to be 30 °C. The surface temperature of the tube increases linearly, thus the maximum temperature will be at the exit of the tube. The temperature of the thermocouple wire also increased due to the current flowing through it. For a current of approximately 1 A passing through each wire (thus a total of 3 A), the temperature of the thermocouple wire was estimated to be 100 °C.

Since worst case conditions were used for these calculations, the surface temperature of the tube was neglected and the temperature of the wire, which was significantly higher, was used instead.

The thermal resistance through the tube wall was neglected due to the relatively small wall thickness and high thermal conductivity of copper. Two Armaflex insulation tubes with thicknesses of 25.4 mm and 32 mm, respectively, were used; therefore the thickness of the insulation was 57.4 mm and the outer diameter of the copper tubes 15.88 mm. Thus, the total thermal resistance was determined as follows:

$$R_{tot} = R_{insulation} + R_{outer} = \frac{\ln\left(\frac{D_2}{D_1}\right)}{2\pi kL} + \frac{1}{h_o A_o} \quad (3.18)$$

The total thermal resistance was calculated to be 5.256 W/°C and the heat loss to the surroundings was calculated from:

$$\dot{Q} = \frac{T_i - T_o}{R_{tot}} \quad (3.19)$$

The heat loss under the worst case scenario conditions (an inner temperature of 100 °C and outer temperature of 15 °C when 1200 W was supplied to the system) was determined to be 16.17 W. Thus, only 1.3 % of the total heat was lost to the surroundings when 57.4 mm thick insulation was used, which is acceptable.

3.3 EXPERIMENTAL SET-UP

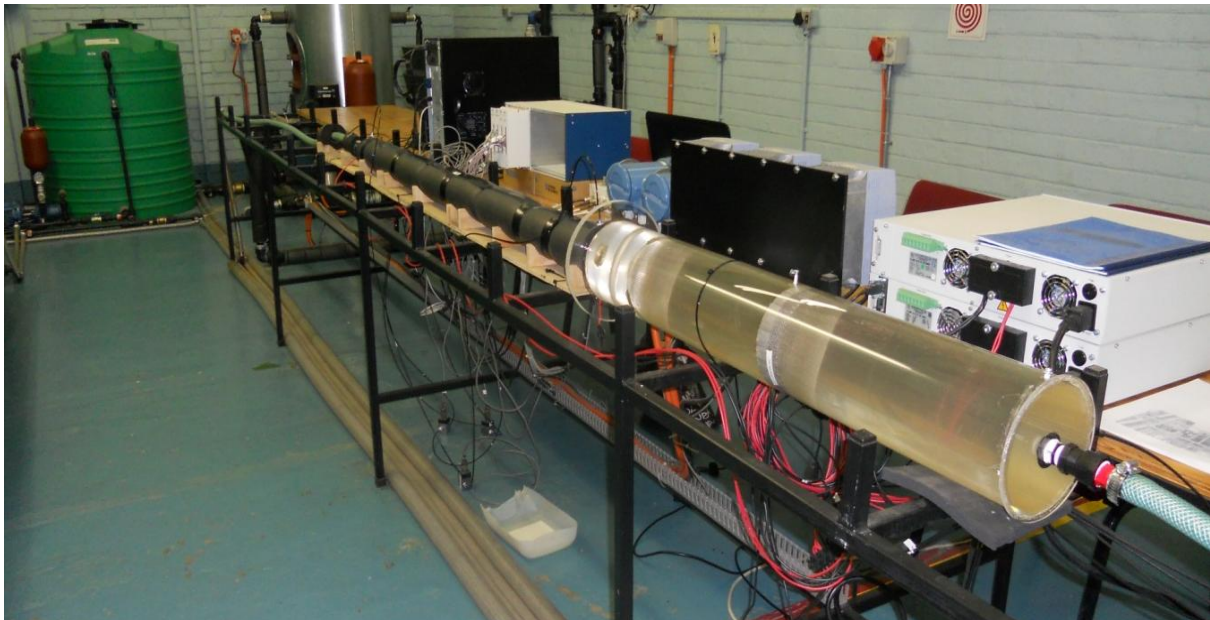


FIGURE 3.1: EXPERIMENTAL SET-UP

The experimental set-up (as shown in Figure 3.1) consisted of a closed water loop which circulated water from the storage tank, through the test section and back. Three different heat fluxes (8.66, 11.49 and 13.67 kW/m²) were applied to the test section by adjusting the applied voltage through the heating wires around the tubes. The test section first contained a smooth

and then a roughened tube, both with an outer diameter of 15.88 mm and a length of 1.8 m, to investigate the influence of surface roughness.

The test fluid was water and the temperature of the 1 000 litre reservoir was maintained at 20 °C. The water was circulated through the system via an electronically controlled positive displacement pump with a maximum flow rate of 2 670 litre/h.

Flow pulsations were introduced into the system due to the positive displacement pumps. A 70 litre accumulator was installed before the flow meters and the test section in order to decrease the pulsations. The accumulator was fitted with a rubber bladder filled with air to dampen the fluctuations. This ensured a constant pressure at the inlet of the test section.



FIGURE 3.2: POSITIVE DISPLACEMENT PUMP AND ACCUMULATOR

A bypass valve was inserted between the accumulator and the flow meters to allow the water to flow back to the tank. The bypass valve was also used to increase the back pressure on the pump, since the pulsations decreased with increasing pump speed. Therefore during experiments, the supply valve was partially closed and the bypass valve partially open, so that the speed of the pump had to be increased in order to supply the correct flow rate of water to the test section, which resulted in reduced pulsations.

Two Coriolis flow meters with different capacities were installed in parallel to measure the mass flow rate. Since the flow meters had different capacities, they were used according to the flow rate requirements. After the flow meters, the fluid flowed through the calming section to the experimental test section and then back into the reservoir.

The flow rates were controlled by the frequency drives that were connected to the positive displacement pumps, therefore the required flow rate was obtained by increasing or decreasing the pump speed. The frequency drives were also connected to a personal computer via the data-acquisition system. A Labview program was used to record the data points and a Matlab program was used to determine the Reynolds numbers, friction factors, Nusselt numbers, and Colburn j-factors.

The basic lay-out of the experimental set-up is shown in Figure 3.3.

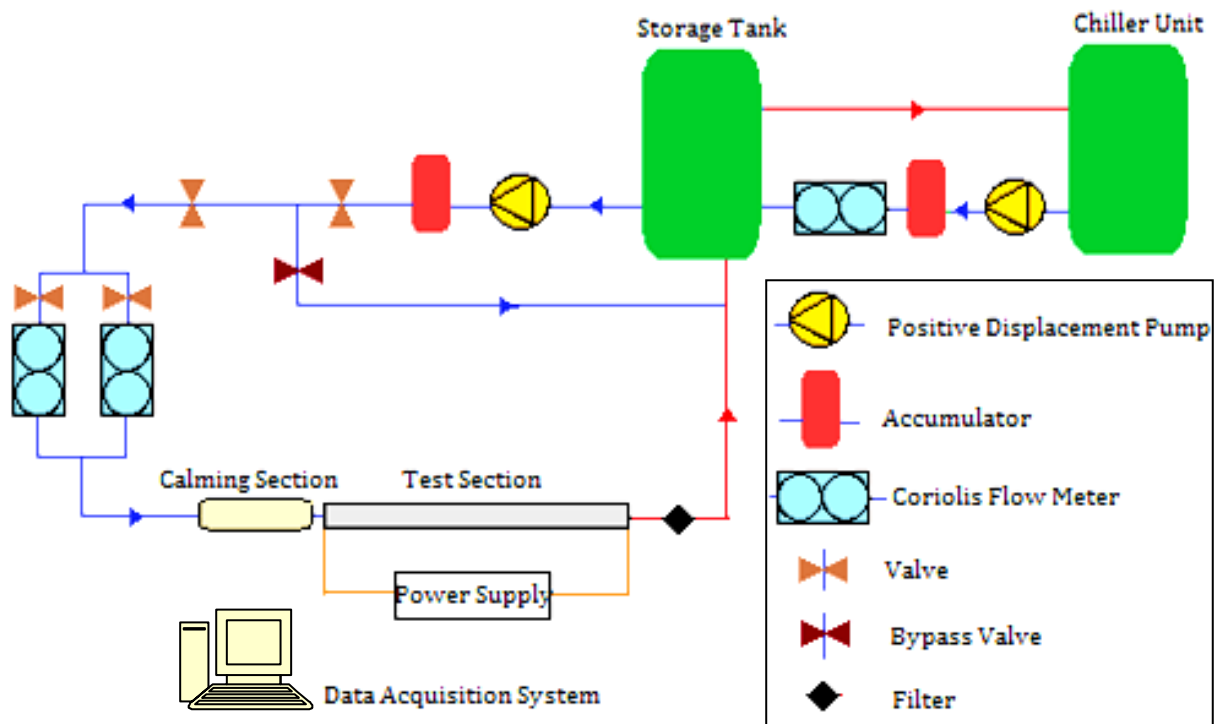


FIGURE 3.3: EXPERIMENTAL SET-UP

3.3.1 TUBE DIAMETERS

Previous experiments conducted by Ghajar and Meyer used hard-drawn copper tubes with outside diameters of 15.88 mm and 19.1 mm. For the present study, tubes with an outside diameter of 15.88 mm have been used, since previous experiments were done with this diameter and the new data can thus be compared with the existing data of Ghajar and Meyer. A theoretical model of the experimental set-up verified that the pump capacity will accommodate this diameter with the required length of the test section.

3.3.2 SURFACE ROUGHNESS

The aim of the experiment was to determine the influence of surface roughness in the transitional flow regime. Thus the experimental results of a smooth and rough tube had to be compared. The Moody Chart was used as a reference to determine whether the relative surface roughness is sufficient, since the relative roughness lines corresponding to the roughened tube should be well above the relative roughness line of a smooth tube between Reynolds numbers of 1 000 and 7 000. From the Moody Chart it was concluded that a relative roughness of 0.001 would be sufficient.

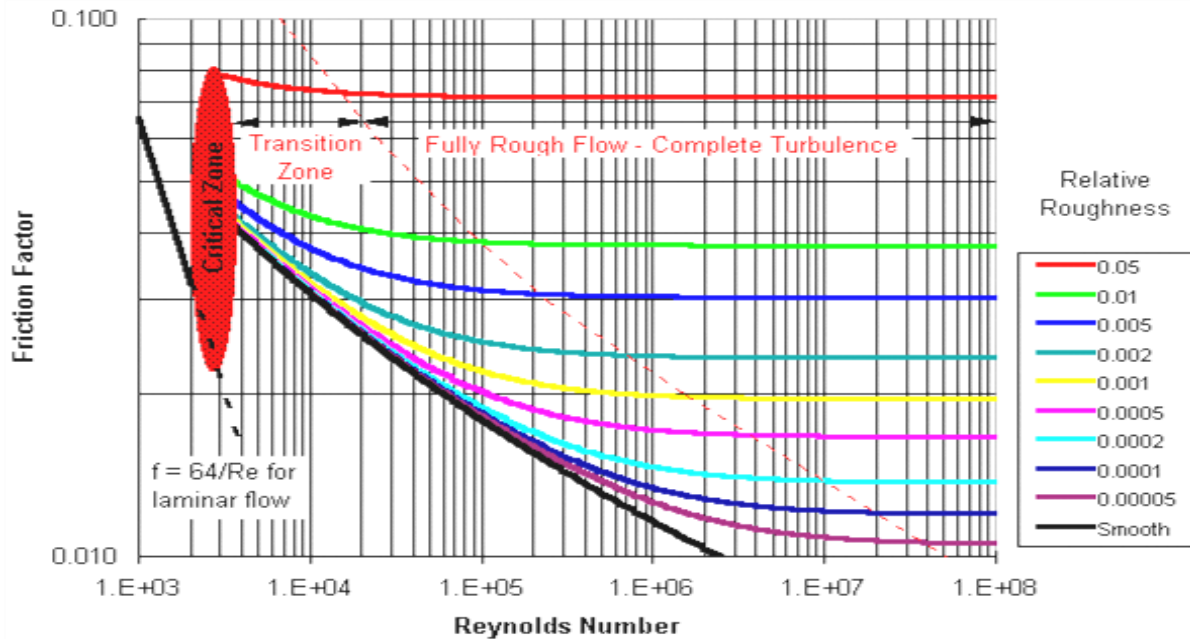


FIGURE 3.4: MOODY CHART (TOPRAK, 2006)

Various attempts were made in order to roughen the tube and the results of the surface roughness tests done by Metlab can be found in Appendix A. The first attempt was carried out by fixing 40-grit sandpaper with double-sided tape to a 10 mm wooden dell. The dell was then forced through the copper tube while turning it in order to obtain a uniform pattern. The surface roughness was determined to be 1.67 μm which corresponded to a relative roughness of 0.00011. From the Moody Chart it was concluded to be insufficient.

A second approach was to use a steel brush. A 31 mm diameter steel brush was trimmed to 14.5 mm and fixed to a steel rod with wire. The rod was forced back and forth through the copper tube while turning it with a vice grip. A surface roughness of 2.091 μm was obtained which was twice as rough as the previous attempt, but still insufficient since it only corresponded to a relative roughness of 0.00015. Figure 3.5 shows a new steel brush that has been slightly trimmed, while the bottom brush has been used to roughen the tube.

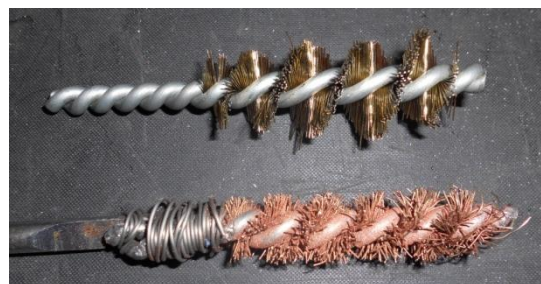


FIGURE 3.5: STEEL BRUSH

A steel wire mesh was also rolled into a tube and then sewn together using one of the mesh wires. The mesh was then placed inside the copper tube and the ends were folded over the tube end to prevent the mesh from moving inside the tube. Although the mesh created a roughness which would have been suitable, this concept was not used since it corresponds to heat transfer enhancement instead of surface roughness. Using a left-hand and right-hand 14 mm tap was also considered, but not used, since it once again corresponded to heat transfer enhancement instead of surface roughness.



FIGURE 3.6: STEEL WIRE MESH

A process similar to knurling was used next. A 14 mm EN24 Steel rod was roughened on a lathe by cutting various random grooves into the rod, until a pattern similar to the desired pattern on the inside of the roughened tube was obtained. The steel rod was then fixed to a 2 m thinner rod by cutting screw thread on the outside of the thin long rod and cutting a threaded hole inside the roughened rod, as shown in Figure 3.7.



FIGURE 3.7: STEEL ROD

The total length of the roughened rod is 10 cm; therefore intervals of 8 cm were marked on the copper tube. Two centimeters were allowed for a safety factor to ensure that the interval which was hammered always had the roughened rod on the inside of the whole interval. Another thin steel rod, with 8 cm intervals marked on it, as well, was inserted from the other side of the copper tube and pressed against the roughened rod. This further ensured that the whole hammered section always contained the roughened rod. A kinetic hammer was used to hammer the copper tube while turning it slowly to ensure that the whole circumference is hammered. After the entire 8 cm interval had been hammered, the roughened rod was pushed forward 8 cm to hammer the next interval. Figure 3.8 further illustrates how the hammered interval was monitored in order to prevent hammering a section that does not contain the rod.



FIGURE 3.8: MEASURING HAMMERED SECTION

Another piece of the same 15.88 mm copper tube that was used for the smooth and roughened tubes was also roughened using the same method. This small tube was then analyzed to determine the surface roughness. Metlab reported that the roughness of the tube could not be measured since the needle got stuck in the grooves of the rough surface and that the tube's surface profile falls outside the capabilities of their roughness tester. The maximum capability

of their equipment is a surface roughness of 16 μm and when dividing this with the inner tube diameter of 14.46 mm, a relative roughness of 0.001 was obtained. This roughness was regarded as sufficient since the corresponding friction factors on the Moody Chart varied between 0.044 and 0.035 for Reynolds numbers between 3 000 and 7 000, which is acceptable.

Unfortunately, during the adiabatic tests on the roughened tube, it was found that the graphs of the Friction Factor against Reynolds number (Figure 3.9) and Pressure against Reynolds number (Figure 3.10) were almost identical to that of the smooth tube. Although there is a slight increase in the friction factor in the transitional region, it is too small to make valid conclusions on the influence of surface roughness. The increase in friction factor in the laminar and turbulent regions, as well as the increase in pressure drop over the whole flow regime, is negligible.

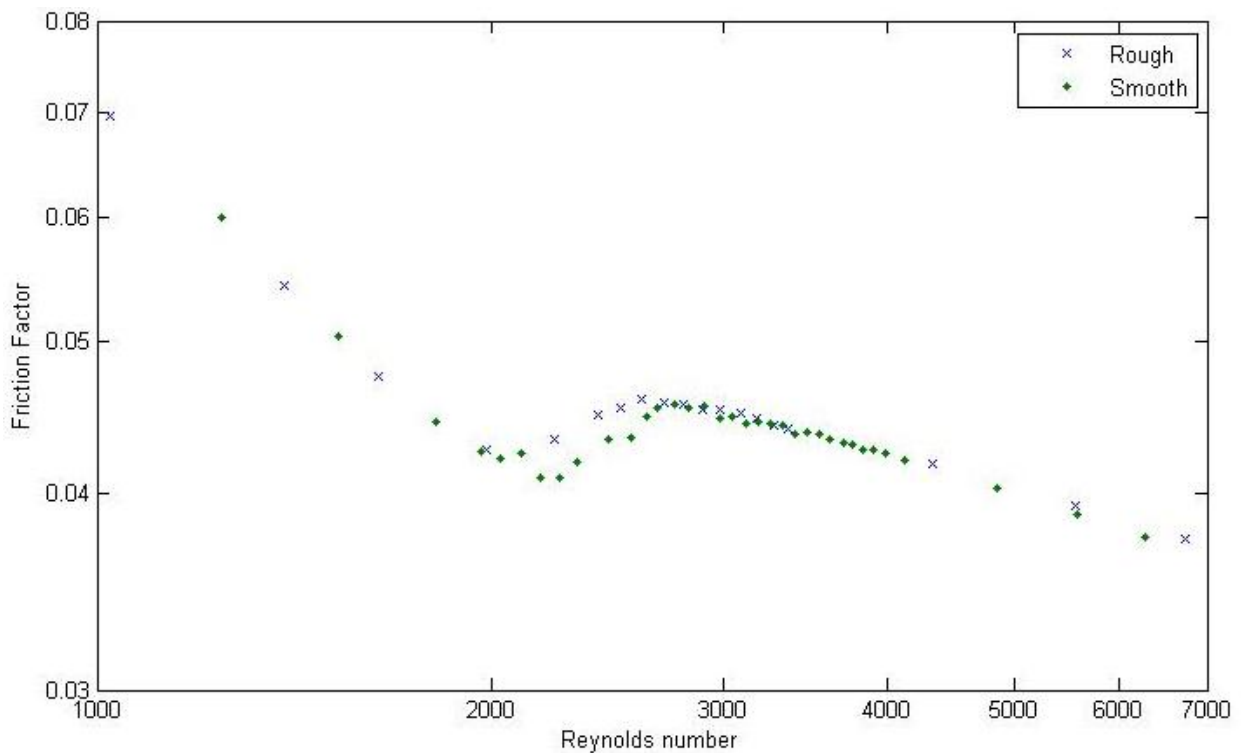


FIGURE 3.9: FRICTIONS FACTOR COMPARISON FOR SMOOTH AND ROUGHENED TUBES

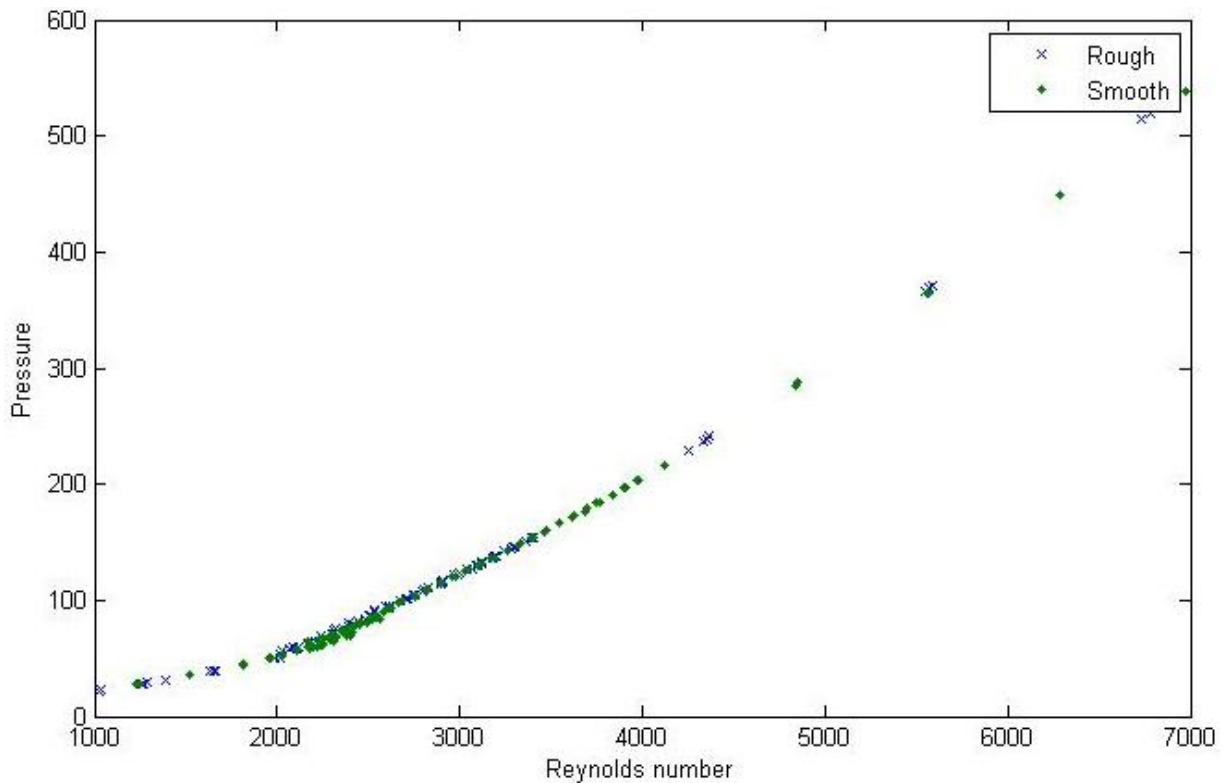


FIGURE 3.10: PRESSURE COMPARISON FOR SMOOTH AND ROUGHENED TUBES

One of Prandtl's students, Nikuradse investigated the influence of relative roughness on the friction factor in the turbulent flow regime by gluing sand grains of a known size onto the inner surface of a tube (Cengel, 2006). Since these experiments were adiabatic, the thermal conductivity of the glue and sand grains was of no importance. For this study, both the heat transfer coefficient and friction factor were investigated, therefore the thermal conductivities of the glue and sand grains should be as high as possible. Unfortunately high thermal conductivity glues need to be imported and due to time constraints, cyanoacrylate (superglue) was used since it bonds instantly when it comes into contact with two surfaces, but flows like water when it is in contact with one surface only. Silica sand was used since the grains are relatively large and of similar size.

The thermal resistance of the glue and silica sand was investigated with a small experiment consisting of a smooth and a roughened tube and an isolated tube in between, as shown in Figure 3.11. Both copper tubes had 3 thermocouples mounted on the top and sides. Water at 60 °C was pumped through the tubes and the temperatures were recorded in order to determine whether there was any significant difference. Since there was no significant difference between the measured temperatures of the two tubes, it was concluded that the influence of the thermal resistance of the sand and the grains was negligible.

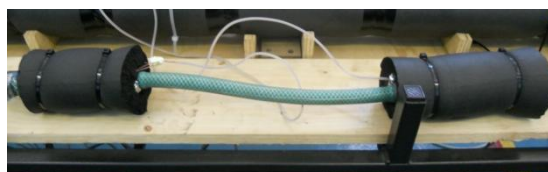


FIGURE 3.11: THERMAL RESISTANCE EXPERIMENT

A filter was also added after the test tubes in this experiment, as well as in the overall test section, to prevent loose sand grains from entering the system. After each test, the filter was checked and since it was clean, it was concluded that the cyanoacrylate and silica sand were able to withstand high temperatures and flow rates.

A Particle Size Distribution test using a Mastersizer 2000E was done in order to determine the average grain size. The result analysis report can be found in Appendix A and since 90 % of the sand grains in the sample had a diameter of 835.737 μm , it was concluded that the average grain size was 0.84 mm. This resulted in a relative roughness of 0.058, which was sufficient for the tube to be considered as a rough tube.



FIGURE 3.12: SAND ROUGHENED TUBE

3.3.3 CALMING SECTION

The set-up contained a calming section to remove any unsteadiness in the flow and ensure a uniform velocity distribution before the fluid entered the test section. An existing calming section shown in Figure 3.13, made by a previous final year student, Mr. Eric Mkhonho, was modified and used (Mkhonho, 2011). It consisted of a 12 cm diameter Perspex tube with two sieves on the inside. The original exit of the calming section was removed and a new Perspex plate with a 15.88 mm fitting was glued to the calming section in order to connect the smooth and roughened tube to it.



FIGURE 3.13: CALMING SECTION

3.3.4 TEST SECTION

Square-edged inlets were used for both tubes. This type of inlet is characterized by a sudden contraction from the calming section diameter to the test tube diameter. Therefore the copper tubes were directly connected to the calming section with a compression fitting, as shown in Figure 3.14. The test sections were manufactured from hard-drawn copper tubes with an inside diameter of 14.46 mm, outside diameter of 15.88 mm and length of 1.8 m. Both tubes were insulated with 54.7 mm thick Armaflex insulation with a thermal conductivity of 0.034 W/mK. The heat loss was estimated to be 1.3 %.

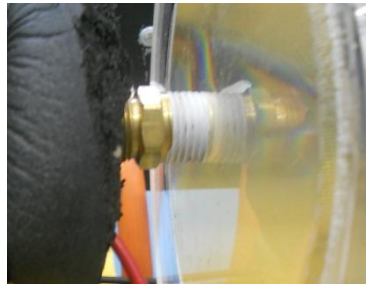


FIGURE 3.14: SQUARE-EDGED INLET

A schematic lay-out of the test section is shown in Figure 3.15.

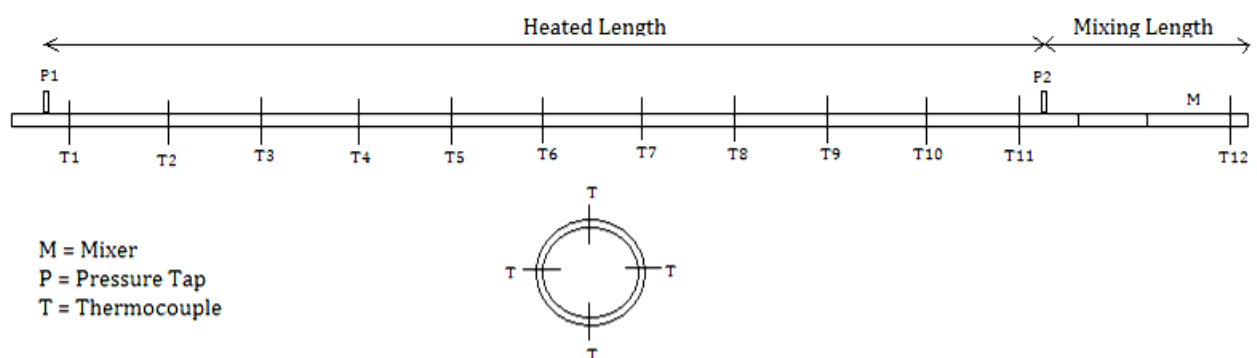


FIGURE 3.15: SCHEMATIC OF TEST SECTION

To obtain a constant heat flux boundary condition, T-type thermocouples with a Constantan wire diameter of 0.25 mm, were wound around both copper tubes in the test section. Three thermocouple wires were wound around the copper tubes in order to decrease the resistance and current flowing through the wire, in comparison to using a single wire.

Thermocouples were also placed along the tubes to measure the temperature at the desired locations. Four thermocouples were fixed 90° apart around the periphery of the tube. There were 11 thermocouple stations spaced 170 mm from each other along the length of the tube and therefore 44 thermocouples were used to measure the wall temperature on each tube. Another thermocouple station at the mixing section consisted of two thermocouples at the top and bottom of the tube. These thermocouples were soldered to the tube by first drilling a 1.5 mm depression into the tube. Flux and solder were then inserted into the depression and heated until melting point. The calibrated thermocouple was then inserted into the depression and the

heat was removed in order for the tube to cool down. The thermocouples were checked to ensure good contact with the tube.



FIGURE 3.16: THERMOCOUPLES ATTACHED TO TUBE

Two pressure taps were installed by silver soldering a 30 mm long capillary tube on each end of the copper tubes. A 1.5 mm hole was then drilled through the capillary tube and the copper tube. This small diameter was chosen to ensure that the taps did not cause flow obstruction in the tubes and that the diameter is less than 10 % of the test tube's inner diameter. All the burrs were removed from the inside of the copper tube, since they could cause a local increase in pressure which would have led to incorrect readings. A bush tap with a "quick release" coupling was inserted over the holes and soldered to the copper tubes, as shown in Figure 3.16. The pressure taps were connected to the differential pressure transducer by using nylon tubing.

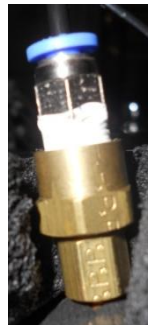


FIGURE 3.17: PRESSURE TAP

A mixer was inserted at the end of the test section. This mixed the water in the pipe to ensure a uniform temperature in the pipe and the temperature measurements were then taken at the end of the mixer tube. It was manufactured from a copper tube with an inside and outside diameter of 20 mm and 22 mm, respectively. Six copper plate fins with a length of 30 mm were soldered together, alternating between horizontal and vertical, as shown in Figure 3.18. The mixers split the thermal layer in half, mixed it, and then split and mixed it again and again to ensure a uniform temperature throughout the cross-section of the tube. Two thermocouples were placed at the end of the mixer to measure the uniform exit temperature.



FIGURE 3.18: MIXER

3.4 DATA REDUCTION

This section discusses the methodology used to obtain the heat transfer coefficients and friction factors for smooth and roughened tubes.

3.4.1 FRICTION FACTOR

The friction factor for one-dimensional flow with a uniform density in smooth tubes of length L and diameter D , can be written in terms of the overall pressure drop, by using equations 3.1 and 3.5:

$$f = \frac{\Delta P \rho D^5 \pi^2}{8 \dot{m}^2 L} \quad (3.20)$$

ΔP was obtained from the differential pressure transducers and the fluid properties are calculated at the bulk fluid temperature, which is the same as the mean temperature defined by equation 3.22. This temperature was also used to determine the Reynolds, Nusselt, Prandtl and other dimensionless groups.

3.4.2 HEAT TRANSFER COEFFICIENT

Heat transfer was achieved by supplying heat to the system by the thermocouples that were wound around both tubes. The electric power delivered to the system was determined from the voltage applied to the system and the known electrical resistance, using equation 3.10. The resistance of the thermocouple wire was then determined using equations 3.8 and 3.9.

Three different heat fluxes were applied to the tubes. The local heat flux can be determined from:

$$\dot{q}(x) = \frac{\dot{Q}(x)}{\pi D x} \quad (3.21)$$

A constant heat flux is applied to the tubes, thus the temperature of the water flowing through it will increase linearly. Therefore, the mean fluid temperature is the average of the inlet and outlet temperature:

$$T_m = \frac{T_i + T_o}{2} \quad (3.22)$$

The surface temperature of the tube at the desired locations can be obtained from the thermocouple readings. Since there are four thermocouples at each location, the average of the four readings will be used. The heat transfer coefficient can then be determined from the following equation since the heat flux, as well as the surface and mean water temperature at a specific location, is known:

$$\dot{q}(x) = h(T_s(x) - T_m) \quad (3.23)$$

The Reynolds and Nusselt numbers could be determined using equations 2.1 and 2.4. The Colburn j-factor could then be determined from equation 2.8 which is the modified Reynolds-analogy.

3.4.3 ENERGY BALANCE

The heat transfer rate can be compared to the electrical power by using the following energy balance:

$$EB = \frac{\dot{q}_{electric} - \dot{q}}{\frac{\dot{q}_{electric} + \dot{q}}{2}} \times 100 \quad (3.24)$$

$$= \frac{\dot{q}_{electric} - \dot{m}C_p\Delta T}{\frac{\dot{q}_{electric} + \dot{m}C_p\Delta T}{2}} \times 100$$

3.5 INSTRUMENTS

3.5.1 DC POWER SUPPLY

A DC Power supply was used in the experimental set-up. The maximum supplied power and voltage was 1.5 kW and 360 V respectively.



FIGURE 3.19: POWER SUPPLY

3.5.2 THERMOCOUPLES

T-type thermocouples with a Constantan wire diameter of 0.25 mm were used to apply the heat flux to the tubes, as well as for the temperature measurements. T-type thermocouple wire consists of two parallel wires, one copper and the other Constantan. The copper and Constantan wires are insulated with blue and red insulation, respectively, and insulated together in a sheath of Teflon. The thermocouples were calibrated in a thermal bath with a Pt-100 probe which was calibrated to 0.01 °C. The thermocouples were calibrated between 20 °C and 60 °C with steps of 2.5 °C. Once the thermal bath had reached the desired temperature and the temperature of the Pt-100 probe was fairly constant, approximately 30 readings were captured for each thermocouple. This process was repeated for a decreasing thermal bath temperature from 60 °C to 20 °C in order to ensure that a constant curve is obtained and to

investigate the effect of hysteresis. The readings for every thermocouple at each temperature were averaged and a plot of the measured temperature against the actual temperature was generated for each thermocouple. The shape of the graphs was a straight diagonal line and the standard deviation for each thermocouple was less than 0.01 °C. A scaling factor was also determined for each thermocouple. This process is explained in Appendix B.

3.5.3 HEATING WIRE

The T-type thermocouple wire was used to apply the heat flux to the tubes. Three constantan wires were connected in parallel in order to reduce the resistance and therefore the current through each wire. A simple device shown in Figure 3.20 was used to wrap the wire around the tubes.

Only the Constantan wires were used for the heating, therefore the three Constantan wires were soldered together at both ends of the tubes, while the copper wires were disconnected.

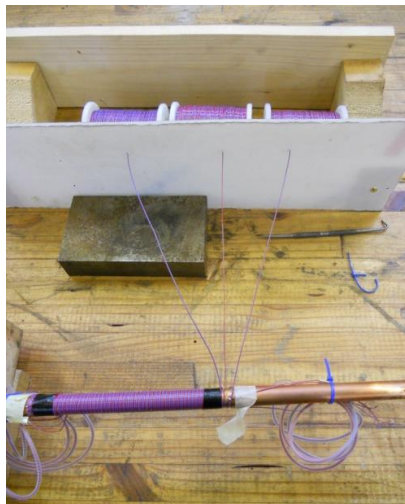


FIGURE 3.20: HEATING WIRE

3.5.4 PRESSURE TRANSDUCERS

A DP15 differential pressure transducer was used to measure the pressure drop across the test section and is shown in Figure 3.21. The diaphragm in the pressure transducer can be changed according to the pressure drops of the system. The minimum and maximum pressure drop across the test section was calculated to be 20 Pa and 580 Pa for the smooth tube and 20 Pa and 8 kPa for the roughened tube. Thus, a number 20 diaphragm with a pressure range of 860 Pa was used for the smooth tube and a number 30 diaphragm with a pressure range of 8.6 kPa was used for the roughened tube. The accuracy of the pressure transducers is 0.25 % of the full scale value. The detail of the calibration method and set-up is explained in Appendix B. The current signal obtained from the Labview program was converted to a pressure reading using interpolation. A plot of the pressure recorded by the Labview program against the actual pressure reading on the manometer was then generated. The slope of this graph was used

during each test to convert the pressure reading from current to Pascal. However, the off-set differed for each test and ranged between 4.8 and 5.2 mA.



FIGURE 3.21: DIFFERENTIAL PRESSURE TRANSDUCER

3.5.5 FLOW METERS

Two Micro Motion Elite Coriolis flow meters were used to measure the flow rate in the tube. The CMF010 had a maximum flow rate capacity of 108 l/h and the CMF025 had a maximum capacity of 2180 l/h. Thus, for low flow rate tests the CMF010 Coriolis CMF025 flow meter was used for higher flow rates. The accuracy of the flow meter was $\pm 0.05\%$ of the full-scale flow rate, therefore ± 0.15 l/h.



FIGURE 3.22: CORIOLIS FLOW METERS

3.6 EXPERIMENTAL PROCEDURE

Steady-state conditions were reached after approximately 20 minutes after start-up. This fairly long time needed was due to the relatively slow thermal inertia of the system before it reached steady temperatures and negligible changes in the mass flow rates. After the initial steady state was achieved, the flow rate was increased or decreased in relatively large increments in the laminar and turbulent regions and smaller increments in the regions where transition was expected. Therefore, enough data points were taken in the transitional region and it took approximately 5 minutes to reach the new steady state after each increment. The reason for the

small time necessary compared to the initial time was because the mass flow increments were relatively small. Steady state conditions were reached once the variations in the wall temperatures of the first (T1), middle (T6) and last (T11) thermocouple stations were minimal and an energy balance of approximately 1% had been achieved. However, the heat transfer data revealed that the energy balance for all the tests varied between 20% and 30%, which is undesirably high. The cause for the heat loss could not be determined yet, since adequate insulation was used. Sufficient time was also given between measurements in order for the system to reach steady state.

The temperatures and pressure drop readings were recorded using a Labview program and a Matlab program was used to determine the Reynolds numbers, Nusselt numbers and friction factors. The Reynolds number of the water flowing through the tube was increased by increasing the mass flow rate using the pumps. The three different heat fluxes were applied to the tubes by adjusting the applied voltage on the DC power supply.

After steady state had been reached, 100 data points were captured at a frequency of 10 Hz. The flow rate was then increased and the next set of data points were recorded once steady state had been reached. The mass flow rate was decreased to reach a minimum Reynolds number of 1 000 for the smooth tube and 500 for the roughened tube and then increased back to a Reynolds number of 7 000, in order to investigate the effect of hysteresis. The process was repeated twice in order to validate the first data and when irregularities occurred, a third set of measurements was taken in that region.

3.7 VALIDATION

The methods to determine the heat transfer coefficients and friction factors were validated by comparing the measurements for the laminar and turbulent flow regimes inside the smooth tube and comparing these with existing heat transfer and friction factor correlations.

For the roughened tube, the adiabatic friction factor data was validated only, since no previous research was done on uniform surface roughness up to date. Although heat transfer correlations for enhanced tube exist, they were not used to validate the results of the roughened tube since the dynamics of the flow in enhanced tubes differ significantly from tubes with a uniform surface roughness.

3.7.1 ADIABATIC FRICTION FACTORS

The friction factor was validated by considering approximately 100 data sets with 100 data points each for each tube. Both increasing and decreasing increments of Reynolds numbers between 1 000 and 7 000 were used to ensure that the laminar and turbulent flow regimes are covered. The measurements were made without any heat transfer to eliminate the effect of varying viscosity and density.

The laminar results ($1\,000 < Re < 2\,300$) were compared with equation 3.2 which is the Poiseuille relation, while the turbulent results ($3\,000 < Re < 7\,000$) were compared with the following equation, which is known as the Blasius correlation:

$$f = 0.316 Re^{-0.25} \quad (3.25)$$

The results were also compared with equation 2.17 obtained by Olivier.

Figure 3.23 shows the friction factor results for increasing and decreasing Reynolds number increments as well as the above-mentioned correlations. There are similarities in the overall trend of the adiabatic friction factors and the laminar friction factor data was approximately 24 % above the theoretical values, while the turbulent data differed by 10 %.

The significantly higher friction factor in the laminar region is due to the fact that the flow is still developing. The following equation can be used to determine the hydrodynamic entry length:

$$L_{h,laminar} = 0.05 * Re * D \quad (3.26)$$

Therefore, for Reynolds numbers between 1 000 and 2 000, the entry length will vary between 74.4 cm and 1.49 m, which is a considerable portion of the tube and therefore the effects of developing flow cannot be neglected. The thickness of the hydrodynamic boundary layer increases with Reynolds number, therefore the wall shear stress is the highest at the tube inlet, where the boundary layer is the thinnest and decreases gradually to the fully developed values. This explains the higher pressure drop, and therefore friction factor, in the entrance region. The equations used to validate the adiabatic friction factors were developed for fully developed flow and subsequently under predict the adiabatic friction factor for developing flow.

In the turbulent flow regime, the following equation can be used to determine the hydrodynamic entry length:

$$L_{h,turbulent} = 10 * D \quad (3.27)$$

The hydrodynamic entry length is independent of the Reynolds number and was determined to be 14.48 cm, which can be considered negligible compared to the overall length of the tube. This also explains the smaller difference between the measured data and the predicted values.

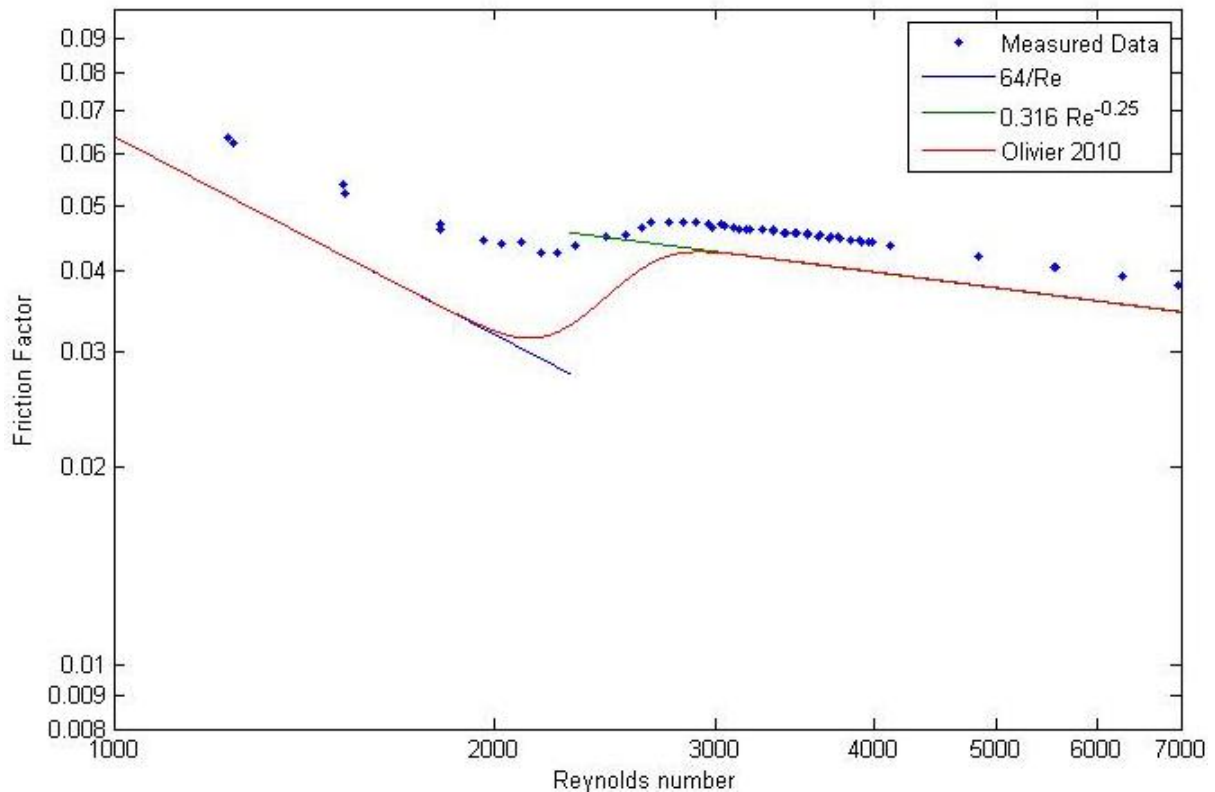


FIGURE 3.23: VALIDATION OF ADIABATIC FRICTION FACTOR RESULTS INSIDE THE SMOOTH TUBE

The friction factor for the roughened tube was validated by considering approximately 83 data sets with 100 data points each for each tube. The average of the increasing and decreasing increments of Reynolds numbers between 500 and 7 000 were used to ensure that the laminar and turbulent flow regimes are covered. These measurements were also made without any heat transfer to eliminate the effect of varying viscosity and density.

The laminar results ($400 < Re < 2\,300$) were compared with the Poiseuille equation again, while the turbulent results ($3\,000 < Re < 7\,000$) were compared with equation 3.4, which is the Modified Colebrook equation. Three different relative roughnesses were used for the validation. The Moody Chart covers a relative roughness range between 0.00001 and 0.05; therefore the relative roughness of this tube is not covered, although a theoretical line has been included.

Figure 3.24 shows the friction factor results for increasing and decreasing Reynolds number increments as well as the above-mentioned correlations. Although the data do not exactly correlate with the existing correlations, there are similarities in the overall trend of the adiabatic friction factors. It was expected that the laminar friction factors would be the same as the smooth tube data and therefore slightly higher than the $64/Re$ correlation, since the laminar friction factor is usually a function of the Reynolds number only and subsequently independent of surface roughness in the laminar region. However, this was not the case and there was a significant increase. In the turbulent region, the friction factor is strongly influenced by any irregularity or roughness on the surface that disturbs the laminar sub layer and therefore affects the flow. Since the relative roughness of this tube was higher than the maximum relative roughness covered in the Moody Chart, it may be possible that the laminar flow was also affected by the roughness, which explains the higher laminar friction factors. The significantly higher turbulent friction factors may be due to the fact that a maximum relative

roughness of 0.05 was used for the Modified Colebrook equation, and therefore the current relative roughness falls outside the boundaries.

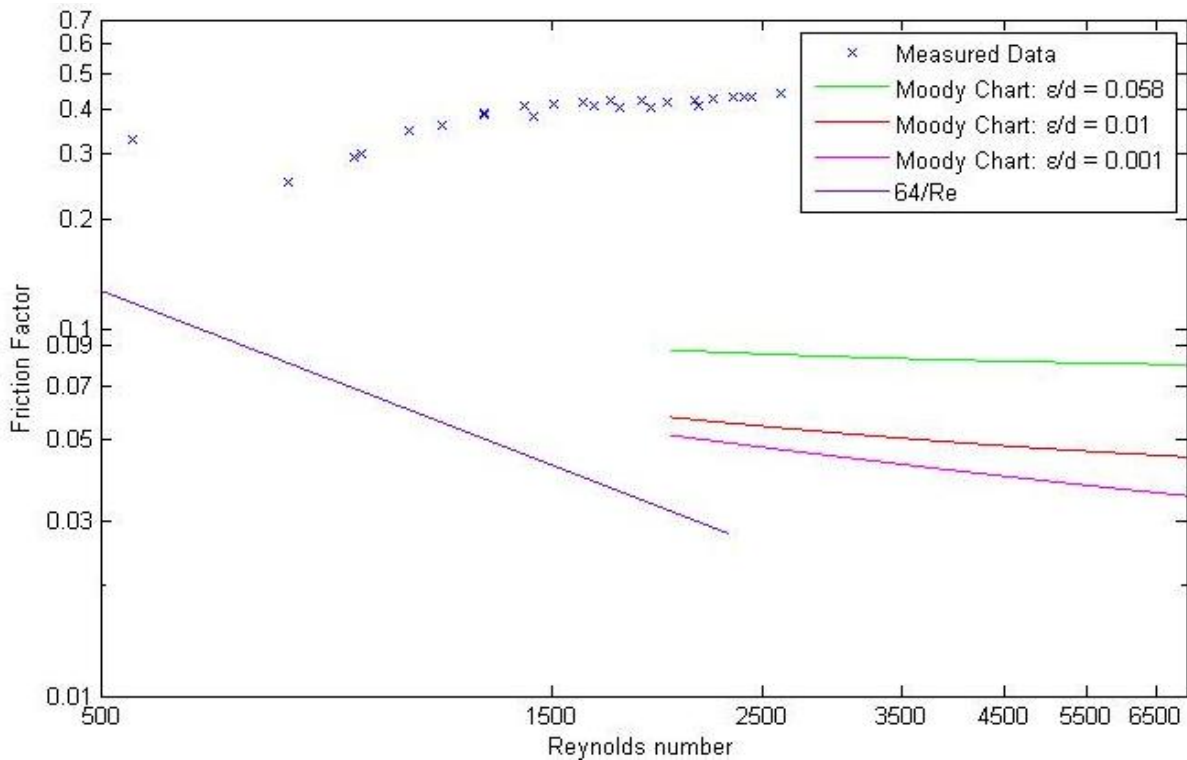


FIGURE 3.24: VALIDATION OF ADIABATIC FRICTION FACTOR RESULTS INSIDE THE ROUGHENED TUBE

3.7.2 DIABATIC FRICTION FACTORS

The diabatic friction factors were validated in Figure 3.25 by using the results of the smooth tube and comparing it with the measured data obtained by Olivier (2010) when he investigated heat transfer through a 15.88 mm tube as well. However, for his experiments, a counterflow tube-in-tube heat exchanger was used; therefore the boundary condition was constant wall temperature instead of the constant heat flux boundary condition used for these experiments. Since the boundary conditions are different, exact correlation with the data of Olivier cannot be expected.

The measured data was also compared with the experimental data obtained by Ghajar (1997). A square-edged inlet tube was used and the test fluid was an ethylene-glycol-water mixture. Although this data was obtained when an 8 kW/m² heat flux was applied, the exact correlation with the 8.66 kW/m² data cannot be expected, since the test fluids and therefore fluid properties, differ.

Both increasing and decreasing increments of Reynolds numbers between 1 000 and 7 000 were used to ensure that the laminar and turbulent flow regimes were covered. Since the increasing and decreasing Reynolds numbers data differed slightly, the average was used for the validation.

The measured data correlates fairly well with the experimental data of Olivier and the overall shape of the curves is similar. The friction factor data obtained when the 11.49 kW/m² heat flux were applied is higher than the adiabatic friction factors, although the friction factors obtained when the other two heat fluxes were applied are significantly lower. This is not possible, since the friction factors are suppose to increase due to the effect of secondary flow. The overall shape of the curves are indeed correct and the transitional region is between Reynolds numbers of 2 100 and 3 000. More detail on possible causes for the inaccurate friction factor data can be found in Chapter 4. The experimental data of Ghajar shows that transition occurs significantly later when an ethylene-glycol-water mixture is used instead of water.

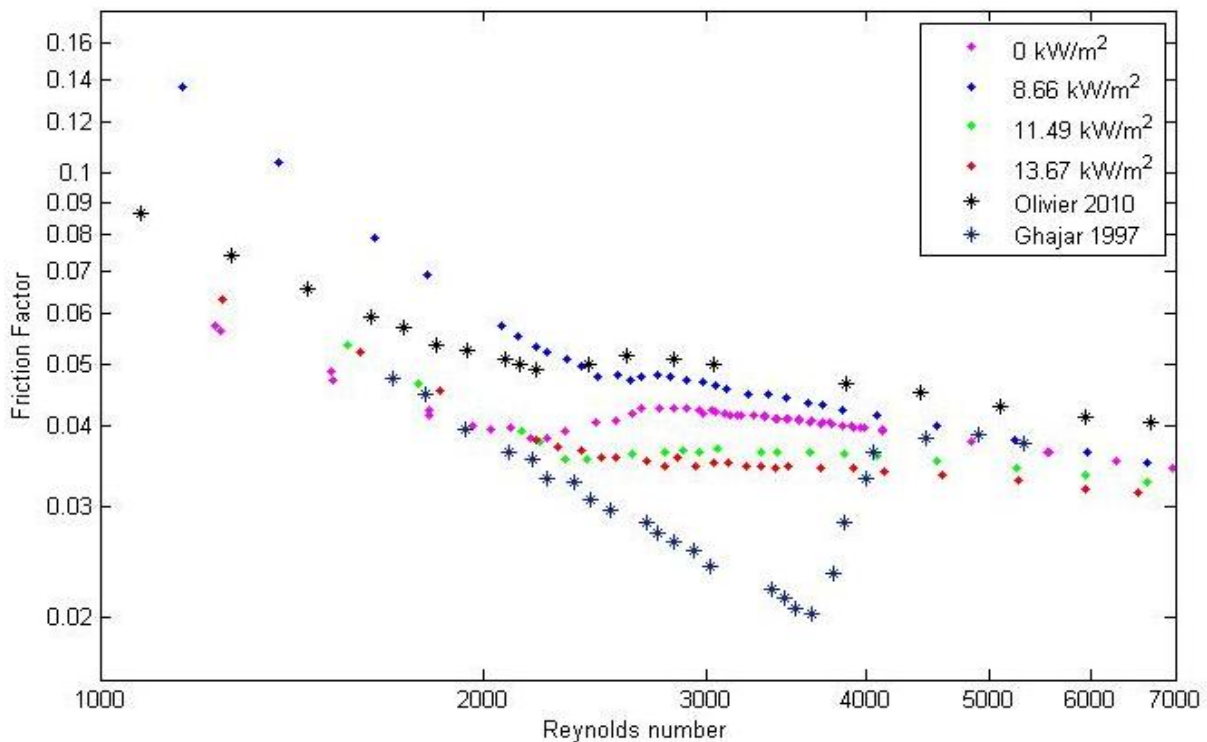


FIGURE 3.25: VALIDATION OF DIABATIC FRICTION FACTOR INSIDE THE SMOOTH TUBE

3.7.3 HEAT TRANSFER COEFFICIENTS

The Nusselt numbers (or indirectly the heat transfer coefficients) of the smooth tube were validated in Figure 3.26 by using the results of the smooth tube again. Approximately 100 data sets with 100 data points each for each heat flux applied used. Both increasing and decreasing increments of Reynolds numbers between 1 000 and 7 000 were used to ensure that the laminar and turbulent flow regimes were covered. Since the increasing and decreasing Reynolds numbers data differed slightly, the average was used for the validation. The measured data was again compared to experimental data obtained by Olivier (2010) and Ghajar (1997).

The measured data in the turbulent region obtained with the 11.49 kW/m² heat flux applied, correlates well with the data of Olivier, although it was obtained from experiments using a different boundary condition. Exact correlation is obtained in the turbulent region; however, there is an 8 % and 12 % difference in the laminar and transitional regions, respectively.

The 8.66 kW/m² measured data is significantly lower than the 8 kW/m² data experimental data obtained by Ghajar. The reason for this difference is because Ghajar used ethylene-glycol-water mixtures as the test fluid. The fluid properties and therefore Prandtl numbers are different. The Prandtl number represents the relative magnitudes of momentum and heat diffusion in the velocity and thermal boundary layers and therefore significantly influences the heat transfer results.

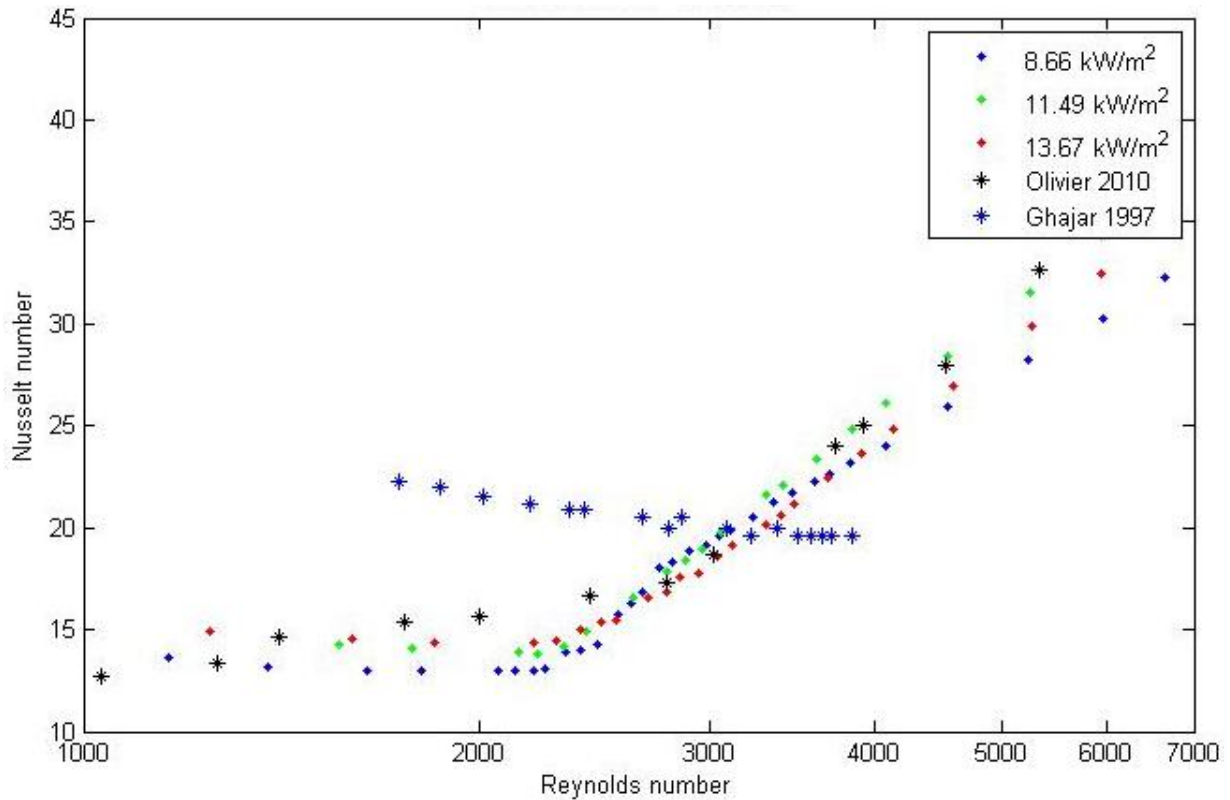


FIGURE 3.26: VALIDATION OF HEAT TRANSFER DATA FOR THE SMOOTH TUBE

3.8 CONCLUSION

The experimental set-up and procedure were described in detail in this chapter. The test section consisted of two tubes, one smooth and the other one roughened, with the same diameter and water used as the working fluid. Three different heat fluxes were applied to the tube and heat transfer and pressure drop measurements were taken. It was ensured that steady state conditions were always met. Therefore adequate time after start-up, as well as between increments, was allowed in order to ensure that the variation in temperature was less than 0.1°C.

The heat transfer coefficient and friction factor were validated using existing correlations as well as the measured data obtained from Olivier (2010) and Ghajar (1997). The adiabatic friction data correlated well with a 10 % error in turbulent region. The laminar friction factors were 25 % above the predicted values due to the fact that the flow was still developing and the correlations were for fully developed flow. The diabatic friction factors did not correlate with existing data of Olivier, although the overall shape of the curves were similar. Possible causes

for the inaccuracies can be found in Chapter 4. An ethylene-glycol-water mixture was used as the test fluid in the experiments done by Ghajar, which explains the significant difference between the measured data and his experimental data.

Although there were slight differences between the measured heat transfer data and those obtained by Olivier, the overall trend was similar and therefore the data has been validated.

4. RESULTS

4.1 INTRODUCTION

Two tubes, one smooth and the other with a relative roughness of 0.058, were investigated. Both tubes were 1.8 m long and had outer diameters of 15.88 mm. The experimental results are divided into two parts, namely the heat transfer results for the smooth tube and then a comparison of the two tubes. The adiabatic friction factor results are included in the diabatic friction factor results using 0 kW/m². Solid markers are used to indicate the measured data for the smooth tube, while crosses are used for the roughened tube.

4.2 SMOOTH TUBE

The Reynolds number was varied between 1 000 and 7 000 since transition was expected to occur at a Reynolds number of approximately 2 300. This ensured that the whole transitional region, as well as part of the laminar and turbulent region, was covered. Approximately 100 data sets with 100 data points each for each heat flux applied used. The average of the increasing and decreasing increments of Reynolds numbers was used in the graphs.

4.2.1 FRICTION FACTORS

Figure 4.2 contains the experimental friction factors of the smooth tube against Reynolds number. In the adiabatic case, transition from laminar to turbulent flow started at a Reynolds number of approximately 2 100 and ended at approximately 2 400, which corresponds to the transitional region at Reynolds numbers of 2 100 – 2 300, which appears in most fluid dynamics textbooks. The s-curve of the diabatic friction factors was much smaller than for the adiabatic case. Therefore it can be concluded that there is very little increase in friction factor in this region.

It is important to investigate the diabatic friction factors, since the viscosity difference between the bulk fluid and the fluid at the wall, as well as the effect of secondary flow, influences the friction factors. From the diabatic friction factor data it follows that the friction factors obtained when the 8.66 kW/m² heat flux was applied, is significantly larger than the adiabatic and other diabatic friction factors. The increase between the adiabatic and diabatic friction factors, especially in the laminar region, may be due to secondary flow, which usually occurs in horizontal heated tubes. The fluid near the tube wall has a higher temperature and lower density and circulates upward, while the fluid in the centre circulates downward due to the lower temperature and higher density. The temperature difference therefore creates secondary flow due to free convection. Mixed convection (a combination of free convection due to secondary flow and forced convection due to the heat flux applied) changes the velocity profile. The friction factor is proportional to the wall shear stress, which in turn is proportional to the

velocity gradient at the wall. The velocity profile is affected in such a way that the velocity gradient is much steeper at the tube wall. As the heat flux is increased, the shear stresses increase due to the steeper velocity gradient, which leads to an increased friction factor. Although the effect of heating is significant in the laminar and transitional regions, the heating effect is almost negligible in the turbulent region. Secondary flow also influences the heat transfer measurements in the laminar flow regime and the effect diminishes as the flow becomes transitional and turbulent.

The influence of secondary flow is shown in Figure 4.1. There is a significant difference between the top and bottom local heat transfer coefficients. These local heat transfer coefficients were determined by using the temperature measurements at the top, bottom and sides, respectively. The side local heat transfer coefficients were expected to be the same. However, this is not the case and a possible reason may be that the tube was slightly turned when it was connected to the rest of the experimental set-up.

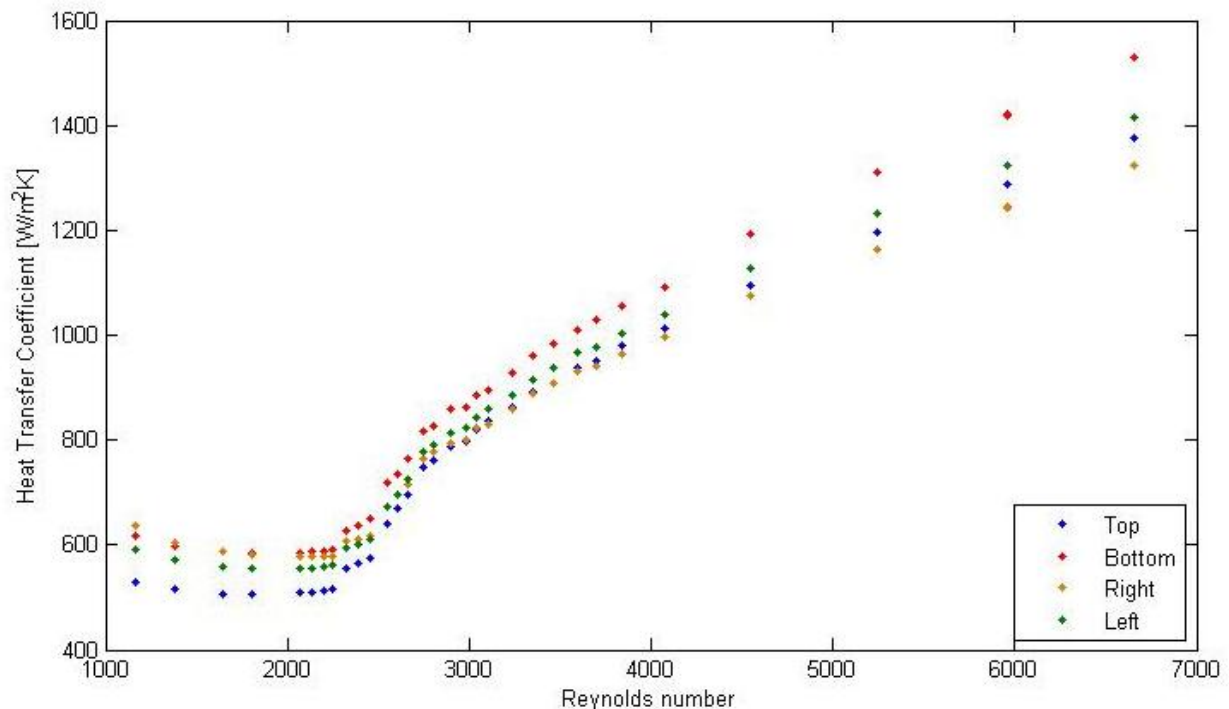


FIGURE 4.1: LOCAL HEAT TRANSFER COEFFICIENTS FOR THE SMOOTH TUBE WHEN 8.66 KW/M² HEAT FLUX APPLIED

The diabatic friction factors obtained when the 11.49 kW/m² and 13.67 kW/m² heat fluxes were applied, in Figure 4.2, were unexpected since they are significantly lower than the adiabatic friction factors, especially in the transitional region. The friction factors were determined using equation 3.20; therefore they are dependent on the pressure drop, density, diameter and length of tube as well as upon the velocity of the fluid. Since the tube dimensions, as well as the fluid velocity and density are correct, the only variable that might be the reason for the incorrect data is the pressure drop. The pressure drop was measured using a differential pressure transducer and since both the pressure transducer and diaphragm have been used by previous students, there is a possibility that it is slightly damaged or incorrect.

Another possibility may be that the diaphragm got damaged. This might well be the reason since the adiabatic turbulent friction factors are only 10 % above the predicted values. The

adiabatic tests were done first and were then followed by the 8.66 kW/m², 11.49 kW/m² and 13.67 kW/m² applied heat fluxes during the diabatic tests. From the results it can be observed that the inaccuracy of the data increases with increasing heat fluxes, which confirms the possibility of a damaged diaphragm. During each start-up of the system, the supply and by-pass valves are adjusted in order to obtain maximum back pressure on the pump and therefore reduce the flow pulsations. It is possible that the diaphragm may have been damaged during this process when the pressure of the system was accidentally increased significantly above the calibrated pressure. The diaphragms are designed to withstand approximately two times their maximum rated pressure before it break. A small diaphragm with a maximum pressure of 860 kPa was used for the smooth tube. Since the pressure was increased significantly above the calibrated value of 580 kPa but not necessarily above 1.72 kPa, the diaphragm did not break, but might got damaged and the calibration might have been less accurate for the rest of the tests. A good safety measure for future experiments will therefore be to check and recalibrate the diaphragms between tests if the pressure was accidentally increased significantly above the maximum pressure.

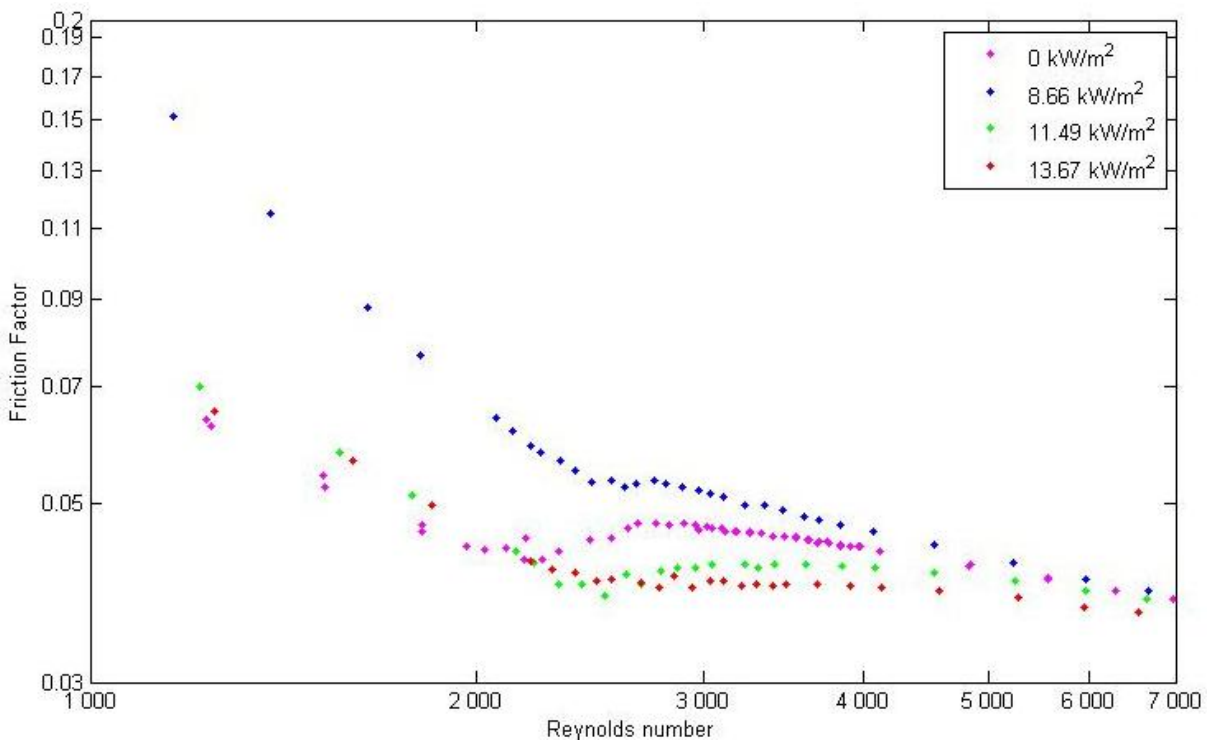


FIGURE 4.2: EXPERIMENTAL FRICTION FACTORS FOR THE SMOOTH TUBE AS A FUNCTION OF REYNOLDS NUMBER FOR DIFFERENT HEAT FLUXES

4.2.2 HEAT TRANSFER

In order to investigate the heat transfer, a graph of the Nusselt numbers against Reynolds numbers was generated. From Figure 4.3 it can be concluded that transition is delayed for increasing heat fluxes. Transition occurs approximately at 2 100 when 8.66 kW/m² is applied and at 2 200 and 2 400 when 11.49 kW/m² and 13.67 kW/m² are applied. In the laminar region, the Nusselt number is higher for higher heat fluxes. In the transitional region, however, the

opposite is true and the gradient of transition is higher for higher heat fluxes. Therefore, the gradient of transition is greater for higher heat fluxes.

The Nusselt numbers in the laminar region are significantly higher than the predicted theoretical constant 4.36 for a constant heat flux boundary condition. These higher values are due to the buoyancy-induced secondary flow in the tube which was caused by the difference in density at the center and wall of the tube. The secondary flow influences forced convection and causes mixed convection heat transfer.

The Nusselt numbers also increases with an increased heat flux applied from approximately 13 when the 8.66 kW/m² heat flux is applied, to approximately 14 when the 13.67 kW/m² heat flux is applied in the laminar region. As the flow rate decreases in the laminar region, the Nusselt numbers increases slightly. This may be due to increased heat loss through the insulation at these low flow rates.

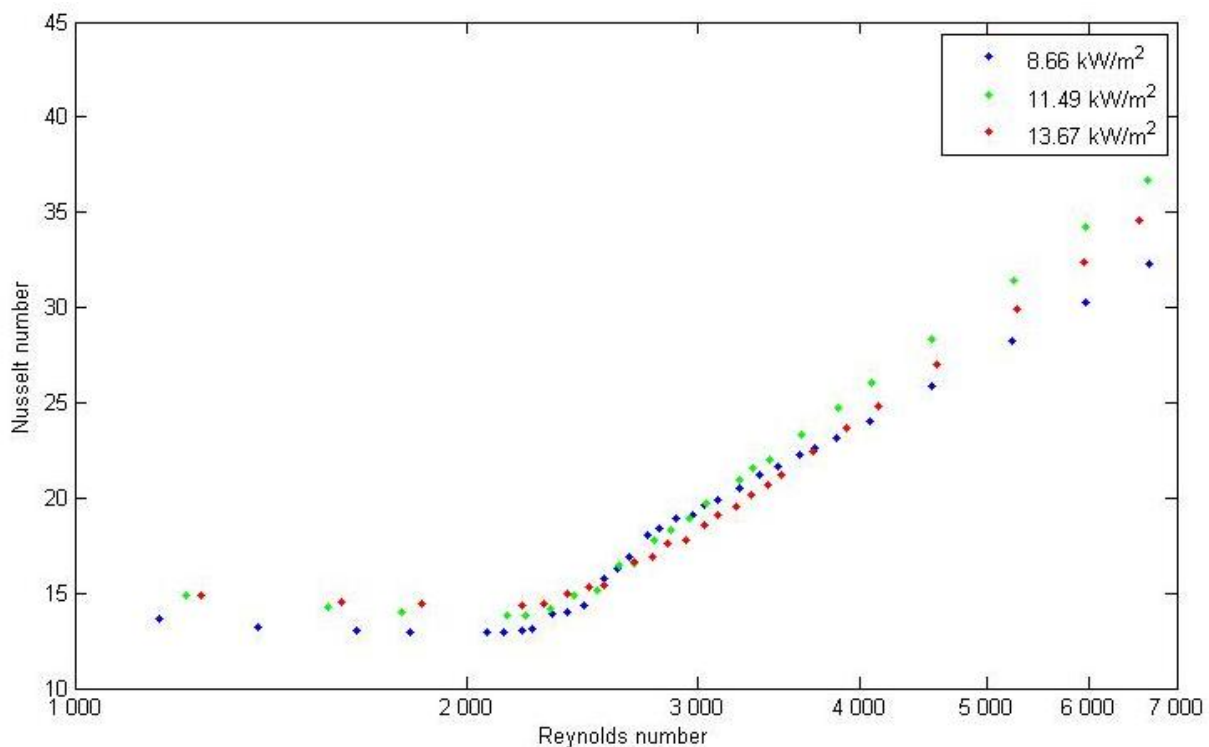


FIGURE 4.3: EXPERIMENTAL HEAT TRANSFER DATA FOR THE SMOOTH TUBE IN TERMS OF NUSSELT NUMBERS AGAINST REYNOLDS NUMBERS FOR DIFFERENT HEAT FLUXES

The effect of secondary flow in the laminar and transitional regions is shown in Figure 4.4 where the ratio of the heat transfer coefficients at the top and bottom of the tube is plotted. For forced convection (in the absence of buoyancy effects), the ratio should be unity, while it should be less than unity for mixed convection. From the figure it follows that the ratio of the local heat transfer coefficients decrease for increasing heat fluxes applied. This trend is consistent with the effect of secondary flow that increases as the applied heat flux increases. As the Reynolds number increases, the ratio of the local heat transfer coefficients approaches unity in the upper bound of the transition region. Therefore it can be concluded that the secondary flow effect is significant in the laminar flow regime, decreases in the transitional regime and is suppressed by the turbulent motion.

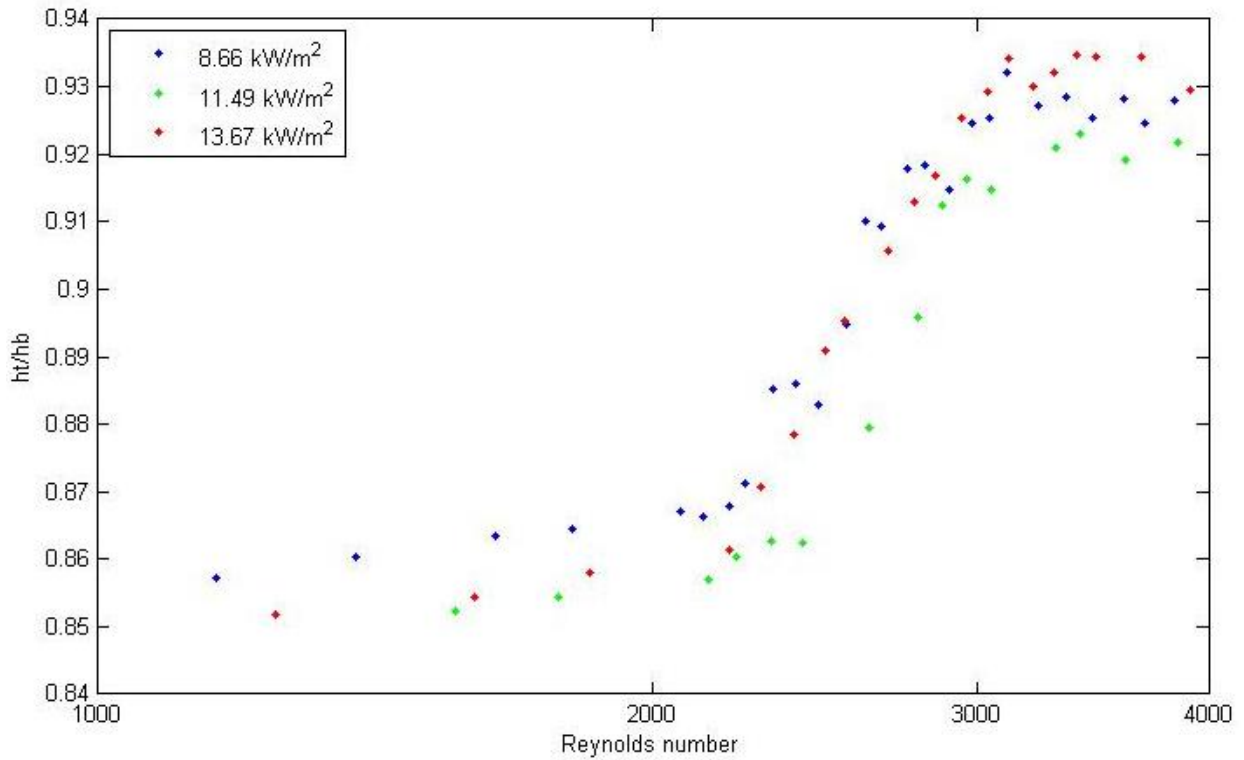


FIGURE 4.4: LOCAL HEAT TRANSFER RATIO FOR THE SMOOTH TUBE FOR DIFFERENT HEAT FLUXES APPLIED

The heat transfer results can also be plotted in terms of the Colburn j-factor, using equation 2.8, since this account for the variation in the fluid Prandtl number. From Figure 4.5, it can be confirmed that transition is delayed for increasing heat fluxes. Transition occurred at Reynolds numbers between 2 200 and 2 800 when the 8.66 kW/m² heat flux was applied, between 2 300 and 3 000 when the 11.49 kW/m² heat flux was applied, and between 2 500 and 3 200 when the 13.67 kW/m² heat flux was applied.

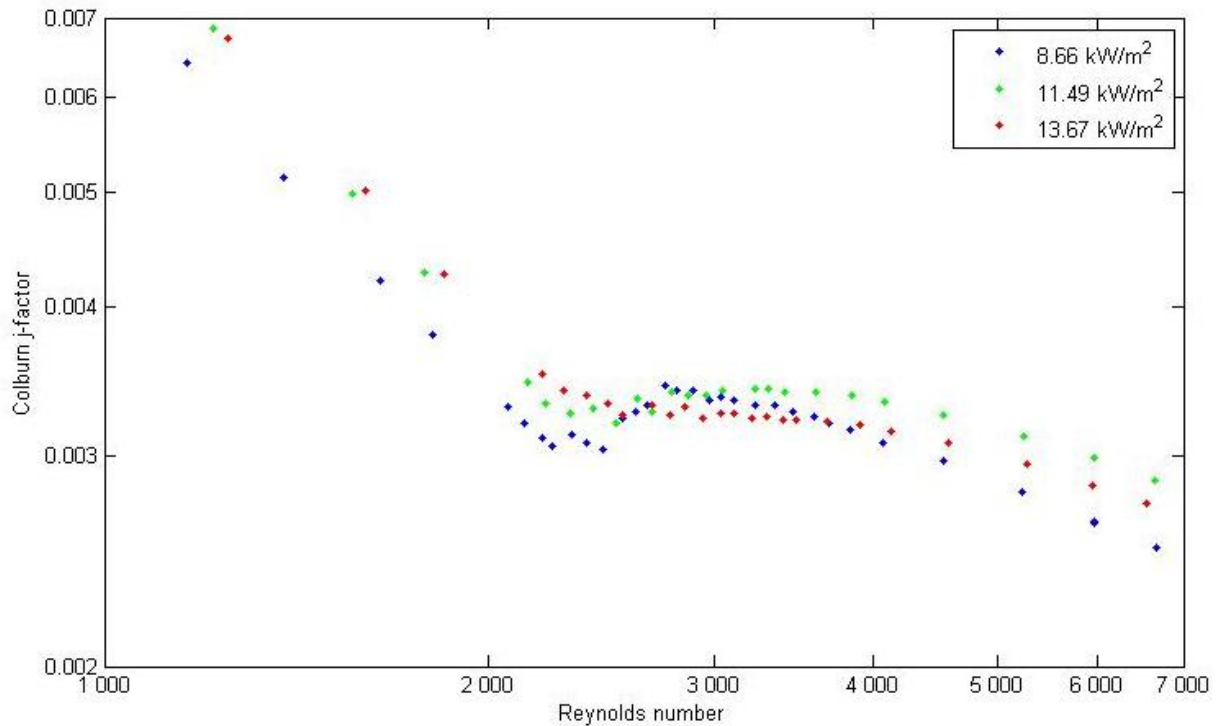


FIGURE 4.5: SMOOTH TUBE HEAT TRANSFER DATA IN TERMS OF THE COLBURN J-FACTORS FOR DIFFERENT HEAT FLUXES

4.3 ROUGHENED TUBE

The Reynolds numbers were varied between 500 and 7 000 in order to cover as large as possible a section of the transitional and laminar flow regimes. This was not always possible since, the experimental set-up was initially designed to operate at Reynolds numbers between 1 000 and 7 000 and a tube with a relative surface roughness of 0.001. However, as mentioned in Chapter 3, there was not a significant difference between the result of this roughness and those of the smooth tube. Therefore, the surface roughness was increased drastically which caused transition to occur much earlier than expected. While the 13.67 kW/m² heat flux was applied, the water at the tube exit reached a maximum temperature of 72 °C and the tube surface a maximum temperature of 95 °C at a Reynolds number of 500. Since the tube was heated to 100 °C when the thermocouples were soldered to the tube, it was undesirable to heat the tube above 95 °C because the thermocouples might loosen again. Therefore, this limited the system from operating at lower Reynolds numbers.

4.3.1 FRICTION FACTORS

The friction factor is strongly influenced by the surface roughness, as shown in Figure 4.6. The laminar sub layer is disturbed by irregularities or roughness on the surface and flow is therefore affected. The friction factors are strongly influenced by the surface roughness in the turbulent region, and this effect is minimal in the laminar region.

During turbulent flow, the entry lengths are short - usually ten tube diameters; it can therefore be assumed that the flow is fully developed in the turbulent region. For fully developed turbulent flow, the friction factors depend on the Reynolds number as well as the relative roughness, which is the ratio of the mean roughness height to the diameter of the tube. The friction factors increase with surface roughness in the transitional and turbulent regions, but this increase is less in the laminar region. This increased friction factor is caused by the increased resistance to flow caused by the surface roughness. Transition also occurs much earlier for the roughened tube.

Although the smooth tube friction factors do not show a definite increase with increasing heat flux applied, the diabatic friction factors of the roughened tube are significantly higher than the adiabatic friction factors. This trend is accurate since the friction factors are expected to increase with an increasing heat flux applied due to the effect of secondary flow. As explained earlier, the velocity profile is disturbed in such a way that the shear stresses increase with an increasing heat flux applied due to the effect of secondary flow. The changing velocity gradient leads to an increased friction factor. The effect of heating is significant in the laminar and transitional regions, and almost negligible in the turbulent region. It can therefore be concluded that secondary flow also influences the heat transfer measurements in the laminar flow regime and that the effect diminishes as the flow becomes transitional and turbulent.

When comparing the adiabatic and diabatic friction factors, it is also clear that transition is delayed when a heat flux is applied. According to the adiabatic friction factor data, transition occurred approximately at Reynolds numbers between 500 and 1 200. The diabatic friction factor data does not show clearly when transition started and ended since part of the laminar region could not be tested due to the limitations of the system. However, a delay in transition for increasing heat fluxes is visible.

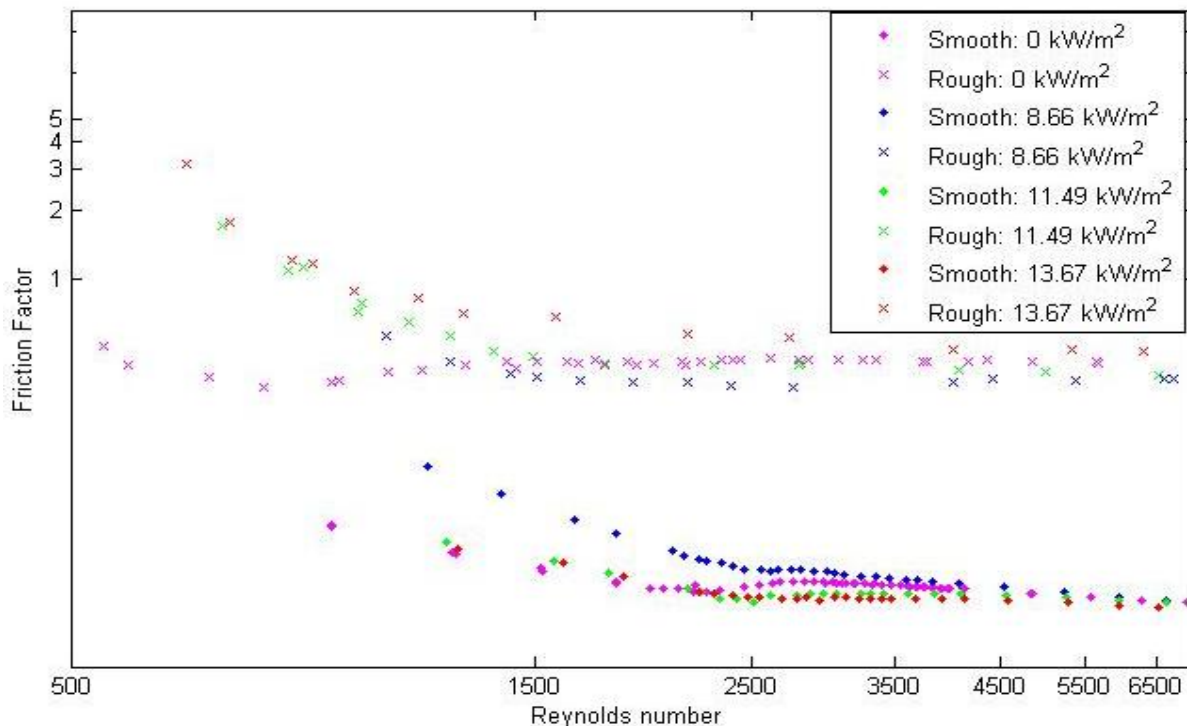


FIGURE 4.6: EXPERIMENTAL FRICTION FACTORS FOR THE SMOOTH AND ROUGHENED TUBE AS A FUNCTION OF REYNOLDS NUMBER FOR DIFFERENT HEAT FLUXES

4.3.2 HEAT TRANSFER COEFFICIENTS

The heat transfer coefficients are investigated by plotting the Nusselt numbers against Reynolds numbers. From Figure 4.7 it follows that the roughened tube has significantly higher heat transfer coefficients compared to the smooth tube in the turbulent region. In the laminar region, the opposite is true and it seems that surface roughness has a negative effect on heat transfer in this region. This may be due to the fact that the surface roughness partially obstructs the secondary flow path. Unfortunately it is not clear from this heat transfer data when transition occurred when the 8.66 kW/m^2 heat flux was applied. However, transition occurred at a Reynolds number of approximately 800 when the 11.49 kW/m^2 heat flux was applied and at approximately 900 when the 13.67 kW/m^2 heat flux was applied. Therefore, once again, transition is also delayed for increasing heat fluxes, which confirms the results obtained with the smooth tube.

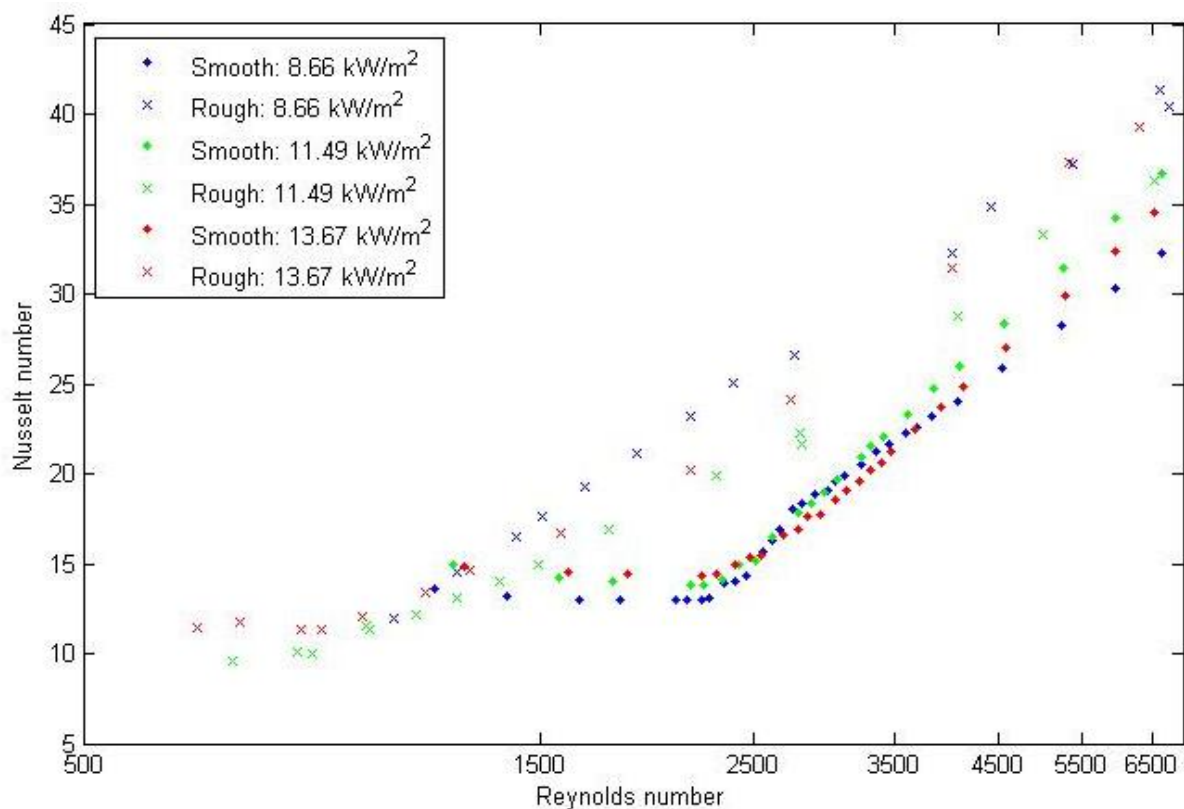


FIGURE 4.7: EXPERIMENTAL HEAT TRANSFER DATA FOR THE SMOOTH AND ROUGHENED TUBE IN TERMS OF NUSSULT NUMBERS AGAINST REYNOLDS NUMBERS FOR DIFFERENT HEAT FLUXES

Once again the laminar Nusselt numbers are significantly higher than 4.36 due to the effect of secondary flow. This is also visible when the ratio of the top and bottom heat transfer coefficients is plotted against the Reynolds number. From Figure 4.8 it follows that the heat transfer ratio increases with increasing Reynolds numbers and approaches unity at the end of the transitional region. Therefore, the secondary flow effect is suppressed by the turbulent motion.

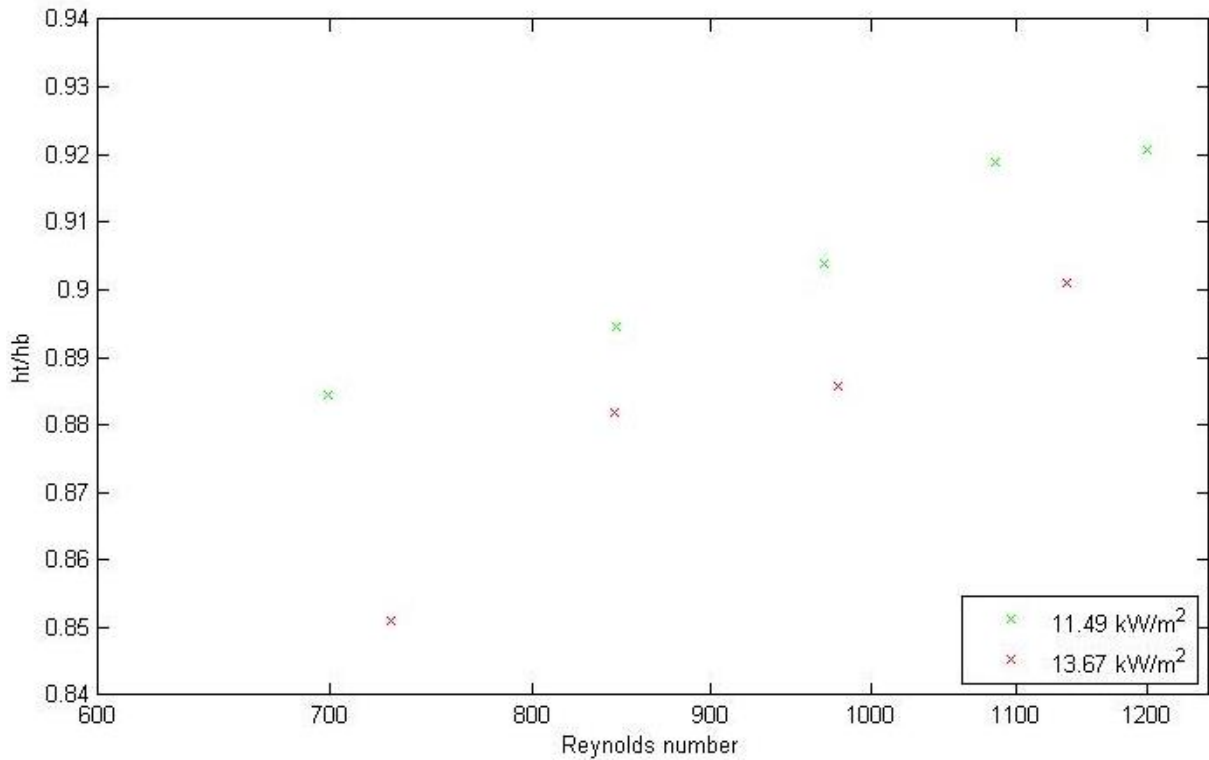


FIGURE 4.8: LOCAL HEAT TRANSFER RATIO FOR THE ROUGHENED TUBE FOR DIFFERENT HEAT FLUXES APPLIED

The heat transfer results were also plotted in terms of the Colburn j-factor in Figure 4.9 in order to account for the variation in the fluid Prandtl number. Similar to the Nusselt number results, the Colburn j-factor is higher for lower heat fluxes in the turbulent region. Transition was slightly delayed for higher heat fluxes since it started at a Reynolds number of approximately 800 when the 11.49 kW/m² heat flux was applied and at approximately 900 when the 13.67 kW/m² heat flux was applied. This confirms the conclusions made from the heat transfer data in terms of the Nusselt number. Unfortunately it is not clear from Figure 4.9 where transition occurred when the 8.66 kW/m² heat flux was applied.

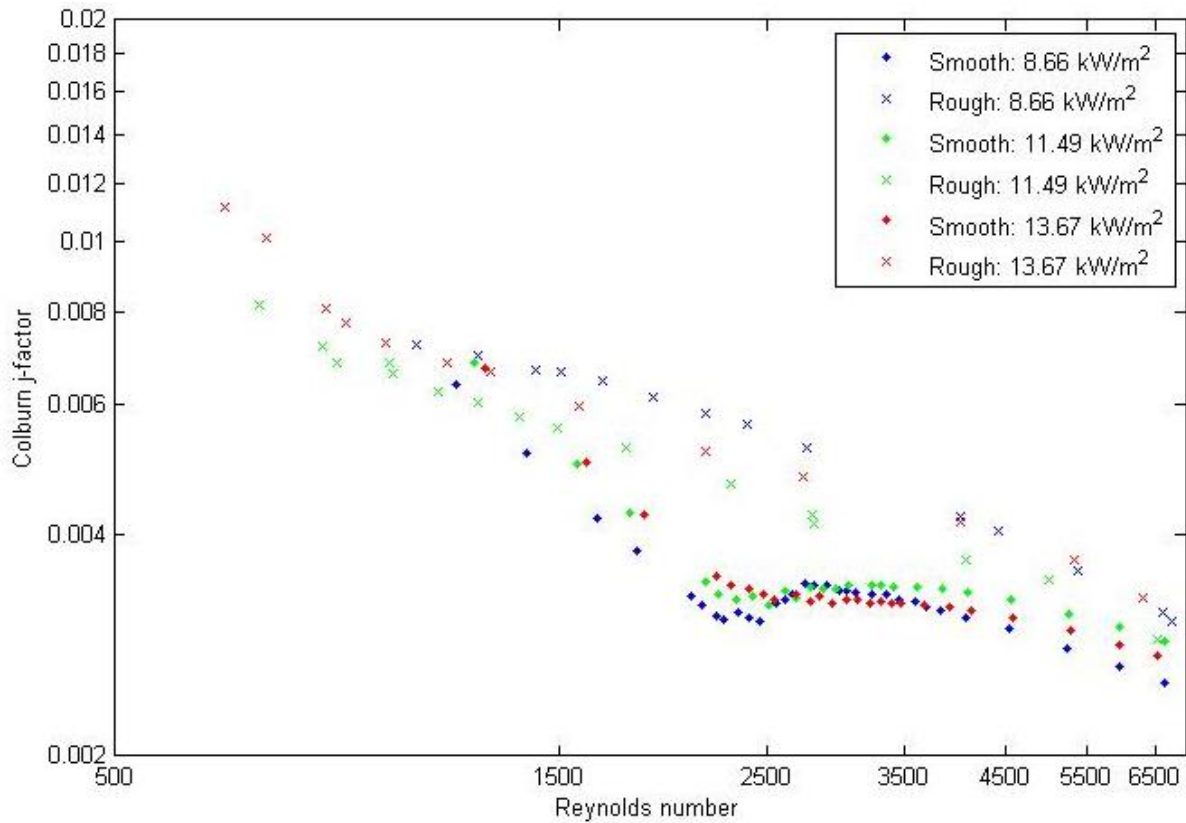


FIGURE 4.9: EXPERIMENTAL DATA FOR THE SMOOTH TUBE IN TERMS OF THE COLBURN J-FACTOR

4.4 CONCLUSION

The friction factor results of the smooth tube were inconsistent and therefore inaccurate, since the diabatic friction factors decreased for increasing heat fluxes applied. It also showed that transition is not delayed for increasing heat fluxes applied. The friction factors are dependent on the pressure drop, density, diameter and length of tube as well as the velocity of the fluid. Since the tube dimensions - as well as the fluid velocity and density - are correct, the only variable that could account for the incorrect data is the pressure drop. The pressure drop was measured using a differential pressure transducer and a diaphragm which was selected according to the pressure drop range that was tested. The inaccuracy between the adiabatic and diabatic data increased drastically which implies that the diaphragm might have been damaged.

A different diaphragm was used for the roughened tube, because the pressure drop was much higher. Since the inaccuracy of the friction factor data for the roughened tube was significantly less than for the smooth tube, it is confirmed that a damaged diaphragm is the reason for the inaccurate friction factor results of the smooth tube.

The adiabatic friction factor data revealed that transition occurred approximately at Reynolds numbers between 500 and 1 200, which is significantly earlier than the transition of the smooth tube which occurred between Reynolds numbers of 2 100 and 2 800. The diabatic friction factor data does not clearly show when transition started and ended since part of the laminar

region could not be tested due to the limitations of the system. However, a delay in transition for increasing heat fluxes is visible

The heat transfer results of the smooth tube show that transition occurs approximately at 2 100 when 8.66 kW/m^2 is applied and at 2 200 and 2 300 when 11.49 kW/m^2 and 13.67 kW/m^2 is applied. In the laminar region, the Nusselt number is higher for higher heat fluxes. However, in the transitional region, the opposite is true and the gradient of transition is higher for higher heat fluxes. The laminar Nusselt numbers were higher than the predicted theoretical constant 4.36 for a constant heat flux boundary condition, due to the buoyancy-induced secondary flow in the tube which was caused by the difference in density at the center and wall of the tube. The secondary flow disturbs the velocity boundary layer in such a way that the shear stress and therefore friction coefficient is increased. The Colburn j-factor plots confirmed that transition is delayed and that the heat transfer increases for increasing heat fluxes.

The roughened tube has significantly higher turbulent heat transfer coefficients, compared to the smooth tube. However, the opposite is true in the laminar region and it can therefore be concluded that surface roughness has a negative effect on heat transfer at low flow rates. This may be due to the fact that the surface roughness partially obstructs the secondary flow path. Transition is also delayed for increasing heat fluxes, since it started at a Reynolds number of approximately 800 when the 11.49 kW/m^2 heat flux was applied and at approximately 900 when the 13.67 kW/m^2 heat flux was applied. Unfortunately it is not clear where transition occurred when the 8.66 kW/m^2 heat flux was applied.

Due to inaccurate friction factor data of the smooth tube and incomplete friction factor data of the roughened tube, it is not possible to develop correlations to accurately describe the influence of surface roughness in the transitional flow regime. The exact boundaries of the transitional flow regime could not be determined since a sufficient part of the laminar region could not be covered due to the limitations of the experimental set-up.

4. CONCLUSION AND RECOMMENDATIONS

Heat exchangers are usually designed to operate in either the laminar or the turbulent flow regime, while the transitional flow regime is avoided due to uncertainties and irregularities. Up to now the transitional flow regime has been investigated, however, there has been no previous work done on influence of surface roughness in the transitional flow regime.

An experimental set-up was built in order to investigate the influence of surface roughness on the heat transfer and pressure drop performance. The system consisted of a smooth and roughened tube, both with an outer diameter and length of 15.88 mm and 1.8 m, respectively. The type of inlet was square-edged and water was used as the test fluid. The roughened tube was roughened by gluing sand grains with an average size of 0.84 mm to the inside surface of the copper tube and the tube therefore had a relative roughness of 0.058.

A total of 810 data sets, each with 100 data points captured at a frequency of 10 Hz, were used to generate 44 graphs which were used to investigate the influence of surface roughness. The adiabatic friction factor results showed that surface roughness increases the friction factor and that transition occurred earlier as well. The diabatic friction factors for the smooth tube were inaccurate due to a damaged diaphragm in the pressure transducer. A different diaphragm was used for the roughened tube, because the pressure drop was significantly higher and since the inaccuracy of these results were significantly less, it was confirmed that the diaphragm used for the smooth tube had been damaged.

The adiabatic friction factor data revealed that transition occurred approximately at Reynolds numbers between 500 and 1 200, which is significantly earlier than the transition of the smooth tube which occurred between Reynolds numbers of 2 100 and 2 800. The diabatic friction factor data does not show clearly when transition started and ended since part of the laminar region could not be tested due to the limitations of the system. However, a delay in transition for increasing heat fluxes is visible.

The heat transfer results of the smooth tube shows that transition occurs approximately at 2 100 when 8.66 kW/m² is applied and at 2 200 and 2 300 when 11.49 kW/m² and 13.67 kW/m² is applied. Transition for the roughened tube started at a Reynolds number of approximately 800 when the 11.49 kW/m² heat flux was applied and at approximately 900 when the 13.67 kW/m² heat flux was applied. Unfortunately it is not clear where transition occurred when the 8.66 kW/m² heat flux was applied. However, it can be concluded that transition is delayed for increasing Reynolds numbers. The laminar Nusselt numbers of both tubes were higher than the predicted theoretical constant 4.36 for a constant heat flux boundary condition, due to the buoyancy-induced secondary flow in the tube which was caused by the difference in density at the center and wall of the tube. The Nusselt numbers for the roughened tube were lower than for the smooth tube in the laminar region, but the opposite was true in the turbulent region. These lower Nusselt numbers may be due to the surface roughness which disrupted the secondary flow path and reduced the amount of mixing. Secondary flow also increased the diabatic friction factors, especially in the laminar region, since it increases the wall shear stress and therefore the overall pressure drop. The effect of secondary flow was almost negligible in the turbulent region.

The Colburn j-factors in the transitional flow regime were higher for increasing heat fluxes in both the smooth and roughened tube, although those in the roughened tube were significantly higher than in the smooth tube. This confirms that surface roughness increases the heat transfer in the transitional flow regime.

Unfortunately, due to inaccurate friction factor data for the smooth tube, and incomplete friction factor data for the roughened tube, correlations could not be developed to describe the influence of surface roughness in the transitional flow regime. It was also not possible to determine the boundaries of the transitional flow regime, since a sufficient part of the laminar flow region could not be covered for the roughened tube due to the limitations of the experimental set-up.

It is therefore recommended that future work should include the following:

- An experimental set-up that is designed to operate at very low Reynolds numbers to accurately cover the whole transitional flow regime, as well as part of the laminar and turbulent flow regimes.
- The measurement equipment, for example the pressure transducers, should be verified between tests to ensure that it is not damaged or inaccurate.
- Although an extensive amount of tests had been performed, a large database is required in order to accurately describe transition; therefore it would be advisable to investigate more heat fluxes and finer increments, especially during tests with the roughened tube.
- Water was the only test fluid used. Different fluids (with different Prandtl numbers), for example an ethylene-glycol-water mixture, should, however, also be tested in order to determine the influence of the Prandtl number.
- A range of diameters, of tubes with the same surface roughness, should be investigated.
- The tube was roughened by gluing sand grains to the inner surface of the copper tube. Although an experiment showed that the influence of the sand grains and glue has a negligible effect on the heat transfer, the accuracy of the results will be improved by roughening the tube with a similar material to that of the tube itself.
- A wider range of surface roughness can also be investigated in order to accurately determine its influence.

5. REFERENCES

- ASHRAE,2009. Fluid Flow, ASHRAE Handbook – Fundamentals, American Society of Heating, Refrigerating and Air-Conditioning Engineers, Inc., Atlanta
- Cengel, Y. A., 2006. *Heat and Mass Transfer*. 3rd ed., Singapore: McGraw-Hill.
- Ghajar, A. J., and Madon, K. F., Pressure Drop Measurements and Correlations in the Transition Region for a Circular Tube with Three Different Inlet Configurations. *Experimental Thermal Fluid Science*. 5, 129-135, 1992.
- Ghajar, A. J., and Tam, L. M., Flow Regime Map for a Horizontal Pipe with Uniform Wall Heat Flux and Three Inlet Configurations. *Experimental Thermal Fluid Science*. 10, 287-297, 1995.
- Ghajar, A. J., and Tam, L. M., Heat Transfer Measurements and Correlations in the Transition Region for a Circular Tube with Three Different Inlet Configurations. *Experimental Thermal Fluid Science*. 8, 79-90, 1994.
- Ghajar, A. J., and Tam, L. M., Effect of Inlet Geometry and Heating on the Fully Developed Friction Factor in the Transition Region of a Horizontal Tube. *Experimental Thermal Fluid Science*. 15, 52-64, 1997.
- Meyer, J.P. and Olivier, J.A., Heat Transfer in the Transitional Flow Regime. *Evaporation, Condensation and Heat Transfer, InTech*, pp. 245-260, 2011.
- Meyer, J.P. and Olivier, J.A., Single-Phase Heat Transfer and Pressure Drop of the Cooling Water inside Smooth Tubes for Transitional Flow with Different Inlet Geometries. *HVAC&R Research*, 16(4), pp. 471-496, 2010.
- Meyer, J.P. and Olivier, J.A., Transitional Flow inside enhanced tubes for fully developed and developing flow with different types of inlet disturbances: Part 1 - Adiabatic Pressure Drops. *International Journal for Heat and Mass Transfer*. 54, 1587-1597, 2010
- Meyer, J.P. and Olivier, J.A., Transitional Flow inside enhanced tubes for fully developed and developing flow with different types of inlet disturbances: Part 2 - heat transfer. *International Journal for Heat and Mass Transfer*. 54, 1598-1607, 2010
- Mkhonotho, E., Flow in the Transitional Flow Regime, Final Year Project, Department of Mechanical and Aeronautical Engineering, University of Pretoria, 2011.
- Obot, N.T., Esen, E.B., Rabas, T.J., The role of transition in determining friction and heat transfer in smooth and rough passages. *International Journal of Heat and Mass Transfer*, 33,2133-2143, 1990.
- Olivier, J.A., Single-Phase Heat Transfer and Pressure Drop of Water Cooled at a Constant Wall Temperature Inside Horizontal Circular Smooth and Enhanced Tubes with Different Inlet Configurations in the Transitional Flow Regime, Ph.D. Thesis, Department of Mechanical and Aeronautical Engineering, University of Pretoria, 2009.

Omega. 2012. *Product Spec Sheet*. [Online]. Available:
http://www.omega.co.uk/ppt/pptsc.asp?ref=FINEWIRE_DUPINSUL [2012, March,18]

Toprak,H. 2006. *Waste Water Engineering*. [Online]. Available:
<http://web.deu.edu.tr/atiksu/enter.html> [2012,October,15]

White, F., 2009. *Fluid Mechanics*. 6th ed. Singapore: McGraw-Hill

APPENDIX A: SURFACE ROUGHNESS

Appendix A contains the results of the surface roughness measurements which was done by Metlab, as well as the results of the grading analysis.

57 Charl Cilliers Street, Boksburg North
 P O Box 1028, Boksburg, 1480
 Tel: (011) 917 5173 • Fax: (011) 917 0546
 Email: metlab@telkomsa.net
 Website: www.metlab.co.za

Director: T.C.W. Brink (Pr. Ing/Eng.)





TEST REPORT IN ACCORDANCE WITH EN 10204 3.1 OF SAMPLE AS SUPPLIED	
Customer:	University of Pretoria
Order no:	COD
Address:	PO Box 39814 Moreleta Park 44
Telephone:	012 997 0296
Email:	meverts@mwweb.co.za
Attention:	Marielize Everts
Material specification:	Copper
Description:	15mm OD tubes
Identification:	See below

REPORT NUMBER:	12 - 3427 A
Date Received:	25 June 2012
Date tested:	26 June 2012

Sample	SURFACE ROUGHNESS MEASUREMENTS*	
	Ra (µm)	Rz (µm)
Long rough	0.424	6.084
Short rough	1.674	14.560
Smooth	0.033	0.463

Surface roughness measurements performed on internal surfaces of tubes.

* Not a SANAS accredited activity

Tests requested, in accordance with spec. provided			
Tests requested, not in accordance with spec. provided			
No requirements provided	X		
REMARKS:			
WITNESS BY:	N/A	MANAGEMENT SIGNATORY	TECHNICAL SIGNATORY
			12 - 3427 A 

TESTING WAS CARRIED OUT IN ACCORDANCE WITH THE FOLLOWING METLAB PROCEDURES (Supporting international procedures): MECH 30, 33, 34 & 39 (ASTM A370; ER: E21; ISO 6892 Method B; EN10002-5) MECH 31 & 32 (ASTM A370; E23; BS EN 10045-1); MET 01 (ASTM E8; E384) MET02 (ASTM E10; A370) MET03 (ASTM E18; A370) MET04 (ASTM B117) MET05 (ASTM A255; E18) MET06 (ASTM E1077) MET07 (ASTM E340; E381) MET08 (ASTM E3; A262) MET09 (ASTM E3; E45) MET10 (ASTM E3; E46; E112; E407) MET13 (ASTM B499) MET14 (ASTM B487) MET 16 (ASTM E110) E110, CHEMS70 & 71 (ASTM E415) CHEMA54 (ASTM E1019)

For conditions relevant to this certificate see reverse side.

57 Charl Cilliers Street, Boksburg North
 P O Box 1028, Boksburg, 1460
 Tel: (011) 917 5173 • Fax: (011) 917 0546
 Email: metlab@telkomsa.net
 Website: www.metlab.co.za

Director: T.C.W. Brink (Pr.Eng/Eng.)



TEST REPORT IN ACCORDANCE WITH EN 10204 3.1 OF SAMPLE AS SUPPLIED

Customer: University of Pretoria	Material specification: Copper
Order no: COD	
Address: PO Box 39814 Moreleta Park 44	Description: ± Ø16mm x 0.7mm wall tube Actual pipe (short)
Telephone: 012 997 0296	
Email: meverts@mmweb.co.za	
Attention: Marlize Everts	Identification: Sample A

REPORT NUMBER:	12 - 3778 A
Date Received:	12 July 2012
Date tested:	13 July 2012

SURFACE ROUGHNESS MEASUREMENTS*			
Ra (µm)		Rz (µm)	
Sample	2.039	2.087	2.091
		12.57	12.64
			12.65

Surface roughness measurements performed on internal surfaces of tubes.

* Not a SANAS accredited activity

Tests requested, in accordance with spec. provided			
Tests requested, not in accordance with spec. provided			
No requirements provided	X		
REMARKS:			
		WITNESS BY: N/A	MANAGEMENT SIGNATORY
			TECHNICAL SIGNATORY
			12-3778-A

Handwritten signature and stamp: 'SILIP HASTA' stamp and signature.

TESTING WAS CARRIED OUT IN ACCORDANCE WITH THE FOLLOWING METLAB PROCEDURES (Supporting international procedures): MECH 30, 33, 34 & 39 (ASTM A370; EB; E21; ISO 6892 Method B; EN10002-5) MECH 31 & 32 (ASTM A370; E23; BS EN 10045-1) MET 01 (ASTM E92; E384) MET02 (ASTM E10; A370) MET03 (ASTM E18; A370) MET04 (ASTM B117) MET05 (ASTM A255; E19) MET06 (ASTM E1077) MET07 (ASTM E340; E381) MET08 (ASTM E3; A262) MET09 (ASTM E3; E45) MET10 (ASTM E3; E45; E112; E407) MET11 (ASTM E3; E45) MET13 (ASTM B489) MET14 (ASTM B487) MET 16 (ASTM E110) E110, CHEMS70 & 71 (ASTM E415) CHEMAS4 (ASTM E1019)



METLAB

TEST REPORT IN ACCORDANCE WITH EN 10204 3.1 OF SAMPLE AS SUPPLIED	
Customer:	University of Pretoria
Order no:	COD
Address:	PO Box 39814 Moreleta Park 44
Telephone:	012 997 0296
Email:	meverts@mweb.co.za
Attention:	Marilize Everts
Material specification:	Copper
Description:	± Ø16mm x 0.7mm wall tube Middle pipe (long)
Identification:	Sample B

REPORT NUMBER:	12 - 3778 B
Date Received:	Date tested:
12 July 2012	13 July 2012

SURFACE ROUGHNESS MEASUREMENTS*				
	Ra (µm)		Rz (µm)	
Sample	2.031	2.034	13.95	12.51
Surface roughness measurements performed on internal surfaces of tubes.				

* Not a SANAS accredited activity

Tests requested, in accordance with spec. provided				
Tests requested, not in accordance with spec. provided				
No requirements provided	X			
REMARKS:				
				12 - 3778 B
				TECHNICAL SIGNATORY
				MANAGEMENT SIGNATORY
				WITNESS BY: N/A

TESTING WAS CARRIED OUT IN ACCORDANCE WITH THE FOLLOWING METLAB PROCEDURES (Supporting international procedures): MECH 30, 33, 34 & 39 (ASTM A370; E8; E21; ISO 6892; Method B; EN10002-5) MECH 31 & 32 (ASTM A370; E23; BS EN 10046-1); MET 01 (ASTM E92; E384) MET02 (ASTM E10; A370) MET03 (ASTM E18; A370) MET04 (ASTM B117) MET05 (ASTM A285; E18) MET06 (ASTM E1077) MET07 (ASTM E940; E381) MET08 (ASTM E3; A282) MET09 (ASTM E3; E45) MET10 (ASTM E3; E45; E112; E407) MET11 (ASTM E3; E45) MET13 (ASTM B487) MET 16 (ASTM E110) E110, CHEMS70 & 71 (ASTM E415) CHEMA54 (ASTM E1019)

TO:	UNIVERSITY OF	REF:	12-4264
	PRETORIA	DATE RECEIVED:	06-08-2012
	P O BOX 39814	DOCUMENT DATE:	12-09-2012
	MORELETA PARK		
	44	ORDER No:	COD
ATT:	MARILIZE EVERTS		

Opinions and Interpretations expressed in this report are outside the scope of SANAS accreditation.

COMMENT ON SURFACE ROUGHNESS TESTING*

Two copper samples were submitted for surface roughness testing* (Not a SANAS accredited activity) on the 6th of August 2012. The internal surface's roughness* could not be tested as the roughness fell outside the testing equipment's capabilities.

The instrument details and parameters are as follows:

Equipment make and model: Hand-held Roughness Tester TR200,
manufactured by the TIME Group Inc.

Ra Parameters: 0.005 μm 16 μm

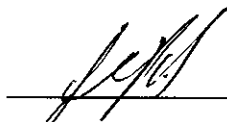
Rz Parameters: 0.02 μm 160 μm

* Results marked "Not SANAS Accredited" in this report are not included in the SANAS Schedule of Accreditation for this laboratory.

Kind regards



COMPILED BY J. STRYDOM
METALLURGIST



APPROVED BY JLP BESTER
METALLURGICAL ENGINEER.

Result Analysis Report

Sample Name:
Sand - Average

SOP Name:

Measured:
01 October 2012 11:24:17

Sample Source & type:
Lab

Measured by:
MASTERSIZER

Analysed:
01 October 2012 11:24:18

Sample bulk lot ref:
25243

Result Source:
Averaged

Particle Name:
Default

Accessory Name:
Hydro 2000MU (A)

Analysis model:
General purpose

Sensitivity:
Normal

Particle RI:
1.520

Absorption:
0.1

Size range:
0.100 to 1000.000 μm

Obscuration:
12.70 %

Dispersant Name:
Water

Dispersant RI:
1.330

Weighted Residual:
1.823 %

Result Emulation:
Off

Concentration:
0.2846 %Vol

Span :
1.472

Uniformity:
0.443

Result units:
Volume

Specific Surface Area:
0.047 m^2/g

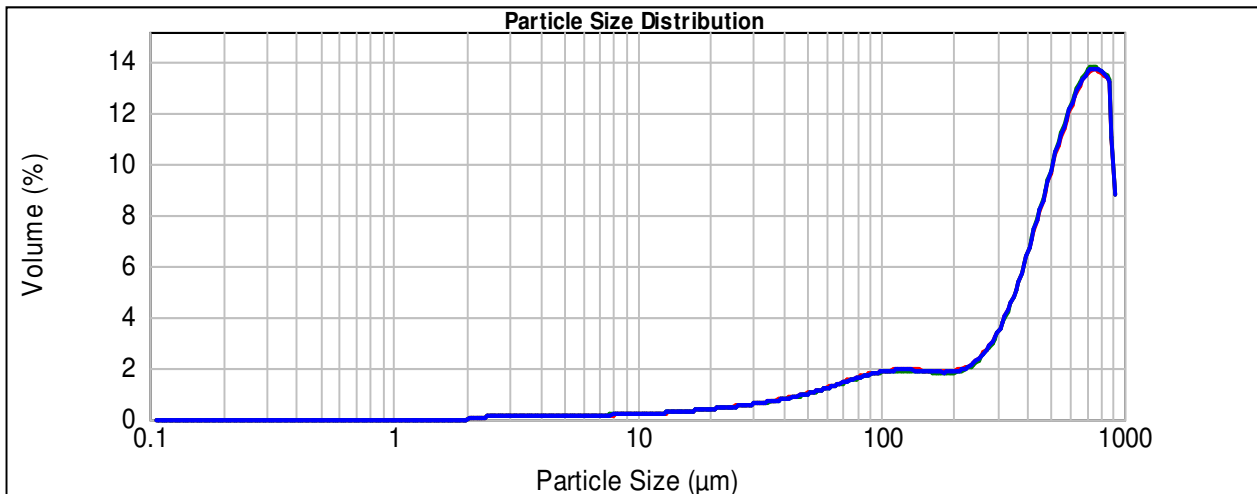
Surface Weighted Mean D[3,2]:
127.790 μm

Vol. Weighted Mean D[4,3]:
483.600 μm

d(0.1): 77.495 μm

d(0.5): 515.280 μm

d(0.9): 835.737 μm



— Sand, 01 October 2012 11:24:17 — Sand, 01 October 2012 11:24:39
— Sand - Average, 01 October 2012 11:24:17

Size (μm)	Volume In %	Size (μm)	Volume In %	Size (μm)	Volume In %	Size (μm)	Volume In %	Size (μm)	Volume In %	Size (μm)	Volume In %
0.100	0.00	0.538	0.00	2.900	0.07	15.614	0.20	84.081	1.11	452.768	5.78
0.110	0.00	0.595	0.00	3.202	0.07	17.240	0.23	92.835	1.18	499.903	6.74
0.122	0.00	0.656	0.00	3.535	0.08	19.035	0.25	102.499	1.22	551.945	7.61
0.135	0.00	0.725	0.00	3.903	0.08	21.016	0.28	113.170	1.24	609.406	8.31
0.149	0.00	0.800	0.00	4.309	0.08	23.204	0.31	124.952	1.24	672.848	8.80
0.164	0.00	0.884	0.00	4.758	0.09	25.620	0.34	137.960	1.23	742.894	8.86
0.181	0.00	0.976	0.00	5.253	0.09	28.287	0.37	152.322	1.20	820.233	8.61
0.200	0.00	1.077	0.00	5.800	0.09	31.232	0.41	168.179	1.18	905.623	3.04
0.221	0.00	1.189	0.00	6.404	0.10	34.483	0.45	185.688	1.19	999.903	0.00
0.244	0.00	1.313	0.00	7.070	0.10	38.073	0.50	205.019	1.25	1103.998	0.00
0.269	0.00	1.450	0.00	7.806	0.11	42.037	0.56	226.362	1.38	1218.929	0.00
0.297	0.00	1.601	0.00	8.619	0.12	46.413	0.62	249.927	1.62	1345.826	0.00
0.328	0.00	1.767	0.00	9.516	0.13	51.245	0.70	275.946	1.98	1485.933	0.00
0.362	0.00	1.951	0.00	10.507	0.14	56.580	0.78	304.673	2.48	1640.625	0.00
0.400	0.00	2.154	0.04	11.601	0.15	62.470	0.86	336.391	3.14	1811.422	0.00
0.442	0.00	2.379	0.06	12.809	0.17	68.973	0.95	371.411	3.93	2000.000	0.00
0.488	0.00	2.626	0.06	14.142	0.18	76.154	1.03	410.077	4.82		
0.538	0.00	2.900	0.06	15.614		84.081		452.768			

Operator notes:

APPENDIX B: CALIBRATION

Appendix B describes the calibration process for the thermocouples and the pressure transducers, as well as the thermocouple scaling factors and the pressure profile for the pressure transducers.

List of Figures

Figure B.2: Temperature Profile of T7.....	4
Figure B.1: Thermocouple Calibration	3
Figure B.3: Temperature Profile of T6.....	7
Figure B.4: Pressure Transducer Calibration	8
Figure B.5: Pressure Transducer 1 Calibration.....	9
Figure B.6: Pressure Transducer 2 Calibration.....	9

List of Tables

Table B1: Scaling Factor and Standard Deviation for Smooth Tube Thermocouples	5
Table B2: Scaling Factor and Standard Deviation for Roughened Tube Thermocouples.....	6

B1 Thermocouple Calibration

The T-type thermocouples were calibrated using a LAUDA ECO RE 1225 thermostat bath with an accuracy of 0.03 °C and a Pt-100 probe which was calibrated to 0.01 °C. The calibration set-up is shown in Figure B.1.



FIGURE B.1: THERMOCOUPLE CALIBRATION

The thermocouples were calibrated between 20 °C and 60 °C at 2.5 °C intervals. Once the thermal bath reached the desired temperature and the temperature of the Pt-100 probe was fairly constant, approximately 30 readings were recorded for each thermocouple at a frequency of 10 Hz. This process was repeated for a decreasing thermal bath temperature from 60 °C to 20 °C in order to ensure that a constant curve is obtained and to investigate the effect of hysteresis. Therefore 29 data sets, containing approximately 30 data points for each of the 44 thermocouples were recorded.

The readings for every thermocouple at each temperature were averaged and a plot of the measured temperature against the actual temperature was generated for each thermocouple. Figure B.2 contains an example of the graph. The shape of the graphs was a straight diagonal line.

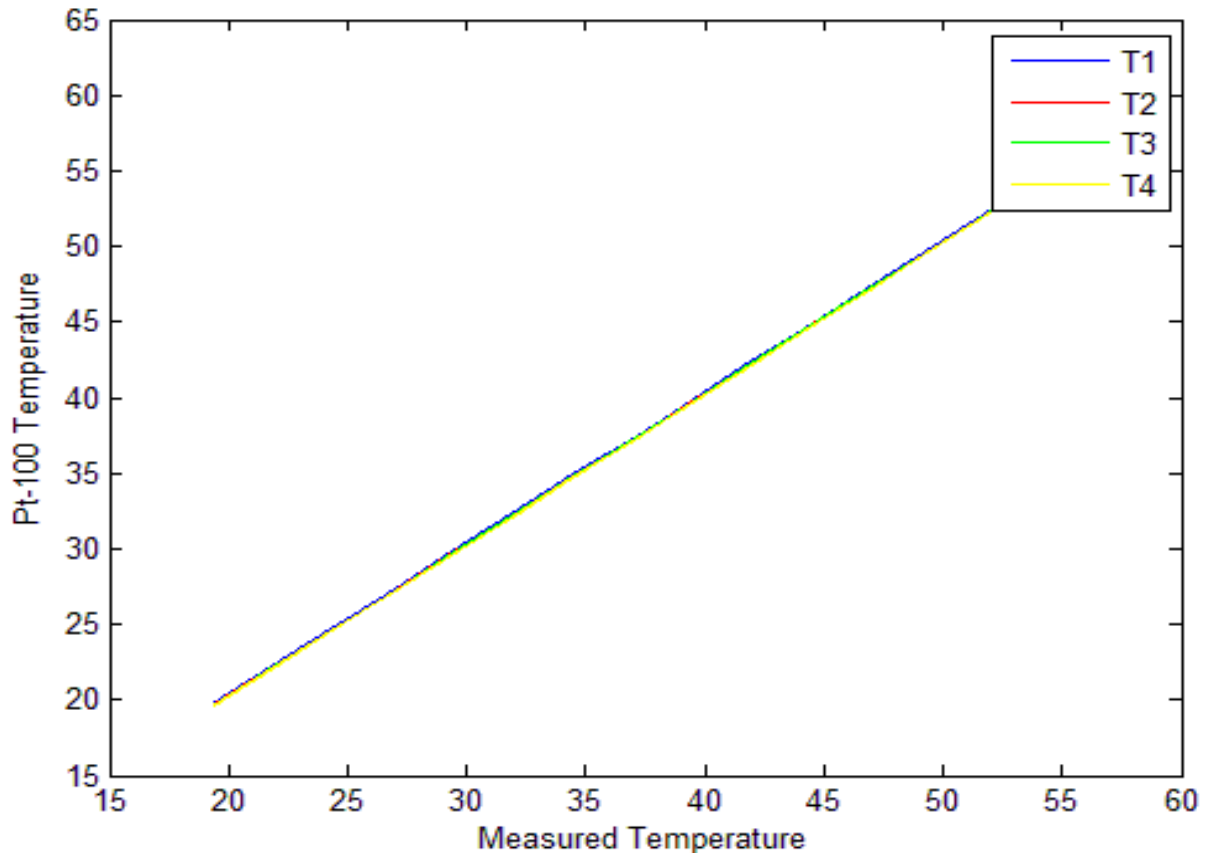


FIGURE B.2: TEMPERATURE PROFILE OF T7

A scaling factor for each thermocouple was calculated by dividing the reference temperature measured with the Pt-100 by the average temperature measures with the thermocouple. This scaling factor was multiplied with the temperatures obtained during the tests. The scaling factors for the smooth tube varied between 0.9731 and 0.9978 and are tabulated in Table B.1. The scaling factors for the roughened tube are tabulated in Table B.2 and varied between 0.8254 and 1.0023.

The standard deviation for each thermocouple was determined using Matlab's built-in function. The standard deviation varied between 0.0015 and 0.0092 for the smooth tube; therefore it can be assumed that the maximum standard deviation was 1%. The standard deviation for each thermocouple on the smooth tube and roughened tube is summarized with the scaling factor in Table B1 and Table B2 respectively.

TABLE B1: SCALING FACTOR AND STANDARD DEVIATION FOR SMOOTH TUBE THERMOCOUPLES

Thermocouple	Scaling Factor	Standard Deviation	Thermocouple	Scaling Factor	Standard Deviation
A1	0.9795	0.0070	G1	0.9881	0.0043
A2	0.9910	0.0031	G2	0.9918	0.0030
A3	0.9913	0.0031	G3	0.9921	0.0028
A4	0.9937	0.0024	G4	0.9934	0.0025
B1	0.9919	0.0030	H1	0.9978	0.0015
B2	0.9900	0.0036	H2	0.9924	0.0028
B3	0.9903	0.0034	H3	0.9974	0.0016
B4	0.9926	0.0027	H4	0.9958	0.0019
C1	0.9793	0.0071	I1	0.9833	0.0058
C2	0.9785	0.0073	I2	0.9809	0.0066
C3	0.9739	0.0089	I3	0.9834	0.0059
C4	0.9731	0.0092	I4	0.9858	0.0050
D1	0.9777	0.0077	J1	0.9844	0.0055
D2	0.9785	0.0073	J2	0.9830	0.0059
D3	0.9849	0.0052	J3	0.9836	0.0057
D4	0.9731	0.0091	J4	0.9851	0.0051
E1	0.9833	0.0058	K1	0.9827	0.0059
E2	0.9783	0.0074	K2	0.9838	0.0057
E3	0.9770	0.0079	K3	0.9828	0.0060
E4	0.9748	0.0085	K4	0.9774	0.0079
F1	0.9796	0.0072			
F2	0.9791	0.0073	Average		
F3	0.9736	0.0092			
F4	0.9734	0.0092			

TABLE B2: SCALING FACTOR AND STANDARD DEVIATION FOR ROUGHENED TUBE THERMOCOUPLES

Thermocouple	Scaling Factor	Standard Deviation	Thermocouple	Scaling Factor	Standard Deviation
A1	0.9884	0.0048	G1	0.9890	0.0043
A2	1.0005	0.0022	G2	0.9961	0.0027
A3	1.0008	0.0022	G3	0.9950	0.0029
A4	1.0023	0.0023	G4	0.9967	0.0025
B1	1.0003	0.0022	H1	1.0002	0.0021
B2	0.9978	0.0023	H2	0.9944	0.0029
B3	0.9973	0.0024	H3	0.9996	0.0021
B4	1.0003	0.0021	H4	0.9979	0.0023
C1	0.9911	0.0040	I1	0.9902	0.0043
C2	0.9903	0.0042	I2	0.9972	0.0049
C3	0.9846	0.0060	I3	0.9850	0.0092
C4	0.9843	0.0061	I4	0.9721	0.0113
D1	0.9881	0.0048	J1	0.9900	0.0043
D2	0.9893	0.0044	J2	0.9889	0.0046
D3	0.9948	0.0028	J3	0.9899	0.0042
D4	0.9810	0.0069	J4	0.9919	0.0037
E1	0.9944	0.0033	K1	0.9875	0.0050
E2	0.9880	0.0048	K2	0.9886	0.0049
E3	0.9868	0.0051	K3	0.9886	0.0048
E4	0.9847	0.0058	K4	0.9845	0.0060
F1	0.9899	0.0044			
F2	0.9889	0.0046	Average		
F3	0.9887	0.0121			
F4	0.8254	0.1608			

From this table it can be concluded that the scaling factor and standard deviation for thermocouple F4 are significantly larger than for the other thermocouples. The plot of T6 is shown in Figure B2 and shows that thermocouple F4 is definitely faulty. Possible reasons for this behaviour are that there are small micro cracks at the junction or that the thermocouple wire is kinked or damaged somewhere inside the Teflon coating and therefore it does not make proper contact all the time. Since a total of 44 thermocouples are positioned on each tube, this thermocouple will be neglected without any significant loss, in order to obtain accurate results.

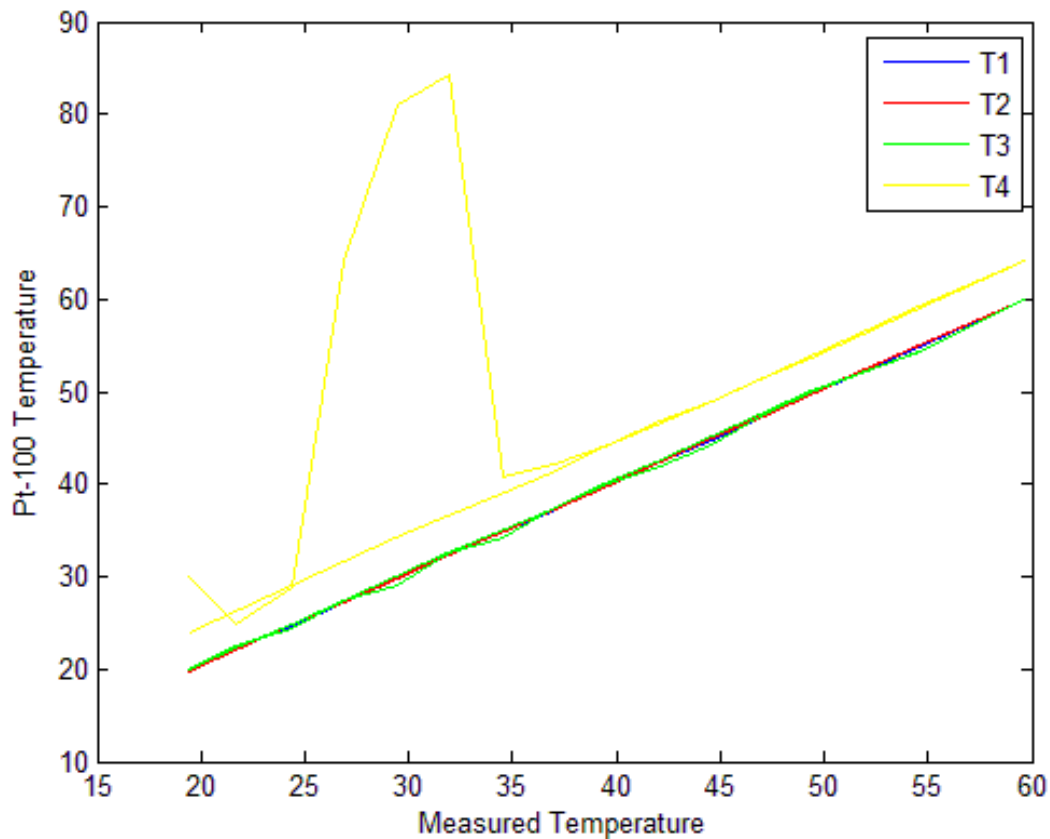


FIGURE B.3: TEMPERATURE PROFILE OF T6

B2 Pressure Transducer Calibration

A DP15 differential pressure transducers were used to measure the pressure drops across the test section. The diaphragms in the pressure transducers can be changed according to the pressure drops of the system. The minimum and maximum pressure drop across the test section was calculated to be 20 Pa and 580 Pa for the smooth tube and for laminar flow in the smooth tube, and 20 and 8 kPa in the roughened tube. Thus, a number 20 diaphragm with a pressure range of 860 Pa was used for the smooth tube and a number 30 diaphragm with a pressure range of 8.6 kPa was used for the roughened tube. The accuracy of the pressure transducers is 0.25 % of the full scale value.

A water manometer, with an accuracy of 50 Pa, was used to calibrate the differential pressure transducer. The set-up used for the calibration is shown in Figure B.4. A thin rubber capillary tube was used to connect the two columns. Water entered the longer column and then the tap was closed. The water then flowed through the connecting tube to the other column until the water level of both tubes was the same, thus, equilibrium was reached. The pressure reading on the manometer was zeroed and the pressure transducer amplifier was adjusted until the pressure reading in the Labview program was approximately 4 mA. The connecting tube was then closed to prevent water flowing to the shorter cylinder and the tap was opened again until the reading on the manometer was approximately 600 Pa, since the maximum pressure needed during testing was 580. The current reading corresponding to the 600 Pa reading was approximately 14 mA. The connecting tube was opened again in order to obtain equilibrium

conditions in the two cylinders. The process was repeated three times in order to reduce the effect of hysteresis and the final current reading in the Labview program, corresponding to a maximum pressure of 600 Pa was 13.16 mA.



FIGURE B.4: PRESSURE TRANSDUCER CALIBRATION

The current signal obtained from the Labview program was converted to a pressure reading in Excell. This was done via interpolation since the pressure ranged between 0 and 600 Pa and the current between 4 and 13.16 mA . A plot of the pressure recorded by the Labview program against the actual pressure reading on the manometer was then generated and is shown in Figure B.5. The equation of the line was determined and used to determine the pressure drop during the tests. However, after each start-up of the pumps, the pressure taps and pressure transducer were bled to ensure that there is no air in the system. A pressure reading was then taken during no-flow conditions and was used as the off-set. The no-flow condition was obtained by opening the by-pass valve and closing the supply-valve in order to ensure that there is water supply for the pump, but not through the test section. One reading consisting of approximately 30 data points was taken and the average pressure reading was used as the off-set value. The final pressure equation used in the Matlab code was therefore

$$y = 64.41x - 257.64 - offset.$$

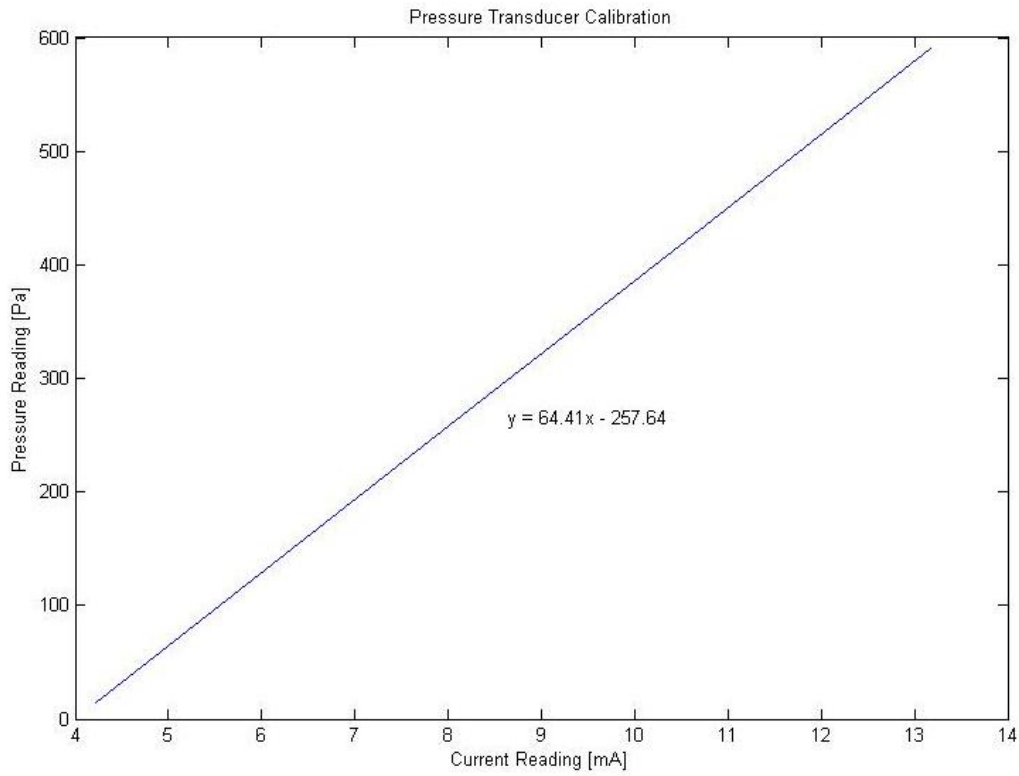


FIGURE B.5: PRESSURE TRANSDUCER 1 CALIBRATION

This process was repeated for the second diaphragm and the following plot was generated:

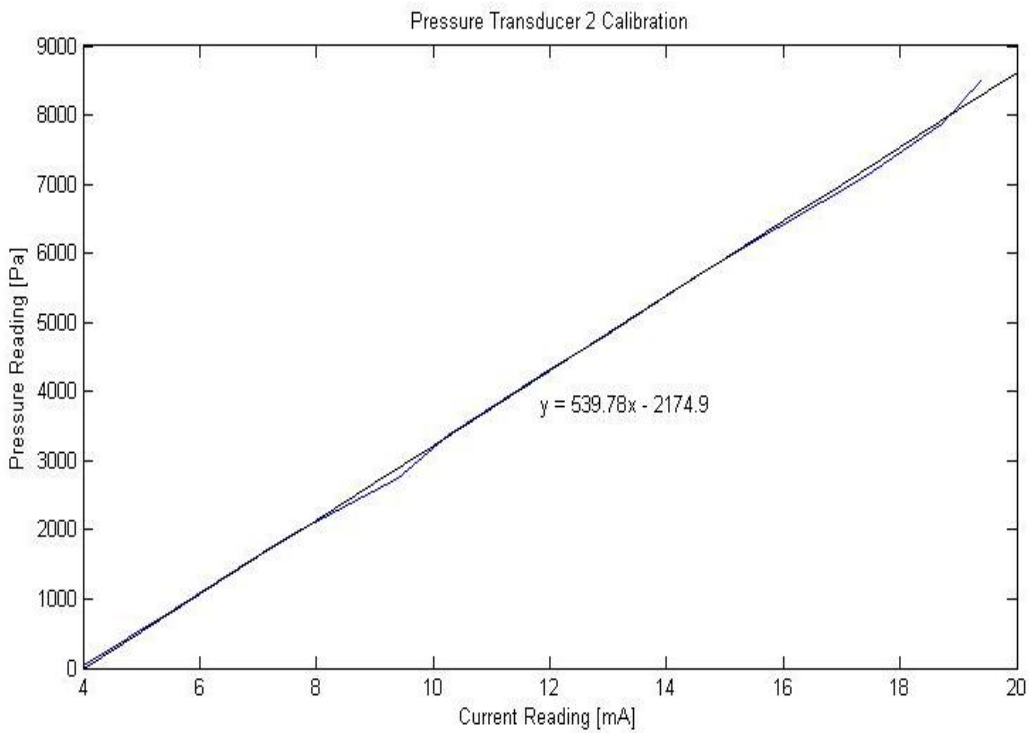


FIGURE B.6: PRESSURE TRANSDUCER 2 CALIBRATION

APPENDIX C: MATLAB CODES

Appendix C contains the Matlab codes that were used to process the calibration and experimental data. The codes for the smooth and roughened tubes are similar, therefore the adiabatic friction factor code and 8.66 kW/m^2 heat flux code for the roughened tube will be included only.

APPENDIX D: PROTOCOL AND PROGRESS REPORTS

Appendix D contains the Protocol and Progress Reports which was used to inform the project leader about the developments of the project.

UNIVERSITY OF PRETORIA

MSC 412 - PROTOCOL

The Influence of Surface Roughness in the Transitional Flow Regime

Marilize Everts S29037078

3/9/2012

Background

A lot of work has been done in the Heat Transfer Laboratory of the University of Pretoria on flow in the transitional flow regime. The transitional flow regime is where the Reynolds number changes from laminar to turbulent flow. Heat exchangers designer usually avoid this region, due to flow instabilities and uncertainties. The type of inlet has significant influence on when transition occurs and from previous work done; it was shown that the smoother the inlet, the more delayed transition will be.

Problem Statement

Although much research has been devoted to flow in the transitional flow regime, little information is available on the influence of surface roughness in this flow regime. Heat transfer and pressure drop measurements at different heat fluxes should be taken for water in a smooth and rough tube of the same diameter.

Aim

The aim of this project is to determine the influence of surface roughness in the transitional flow regime.

Scope

A literature study will be done to acquire the relevant information on the background of the problem, as well as previous work done on this subject and especially in the Heat Transfer Laboratory of the University of Pretoria.

The Reynolds number varies between approximately 2100 and 4000 for transitional flow and in round tubes the Reynolds number is at approximately 2100 to 2300. For this study, a range of Reynolds numbers between 1000 and 8000 will be used.

Heat transfer and pressure drop measurements must be taken at different heat fluxes for water in a smooth and rough tube over the transitional regime. The two pipes must have the same diameter with a square edge inlet and a length of 1.8m. The experimental set-up must also contain a calming section. Copper pipes with a diameter of about 15mm (depending on availability) will be used for the experiment and it must be sufficiently isolated.

The 'rough' tube should be roughened in such a way that the roughness is consistent over the length of the pipe. The roughness should be measured to obtain the relative roughness. Before the commencement of the testing, the pipe must be cleaned properly to ensure that there are no loose particles in the pipe.

An experimental set-up must be developed and built and the data obtained from the experiments must be compared to recently published results, as well as the data of the other student who is doing the same project on a different tube diameter.

Method

The following method will be used to determine the influence of surface roughness in the transitional flow regime:

- Protocol
- Literature study
- Theoretical Simulation
- Experimental set-up
- Experiments
- Correlations
- Compare, discuss and process data
- Compile Final Report
- Prepare Presentation and oral
- Poster exhibition

Deliverables

- Research Report
- An experimental set-up to test the influence of surface roughness in the transitional flow regime.
- An oral presentation and poster exhibition

Target Dates

- | | |
|-------------------------------|------------------|
| • Protocol | 9 March 2012 |
| • First Progress Report | 30 March 2012 |
| • Half year Report | 28 May 2012 |
| • Half year evaluation | 22 June 2012 |
| • Second Progress Report | 27 August 2012 |
| • Closure of workshops | 6 October 2012 |
| • Final Report | 22 October 2012 |
| • Final Presentation and oral | 16 November 2012 |
| • Poster Exhibition | 29 November 2012 |

Number	Task	Start	End	Duration	% Complete	2012									
						March	April	May	June	July	August	September	October	November	
1	MSC Research Project	3/1/2012	11/29/2012	196											
1.1	Protocol	3/1/2012	3/9/2012	7	100.0										
1.2	Literature Study	3/5/2012	3/30/2012	20											
1.3	First Progress Report	3/25/2012	3/30/2012	5											
1.4	Theoretical Simulation	3/31/2012	5/1/2012	22											
1.5	Experimental Set-up	5/1/2012	5/28/2012	20											
1.6	Half Year Report	5/18/2012	5/28/2012	7											
1.7	Experiments	5/29/2012	7/20/2012	39											
1.8	Correlations	7/21/2012	8/20/2012	21											
1.9	Second Progress Report	8/22/2012	8/28/2012	5											
1.10	Final Report	8/29/2012	10/22/2012	39											
1.11	Final Presentation and Oral	10/23/2012	11/16/2012	19											
1.12	Poster Exhibition	11/17/2012	11/29/2012	9											

UNIVERSITY OF PRETORIA

INFLUENCE OF SURFACE ROUGHNESS IN THE TRANSITIONAL FLOW REGIME

MSC – FIRST PROGRESS REPORT

Study Leader: Prof JP Meyer

Marilize Everts S29037078

3/30/2012

Marilize Everts

Prof J.P. Meyer

Work completed up to date

Since there are mainly two groups of people who investigated the transitional flow regime, a literature study has been done on the work done by Meyer and Ghajar. Diabatic and adiabatic cases, as well as enhanced tubes were investigated.

Project Plan

Since the required background knowledge needed for the project has been obtained, the theoretical simulation process can be started before the actual experimental set-up can be designed. The relevant information concerning the available laboratory equipment must be obtained, since this is needed for the calculations. Options to roughen the inside of the tube must also be investigated in order to select the best one.

Personal Opinion

Up to now, no serious problems are foreseen except to find a suitable method to roughen the inside of the tube uniformly. The project is still on schedule and if this schedule is further adhered to, all the deadlines will be met and influence of the surface roughness in the transitional flow regime will be determined.

Number	Task	Start	End	Duration	% Complete	2012											
						March	April	May	June	July	August	September	October	November			
1	MSC Research Project	3/1/2012	11/29/2012	196													
1.1	Protocol	3/1/2012	3/9/2012	7	100.0												
1.2	Literature Study	3/5/2012	3/30/2012	20	100.0												
1.3	First Progress Report	3/25/2012	3/30/2012	5	100.0												
1.4	Theoretical Simulation	3/31/2012	5/1/2012	22													
1.5	Experimental Set-up	5/1/2012	5/28/2012	20													
1.6	Half Year Report	5/18/2012	5/28/2012	7													
1.7	Experiments	5/29/2012	7/20/2012	39													
1.8	Correlations	7/21/2012	8/20/2012	21													
1.9	Second Progress Report	8/22/2012	8/28/2012	5													
1.10	Final Report	8/29/2012	10/22/2012	39													
1.11	Final Presentation and Oral	10/23/2012	11/16/2012	19													
1.12	Poster Exhibition	11/17/2012	11/29/2012	9													

UNIVERSITY OF PRETORIA

INFLUENCE OF SURFACE ROUGHNESS IN THE TRANSITIONAL FLOW REGIME

MSC – SECOND PROGRESS REPORT

Study Leader: Prof JP Meyer

Marilize Everts

Marilize Everts

Prof J.P. Meyer

Status of work completed up to date

The experimental set-up is almost done and the thermocouples have been calibrated and attached to the two tubes. The second tube was roughened by a process similar to knurling. A steel bar was roughened on the outside and inserted into the copper tube. A kinetic hammer was used to hammer the copper tube and imprint the roughness on the inside. Metlab reported that the roughness of the tube could not be measured since the needle got stuck in the grooves of the rough surface and that the surface profile of the tube falls outside the capabilities of their roughness tester. The maximum capability of their equipment is a surface roughness of 16 μm and when dividing this with the inner tube diameter of 14.46 mm, a relative roughness of 0.001 was obtained. This roughness was sufficient since the corresponding friction factors on the Moody Chart varied between 0.044 and 0.035 for Reynolds numbers between 3 000 and 7 000, which is acceptable.

Project Plan

The experimental set-up will be completed within the next two week and afterwards the tests will be conducted. During these last two weeks of the experimental set-up, Matlab codes will also be written. Once the results are obtained, it can be inserted into the existing codes. These codes will assist in investigating the friction factors and pressure drop and compare the two tubes with each other.

Budget

The experimental set-up is almost finished; therefore the majority of the costs is already made. The rest of the costs are expected to be minimal. A summary of the total costs is given in the table below. The material costs include everything that have been bought in order to build the experimental set-up and to roughen the tube. The testing costs refer to the testing of the surface roughness which was done by Metlab in order to determine the relative roughness of the tube.

Description	Cost
Material	984.42
Testing	769.5
Total	1753.92

Personal Opinion

Roughening the one tube was far more difficult and time consuming than initially expected, but since the experimental set-up is nearly completed and the testing will soon commence, the project will be completed on time.

The Gantt chart has been altered since there was not enough time allocated for building the experimental set-up, and too much time was allocated for testing. The rest of the Gantt Chart is similar to the previous one.

Number	Task	Start	End	Duration	% Complete	2012											
						March	April	May	June	July	August	September	October	November	December		
1	MSC Research Project	3/1/2012	11/29/2012	196													
1.1	Protocol	3/1/2012	3/9/2012	7	100.0												
1.2	Literature Study	3/5/2012	3/30/2012	20	100.0												
1.3	First Progress Report	3/25/2012	3/30/2012	5	100.0												
1.4	Theoretical Simulation	3/31/2012	5/9/2012	28	100.0												
1.5	Half Year Report	5/10/2012	5/27/2012	12	100.0												
1.6	Half Year Evaluation	6/18/2012	6/21/2012	4	100.0												
1.7	Experimental Set-up	6/21/2012	9/7/2012	57	90.0												
1.8	Second Progress Report	8/27/2012	8/28/2012	2	100.0												
1.9	Experiments	9/10/2012	9/14/2012	5													
1.10	Data processing and Correlations	9/10/2012	9/21/2012	10													
1.12	Final Report	9/21/2012	10/5/2012	11													
1.13	Final Presentation and Oral	11/9/2012	11/16/2012	5													
1.14	Poster Exhibition	11/20/2012	11/29/2012	8													